

GÖTTINGER ZENTRUM
FÜR BIODIVERSITÄTSFORSCHUNG UND ÖKOLOGIE
– GÖTTINGEN CENTRE FOR BIODIVERSITY AND ECOLOGY –

Soil nitrogen oxide and carbon dioxide emissions from a
tropical lowland and montane forest exposed to elevated
nitrogen input

Dissertation zur Erlangung des Doktorgrades der
Mathematisch-Naturwissenschaftlichen Fakultäten der
Georg-August-Universität Göttingen

vorgelegt von

Diplom-Geoökologin

Birgit Köhler

aus

Rendsburg

Göttingen, Januar 2009

Referentin: Dr. Marife Corre

Korreferent: Prof. Dr. Erwin Zehe

Tag der mündlichen Prüfung: 18. 02. 2009

MEINER FAMILIE

- DEDICATED TO MY FAMILY -



‘OVERALL, OUR UNDERSTANDING OF THE NITROGEN CYCLE AND THE DEVELOPMENT OF EFFECTIVE POLICIES TO REDUCE INADVERTENT LOSSES OF ANTHROPOGENIC NITROGEN TO THE ENVIRONMENT IS ANALOGOUS TO OUR UNDERSTANDING OF THE CARBON CYCLE IN THE LATE 1960S.

HUMANS ARE ADDING NITROGEN TO THE EARTH’S SURFACE; WE DO NOT KNOW WHERE IT ALL GOES, BUT WE DO KNOW THAT INCREASING CONCENTRATIONS OF NITROGEN IN UNEXPECTED PLACES WILL CAUSE SIGNIFICANT ENVIRONMENTAL DAMAGE (...).’

William H. Schlesinger (2009)

TABLE OF CONTENTS

SUMMARY	11
1 INTRODUCTION	13
1.1 Tropical forests in a changing environment	14
1.2 Transformation of the nitrogen cycle and the globalization of nitrogen deposition	14
1.3 The relation between soils, atmospheric trace gases and climate change	17
1.4 Contrasting tropical lowland and montane forests	18
1.5 Objectives of the thesis.....	18
1.6 Location of the study forests.....	19
1.1 Design of the nitrogen-addition experiments.....	19
1.1 Methodological outline of the trace gas measurements.....	20
1.2 Outline of the chapters	22
1.3 References	24
2 IMMEDIATE AND LONG-TERM NITROGEN OXIDE EMISSIONS FROM TROPICAL FOREST SOILS EXPOSED TO ELEVATED NITROGEN INPUT.....	27
2.1 Abstract.....	28
2.2 Introduction	28
2.3 Materials and methods.....	32
2.3.1 Approach.....	32
2.3.2 Study Area.....	32
2.3.3 Experimental design.....	34
2.3.4 Soil characteristics	35
2.3.5 N-oxide flux measurements.....	37
2.3.6 Soil mineral N, soil moisture, and net rates of soil N cycling	38
2.3.7 Statistical analyses	39
2.4 Results	40
2.4.1 Soil conditions, N-cycling rates and N-oxide fluxes from control forests	40
2.4.2 Transitory N addition effects ('fertilization peaks')	46
2.4.3 Long-term effects of N enrichment.....	48
2.4.4 N-oxide fluxes following first-time N addition	50
2.5 Discussion	51
2.5.1 Soil N cycle and N-oxide fluxes from control forests.....	51
2.5.2 Response of soil N-oxide fluxes to N addition in the lowland forest.....	52
2.5.3 Response of soil N-oxide fluxes to N addition in the montane forest.....	53

2.5.4	Factors influencing soil N-oxide emissions following anthropogenic N additions	54
2.5.5	Consequences of chronic N deposition on soil N-oxide emissions from tropical lowland and montane forests	56
2.6	References	57
3	CHRONIC NITROGEN ADDITION CAUSES A REDUCTION IN SOIL CARBON DIOXIDE EFFLUX DURING THE HIGH STEM-GROWTH PERIOD IN A TROPICAL MONTANE FOREST BUT NO RESPONSE FROM A TROPICAL LOWLAND FOREST ON A DECADAL TIME SCALE.....	63
3.1	Abstract	64
3.2	Introduction	64
3.3	Materials and methods.....	66
3.3.1	Study Area.....	66
3.3.2	Experimental design.....	67
3.3.3	Soil CO ₂ efflux, temperature and moisture measurements.....	68
3.3.4	Statistical analyses and calculations.....	69
3.4	Results	70
3.4.1	Water-filled pore space and temperature in the control forest soils.....	70
3.4.2	Soil CO ₂ efflux of the control forests.....	70
3.4.3	Effects of elevated N input on the chronic soil CO ₂ efflux	74
3.5	Discussion	76
3.5.1	Soil moisture and temperature regulation on soil CO ₂ efflux from the control forests....	76
3.5.2	Effects of N addition on soil CO ₂ efflux from the lowland forest	77
3.5.3	Effects of N addition on soil CO ₂ efflux from the montane forest	79
3.5.4	Consequences of chronic N deposition on carbon cycling in tropical forests	80
3.6	References	82
4	AN INVERSE ANALYSIS REVEALS LIMITATIONS OF THE SOIL-CO₂ PROFILE METHOD TO CALCULATE CO₂ PRODUCTION FOR WELL-STRUCTURED SOILS.....	87
4.1	Abstract	88
4.2	Introduction	88
4.3	Materials and methods.....	91
4.3.1	Measurements	91
4.3.2	Model approach and calculation methods	94
4.4	Results	100
4.4.1	Volumetric water content, temperatures, ²²² Rn and CO ₂ concentrations down to 2 m soil depth	100
4.4.2	Soil porosity and empirical diffusion coefficients	100

4.4.3	Simulated steady state ^{222}Rn concentrations.....	100
4.4.4	CO ₂ fluxes and production rates calculated with the empirical D and different implementations of the profile method	101
4.4.5	CO ₂ fluxes and production rates calculated with the inverse D in the profile method...	103
4.5	Discussion	107
4.5.1	The influence of the function to interpolate between the measured CO ₂ concentrations....	107
4.5.2	The influence of uncertainties in the depth distribution of D	108
4.5.3	Processes governing soil CO ₂ dynamics	109
4.5.4	Implications of this study for soil CO ₂ production modeling.....	111
4.6	References	112
5	SYNTHESIS.....	117
5.1	How will tropical regions respond to rising nitrogen input?	118
5.2	What is the ultimate fate of reactive nitrogen?	118
5.3	What are the net climate effects of increasing reactive nitrogen?.....	120
5.4	From trace gas production to soil surface flux.....	122
5.5	Suggestions for future research.....	123
5.6	References	125
DECLARATION OF ORIGINALITY, CERTIFICATE OF AUTHORSHIP AND DECLARATION ABOUT DATA CONTRIBUTIONS OF THE CO-AUTHORS TO THE PRESENTED MANUSCRIPTS.....		127
CURRICULUM VITAE		128
ACKNOWLEDGEMENTS		129

LIST OF FIGURES

Figure 1-1: The pace of prominent human-induced global changes.	15
Figure 1-2: Example how a molecule of reactive nitrogen may ‘cascade’ through the environment.....	16
Figure 1-3: Global atmospheric deposition of reactive nitrogen in 2000.....	17
Figure 1-4: Location of the lowland and montane study forests within the Republic of Panama.....	19
Figure 1-5: Photographs of the tropical lowland and montane forests, Republic of Panama.....	20
Figure 1-6: Design of the nitrogen-addition experiments.....	21
Figure 1-7: Photographs of the field and laboratory equipment for gas flux measurements and analysis.....	22
Figure 1-8: Photographs of the pits for soil air sampling in the lowland forest	23
Figure 2-1: Soil temperature and water-filled pore space in the control and N-addition lowland and montane forests.....	41
Figure 2-2: Soil extractable NH_4^+ and NO_3^- in the control and N-addition lowland forest.....	42
Figure 2-3: Soil extractable NH_4^+ and NO_3^- in the control and N-addition montane forest....	42
Figure 2-4: NO and N_2O emissions from the control and N-addition lowland forest.....	47
Figure 2-5: NO and N_2O emissions from the control and N-addition montane forest.....	48
Figure 2-6: Linear regressions between water-filled pore space and NO emissions, $\log(\text{N}_2\text{O})$ emissions and $\log(\text{N}_2\text{O}/\text{NO})$ ratio for the N-addition lowland forest.....	49
Figure 2-7: NO and N_2O emissions from the first-time N-addition lowland and montane forest.	51
Figure 3-1: Water-filled pore space and soil temperature in the control and N-addition lowland and montane forests.....	71
Figure 3-2: Soil CO_2 efflux from the control and N-addition lowland and montane forests. .	72
Figure 3-3: Regression analyses between water-filled pore space and CO_2 efflux for the control and N-addition lowland and montane forests.....	73
Figure 3-4: Linear regressions between soil temperature and CO_2 efflux for the control and N-addition lowland and montane forests.	74

Figure 3-6: Cumulative soil CO ₂ efflux from the control and 2-3-yr N-addition montane forest	75
Figure 3-6: Normalized ratio of soil CO ₂ efflux to monthly tree stem growth from the control and N-addition montane forest	76
Figure 4-1: Sigmoidal interpolation function and its first and second derivative.....	96
Figure 4-2: Measured and simulated ²²² Rn concentration profiles in soil air during dry and wet season in the lowland forest.....	101
Figure 4-3: CO ₂ concentrations in soil air down to 2 m depth in the lowland forest.....	102
Figure 4-4: Empirical and inversely modeled diffusion coefficients, and measured and interpolated CO ₂ concentrations in soil air during dry and wet season.	104
Figure 4-5: Soil CO ₂ fluxes and ‘production rates’ calculated with the soil-CO ₂ profile method.....	105
Figure 4-6: Time-series of the measured and modeled mean soil CO ₂ flux.....	106
Figure 4-7: a) X-ray computed tomography scan of the inter-aggregate pores in a Terra fusca soil. b) Conceptual graph illustrating the steady state CO ₂ exchange fluxes at the interfaces between air- and water-filled pores.	106

LIST OF TABLES

Table 2-1: Soil classification and characteristics of the lowland and montane forest.....	33
Table 2-2: Forest characteristics of the lowland and montane sites.....	36
Table 2-3: Net rates of soil N cycling in the lowland and montane forest	43
Table 2-4: NO and N ₂ O emissions from old-growth tropical lowland forests	44
Table 2-5: NO and N ₂ O emissions from old-growth tropical montane forests	45
Table 2-6: Annual NO and N ₂ O emissions of the control and N-addition plots.....	46
Table 3-1: Annual soil CO ₂ efflux of the control and N-addition plots	73
Table 4-1: Profiles of total porosity, its inter-aggregate and air-filled fractions, and radon production rates of the lowland forest soil.....	103

Summary

Tropical nitrogen (N) deposition is projected to increase substantially within the coming decades, but the effects on forest soil emissions of climate-relevant trace gases are poorly investigated. In the experimental part of this study, long-term N-addition experiments were used to achieve N-enriched conditions in old-growth montane and lowland forests in the Republic of Panama. The experiments consisted of four replicate 40x40 m control and N-addition plots, with the latter receiving 125 kg N ha⁻¹ yr⁻¹ split in four equal applications. Soil nitrous oxide (N₂O) and carbon dioxide (CO₂) fluxes were determined using vented static chambers and gas chromatographic analysis; soil nitric oxide (NO) fluxes were measured using open dynamic chambers and chemiluminescent detection. The emission responses to N addition were divided into transitory effects, which occurred within a six-week period after N additions, and long-term effects. In the lowland forest, also soil CO₂ concentration profiles were assessed down to 2 m depth. The measurements were conducted within the 1st to 3rd year of N addition in the montane, and the 9th to 11th year of N addition in the lowland forest. In the mathematical modeling part of this study, the ‘soil CO₂-profile method’ to calculate soil CO₂ production was inversely analyzed to test its validity and assumptions for our well-structured lowland forest soils.

The montane forest has N-limited stem diameter growth and fine litterfall and is located on an Andisol soil with low buffering capacity and an organic layer. First-time N additions caused rapid increases in soil N-oxide emissions. During 1-2 yr N-addition, the annual fluxes were five times (transitory effect) and two times (long-term effect) larger than the control. This was largely attributed to a fast and substantial increase of the nitrification activity in the organic layer. Concerning the variance in soil CO₂ effluxes, temperature was the main explanatory variable. First year N addition did not cause a response but annual CO₂ efflux decreased by 14% and 8% in the 2nd and 3rd year N-addition plots, respectively, compared to the control. The reduction occurred during the high stem-growth period of the year, simultaneously with a stimulation of stem diameter growth. This observation indicates a shift in carbon partitioning from below- to aboveground which, in the longer term, would cause imprints on the magnitude of soil C storage.

The seasonal lowland forest, where stem diameter growth and annual fine litterfall mass are not N-limited, is located on a clay-textured Cambisol soil with high base saturation and buffering capacity. N enrichment decreased soil pH and base saturation and increased the

exchangeable aluminum content. Soil N-oxide and CO₂ emissions from the control forest were larger than from the montane control. First-time N additions caused only gradual and minimal increases in soil N-oxide emissions, while annual N-oxide emissions under chronic N addition were seven times (transitory effect) and four times (long-term effect) larger than the controls. The ratio of soil N₂O/NO emissions was positively correlated with the water-filled pore space in the N-addition but not in the control plots: An originally rather conservative soil N cycle, where N-oxide emissions were regulated by N availability, has been changed to an increasingly leaky soil N cycle where the soil aeration status reflects in a pronounced seasonality of emissions. Concerning the variance in soil CO₂ effluxes, soil moisture was the main explanatory variable. Soil CO₂ efflux did not differ between the 9-11-year N-addition and control plots: After a decade of N addition, the soils good nutrient-supplying and buffering capacity still mitigated acidity- or Al-induced reductions of soil respiration; chronic N input to nutrient-rich lowland forests, where primary productivity is not N-limited, may not change their C balance on a decadal time scale.

Soil CO₂ production at a specific depth can not be measured in the field. The production has frequently been calculated from the vertical gas diffusive flux divergence, known as ‘soil-CO₂ profile method’. For our lowland forest, this method gave inconsistent results when using ‘empirical’ diffusion coefficients (*D*) calculated based on soil porosity and moisture. An inverse analysis served to deduce which *D* would be required to explain the observed CO₂ concentrations if the profile method were valid. In the top soil, the ‘inverse’ *D* closely resembled the empirical *D*. In the deep soil, however, the inverse *D* increased sharply while the empirical did not. This deviation disappeared upon conducting a constrained fit parameter optimization. A radon (Rn) mass balance model, in which diffusion was calculated based on these *D*, simulated the observed Rn profiles reasonably well. However, the constrained inverse *D* underestimated the observed CO₂ concentrations. Finally, it gave depth-constant fluxes and hence zero production in the CO₂-profile method. These problems to inversely achieve consistent results with the profile method are attributed to a missing description of steady state CO₂ exchange fluxes across water-filled pores. These are driven by the different diffusivities in inter- vs. intra-aggregate pores which create permanent CO₂ gradients if separated by a ‘diffusive water barrier’. The assumptions of the profile method are inaccurate for well-structured soils with high water content, where places of CO₂ production and upward diffusion exhibit spatial separation.

CHAPTER

1

Introduction

1.1 Tropical forests in a changing environment

Tropical and subtropical forests contribute to more than half of the global forest area (FAO, 2000). They have a disproportionate role in the global carbon (C) cycle (Malhi, 2005), which is tightly coupled with other biogeochemical cycles as the one of nitrogen (N) (Gruber & Galloway, 2008). The population of tropical countries amounted to 4.9 billion people in 2000 and is projected to grow by a further 2 billion before 2030 (United Nations, 2004). Human activities threaten tropical forest systems at both local and global scale. Local anthropogenic impacts include deforestation, fragmentation, poaching and the introduction of invasive species. At a global scale, the effects are mainly due to human-induced climate change. With increasing atmospheric carbon dioxide (CO₂) concentration, temperature and nutrient deposition, and changes in precipitation patterns, ecosystem moisture status and disturbance regimes climate change alters several characteristics of the tropical environment (Chambers & Silver, 2004; Wright, 2005). Concerning the forests nutrition, especially the N cycle is undergoing a major transformation due to human activities.

1.2 Transformation of the nitrogen cycle and the globalization of nitrogen deposition

The N cycle is integral to functioning of the Earth system and to climate. As N is an essential component of proteins, genetic material, chlorophyll and other key organic molecules all organisms require N in order to live. Although the Earth's atmosphere is composed by 78% nitrogen gas (N₂) this is a largely bio-unavailable reservoir because most organisms cannot use N directly from the air. Therefore, N is usually the major limiting factor for aboveground primary production in undisturbed temperate ecosystems (Vitousek *et al.*, 1997). 'Mobilization' of N₂ is initiated by breaking the triple bond between the two N-atoms, producing available 'reactive' N (N_r) in both oxidized and reduced forms- principally nitrate and ammonium. Naturally, N can only be mobilized by N-fixing organisms (major contribution) or by lightning (minor contribution). It can be sequestered back to the atmosphere by complete denitrification to N₂. Prior to the industrial age, N_r did not accumulate in environmental reservoirs because microbial N fixation and denitrification were approximately equal (Ayres *et al.*, 1994). In the early 20th century, however, the Haber-Bosch process was developed as a way to industrially mobilize the chemically inert N₂ from the atmosphere. This industrial N fixation, mainly used to produce N fertilizer, has increased

exponentially from near zero in the 1940s, consequently boosting food production (Vitousek *et al.*, 1997). It is estimated that the Haber-Bosch process consumed about 1% of the world's total annual energy supply in the late 1990s (Smith, 2002). In comparison to other prominent global changes the increase in industrial N fixation began quite recently but is proceeding very rapidly (Vitousek *et al.*, 1997, Fig. 1-1). Further main causes of the global increase in N_r , aside from the increasing use of N fertilizer in agriculture, are fossil fuel combustion and the cultivation of N-fixing plants (Galloway *et al.*, 2003; 2008). Also land clearing, biomass burning and wetland drainage have enhanced the mobility of N_r within and between terrestrial ecosystems (Vitousek *et al.*, 1997). Since 1970, world population has increased by another 78% and N_r creation by 120%, such that in the last decades the anthropogenic production of N_r has been greater than the production from all natural terrestrial systems. Once atmospheric N_2 is mobilized into a reactive form it will cycle through the ecosystems, called 'N cascading', and can influence the environment in a variety of ways (Galloway *et al.*, 2003, 2008; Fig. 1-2).

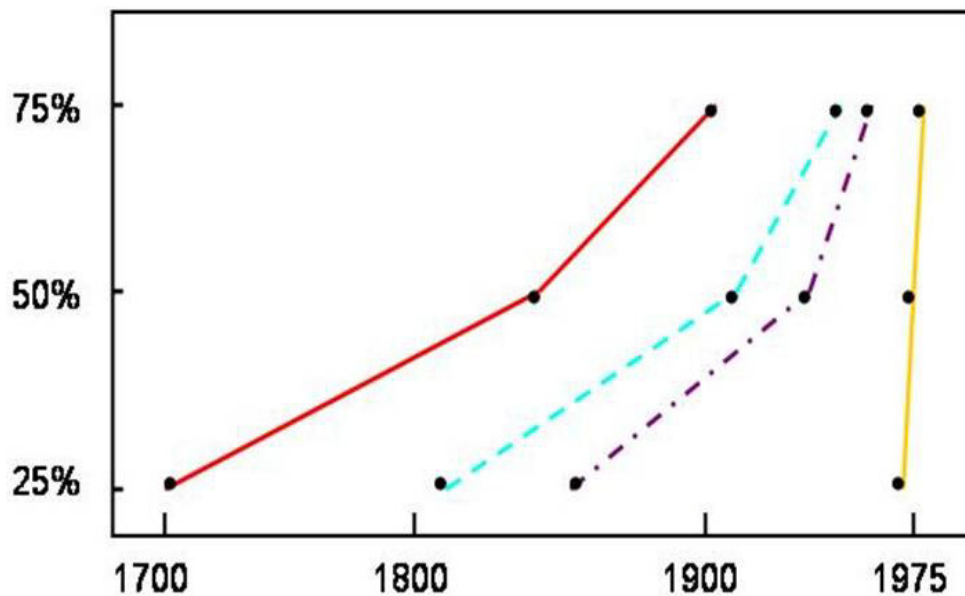


Figure 1-1. Comparative timing and rate of a number of global changes, namely deforestation (—), CO₂ release (---), human population increase (-·-) and industrial N-fertilizer production (—). The figure shows the year by which 25%, 50% and 75% of the extent of change in the late 1980's had occurred. From Vitousek *et al.* (1997).

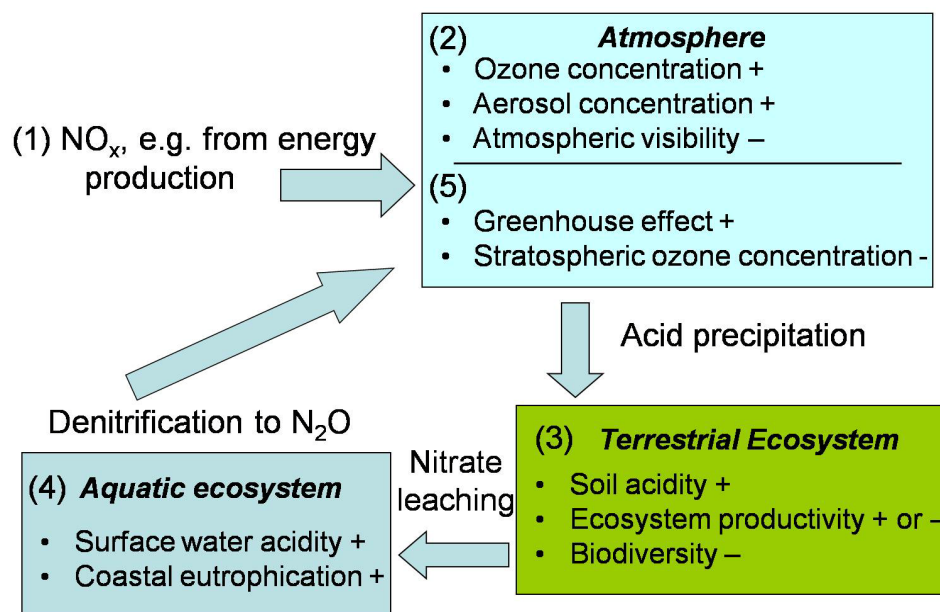


Figure 1-2. Example how a molecule of ‘reactive’ nitrogen may ‘cascade’ through environmental reservoirs ((1) to (5)) and cause a variety of effects. A positive sign indicates an increase, a negative sign a decrease in the respective process or characteristic. Visualized from Galloway *et al.* (2003).

It has become a great challenge to try and optimize the need for the key human resource N while minimizing unwanted negative consequences of increasing N cycling, but ever since the industrialization such an optimum has not been achieved (Galloway *et al.*, 2008). In the absence of human influence atmospheric N deposition to ecosystems is maximally 0.5 kg ha⁻¹ yr⁻¹ (Dentener *et al.*, 2006). In some regions of the world, namely in sub-Saharan Africa, soil nutrient deficiencies are still a major limiting factor in crop production, causing a rising prevalence of hunger and malnutrition (Sanchez & Swaminathan, 2005). On the other hand there are now large regions of the world where average N deposition rates exceed 30 kg ha⁻¹ yr⁻¹ (Fig. 1-3). High N deposition can cause a host of environmental problems, including soil acidification resulting in cation losses, decreases in biodiversity, estuarine eutrophication and groundwater pollution. Ecosystem N enrichment may also cause responses which feed back on global climate, for example by changing ecosystem C storage and fluxes of climate relevant trace gases at the soil-air interface (Matson *et al.*, 1999; Galloway *et al.*, 2008).

While, in the past, enhanced atmospheric N deposition was largely concentrated in economically developed regions of the temperate zone it is currently subject to globalization. For the coming decades, N deposition is projected to increase substantially in economically emerging tropical regions such as Southeast Asia and Latin America (Galloway *et al.*, 2003; 2004; 2008). In some tropical regions atmospheric N input is already severely elevated, for

example in southern China where wet N deposition has exceeded $30 \text{ kg ha}^{-1} \text{ yr}^{-1}$ since at least 1990 (Mo *et al.*, 2007). Despite these occurring and projected increases in tropical N deposition its effects on the biogeochemistry of tropical forests are poorly investigated (Matson *et al.*, 1999; Galloway *et al.*, 2008).

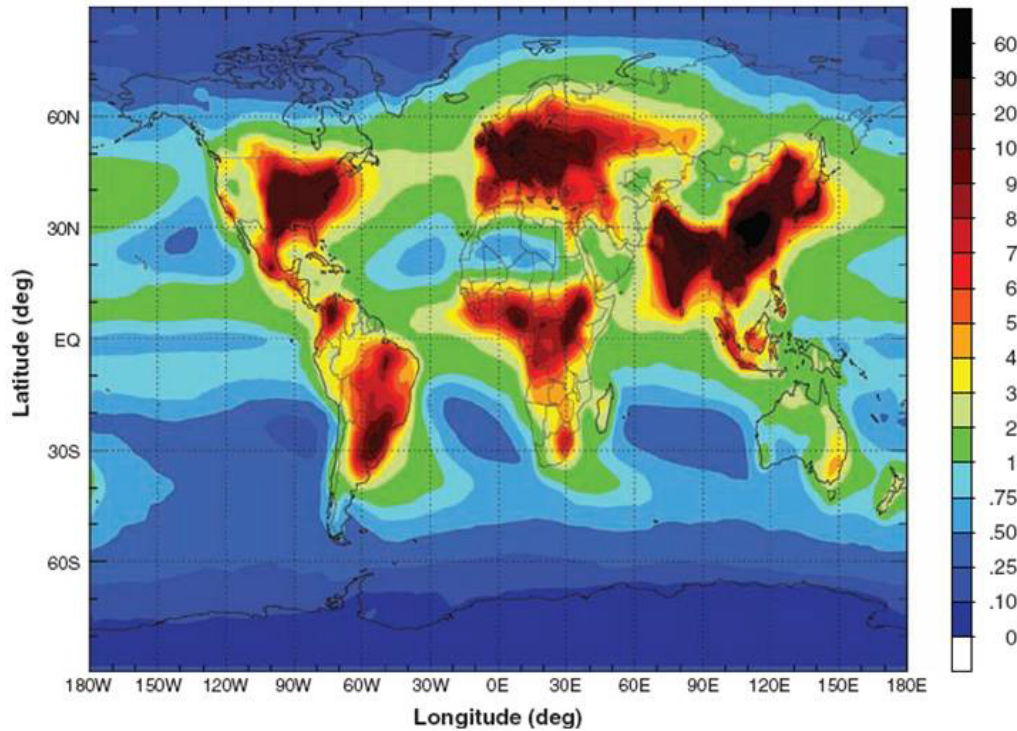


Figure 1-3. Global atmospheric deposition of reactive nitrogen in 2000 ($\text{kg N ha}^{-1} \text{ yr}^{-1}$). From Galloway *et al.* (2008).

1.3 The relation between soils, atmospheric trace gases and climate change

Several atmospheric trace gases are naturally produced in soils and emitted to the atmosphere. Nitric oxide (NO) and nitrous oxide (N_2O) are produced in soils largely by nitrification and denitrification. Tropical forests are the largest natural source of terrestrial N_2O emissions (Bouwman *et al.*, 1995) and the third largest emitter of NO (Yienger & Levy, 1995). CO_2 is produced in soils mainly by roots and microbial decomposition of litter and organic matter, and its emission, called ‘soil respiration’, is the second largest flux in the global terrestrial C cycle (Rustad *et al.*, 2000). Every year, tropical forests cycle more than 10% of the atmospheric CO_2 through photosynthesis, respiration and microbial decay (Malhi, 2005). These soil emitted gases are relevant for the global climate: Among the anthropogenically altered agents the long-lived greenhouse gases CO_2 and N_2O are the largest and fourth largest single contributors to positive radiative forcing, respectively. The dominant impact of NO

emissions on climate is through the photochemical formation of tropospheric ozone, the third largest single contributor to positive radiative forcing (IPCC, 2007). Elevated N input to tropical forests is projected to stimulate soil N-oxide emissions (Hall & Matson, 1999) and may increase or decrease soil CO₂ efflux (Cleveland & Townsend, 2006; Mo *et al.*, 2007), which in turn will affect radiative forcing and hence global warming.

1.4 Contrasting tropical lowland and montane forests

Tropical montane forests differ from lowland forests in their structure and functioning (Bruijnzeel & Veneklaas, 1998). These differences are related to altitudinal changes in abiotic environmental factors. For instance, temperature, evapotranspiration and rainfall seasonality decrease while rainfall amount, cloudiness, fog, soil water saturation and UV-B radiation intensity increase with increasing elevation (Richter, 2008; Gerold, 2008). Tree height, aboveground biomass, leaf size, leaf area index as well as forest productivity are larger (Bruijnzeel & Veneklaas, 1998; Leuschner & Moser, 2008) while fine root biomass and the root-to-aboveground biomass ratio are smaller in lowland than montane forests (Leuschner & Moser, 2008). Soils are often highly and deeply weathered in lowland forests (McGroddy & Silver, 2007) while they are often shallow and with little horizon development in montane forests (Foster, 2001). With respect to the study focus of this thesis the most important differences between lowland and montane forests are the following: (1) Altitude influences the N status of old-growth tropical forests. While N may be limiting above-ground primary productivity in montane forests it is often in relative excess in lowland forests (Tanner *et al.*, 1998). (2) Decomposition is often rapid in lowland, but restricted in montane forests. In lowland forests, litter accumulates only transitory on the forest floor when decomposition is inhibited during dry season (Swift *et al.*, 1979; Montagnini & Jordan, 2005). In contrast, the mineral soil in montane forests is usually covered with a thick and densely rooted organic layer, resulting in a relatively high soil C storage (Schuur, 2001; Schuur *et al.*, 2001).

1.5 Objectives of the thesis

This study was conducted within the research framework of the NITROF-Project which investigates the effects of elevated N input on biogeochemistry and productivity of tropical forests. NITROF is funded by the Robert Bosch Foundation as an independent research group headed by Marife D. Corre. The main objectives of the thesis were to 1) investigate the effects of elevated N input on soil emissions of N₂O, NO and CO₂ from contrasting lowland and

montane forests and 2) use the soil CO₂ profile method to calculate depth-specific soil CO₂ production rates for the deeply weathered lowland forest soil.

1.6 Location of the study forests

The old-growth and species rich study forests are situated in the Republic of Panama (Fig. 1-4). The lowland forest site in the Panama Canal Area (Fig. 1-5a) is located on Gigante Peninsula (9°06'N, 79°50'W) which is part of the Barro Colorado Nature Monument. The lower montane forest site (Fig. 1-5b) is located in the Fortuna Forest Reserve in the Cordillera Central (8°45'N, 82°15'W), Chiriquí province. Both forests belong to the principal research sites of the Smithsonian Tropical Research Institute (STRI), and are described in detail in paragraph 2.3.2.



Figure 1-4. Location of the lowland and montane study forests within the Republic of Panama (satellite image from the Smithsonian Tropical Research Institute (2009)).

1.1 Design of the nitrogen-addition experiments

At both study sites, N enrichment was achieved using long-term N-addition experiments. N-addition and control plots, each treatment with four replicates, are 40x40 m in size. The N-addition plots receive 125 kg urea-N ha⁻¹ yr⁻¹ split in four equal applications. In the lowland, the study was conducted in an on-going nutrient addition experiment which was set up by S. Joseph Wright from STRI. The plots are laid out in four replicates across a 26.6-ha area in a stratified random design (Fig. 1-6a). N-addition started in 1998. In the montane forest, the N-

addition experiment was set up by the NITROF-project in a paired-plots random design (Fig. 1-6b). N addition started in 2006. A detailed description of the experimental design is given in paragraph 2.3.3.



Figure 1-5. a) Seasonal tropical lowland forest in the Barro Colorado Nature Monument (here Barro Colorado Island with research station; photograph from Marcos Guerra, Smithsonian Tropical Research Institute (2009)) close to the Gatún Lake of the Panama Canal, Republic of Panama and b) lower tropical montane forest in the Fortuna Forest Reserve, Chiriquí Province, Republic of Panama (photograph from Jonas Loss).

1.1 Methodological outline of the trace gas measurements

The measurements were conducted within the 1st to 3rd year of N addition in the montane, and the 9th to 11th year of N addition in the lowland forest. Trace gas exchange rates at the soil-air interface were assessed using chamber measurements. In contrast to the long-lived greenhouse gases N₂O and CO₂, NO is a highly reactive trace gas and can thus not be stored for later analysis. Therefore, NO fluxes were measured in the field using air-sampling from open dynamic chambers (Fig. 1-7a) and chemiluminescent detection after oxidation to NO₂ by

a CrO_3 catalyst (Fig. 1-7b). Fluxes of N_2O and CO_2 were determined by air-sampling from vented static chambers (Fig. 1-7c) and gas-chromatographic analysis in the laboratory using an electron capture detector (Fig. 1-7d). Details concerning the gas flux measurements and subsequent calculations are presented in paragraphs 2.3.5 and 3.3.

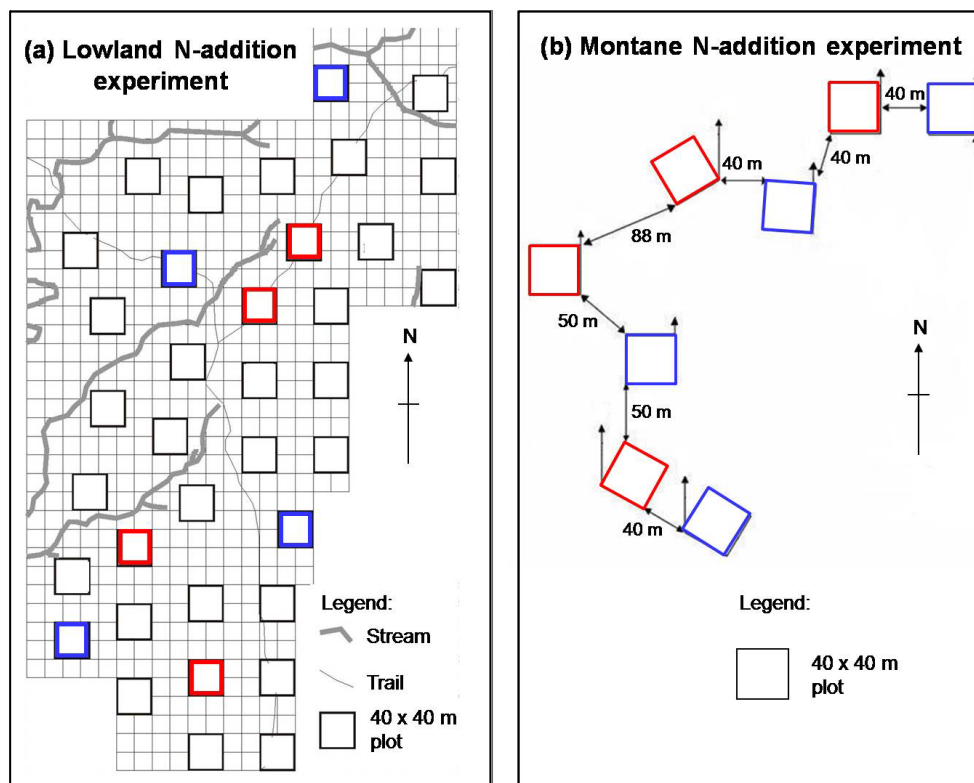


Figure 1-6. Design of the nitrogen-addition experiments; a) Stratified random design in the lowland forest (map modified from S. Joseph Wright) and b) paired-plot random design in the montane forest (modified from Harbusch (2007)). The control plots are marked in blue and the N-addition plots are marked in red.

Furthermore, six pits –each treatment with three replicates– were established in the deeply weathered lowland soil (Fig. 1-8a and b). Air was sampled from stainless-steel tubes installed into the pit walls at six depths down to 2 m (Fig. 1-8c). The CO_2 concentrations were determined by gas chromatographic analysis using an electron capture detector (Fig. 1-7d). The pits, which are permanently installed, can be opened and closed with a lid (Fig. 1-8d). Further explanations concerning the pit setup, installations and measurement methodology are given in paragraph 4.3.1.

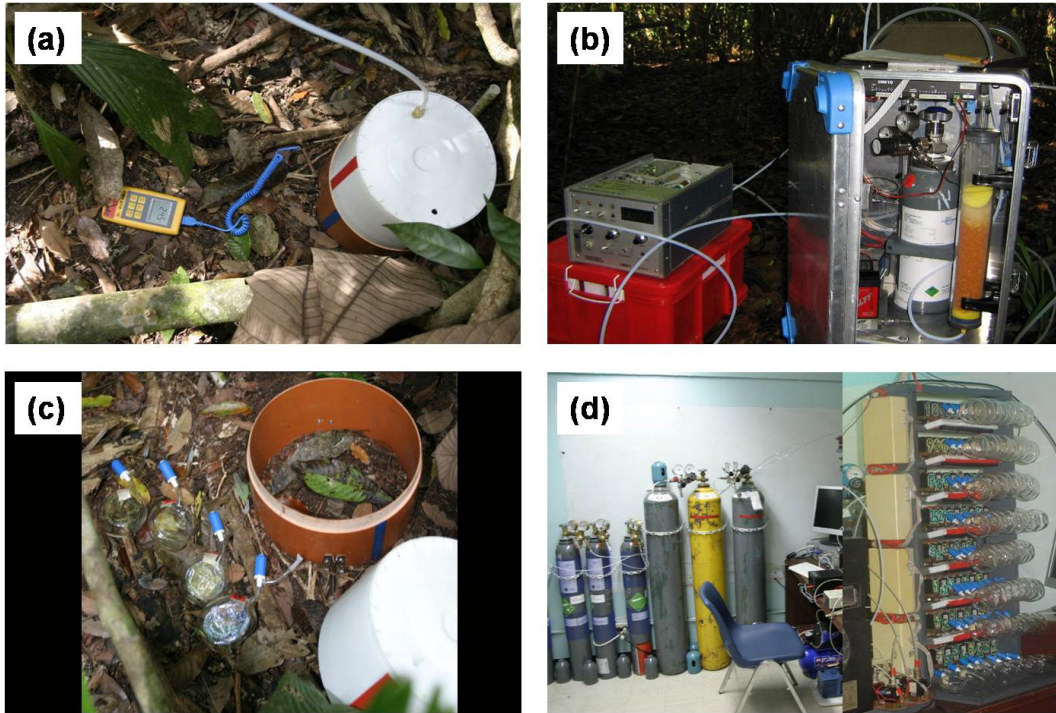


Figure 1-7. Field and laboratory equipment for gas flux measurements and gas analysis. a) Open dynamic chamber to measure nitric oxide (NO) fluxes in the field; b) NO field equipment with NO₂ detector and NO standard gas for calibration on site; c) chamber base with lid (vented static chamber) and glass bottles for air sampling; d) gas chromatograph with carrier- and calibration gases and automatic sampling unit. The sampling unit is loaded with glass bottles containing the air samples to be analyzed for N₂O and CO₂ concentrations. Photographs a)-c) from Jonas Loss, d) (modified) from Edzo Veldkamp.

1.2 Outline of the chapters

Chapter 2 (Koehler *et al.*, 2009a) deals with the question how the timing and magnitude of soil N-oxide emissions change with elevated N input to tropical forests. Both transitory and long-term effects are discussed, and the emission response is related to the forests soil N cycling. **Chapter 3** (Koehler *et al.*, 2009b) covers the response of soil CO₂ efflux to elevated N input, and relates it to tree phenological studies from the same sites. **Chapter 4** (manuscript in preparation) presents an inverse analysis of the ‘soil-CO₂ profile method’ to calculate soil CO₂ production. The validity of the model assumptions and its applicability are tested for our well-structured and wet lowland soil. The hypotheses of each sub-study are deduced and explained within the respective chapter.

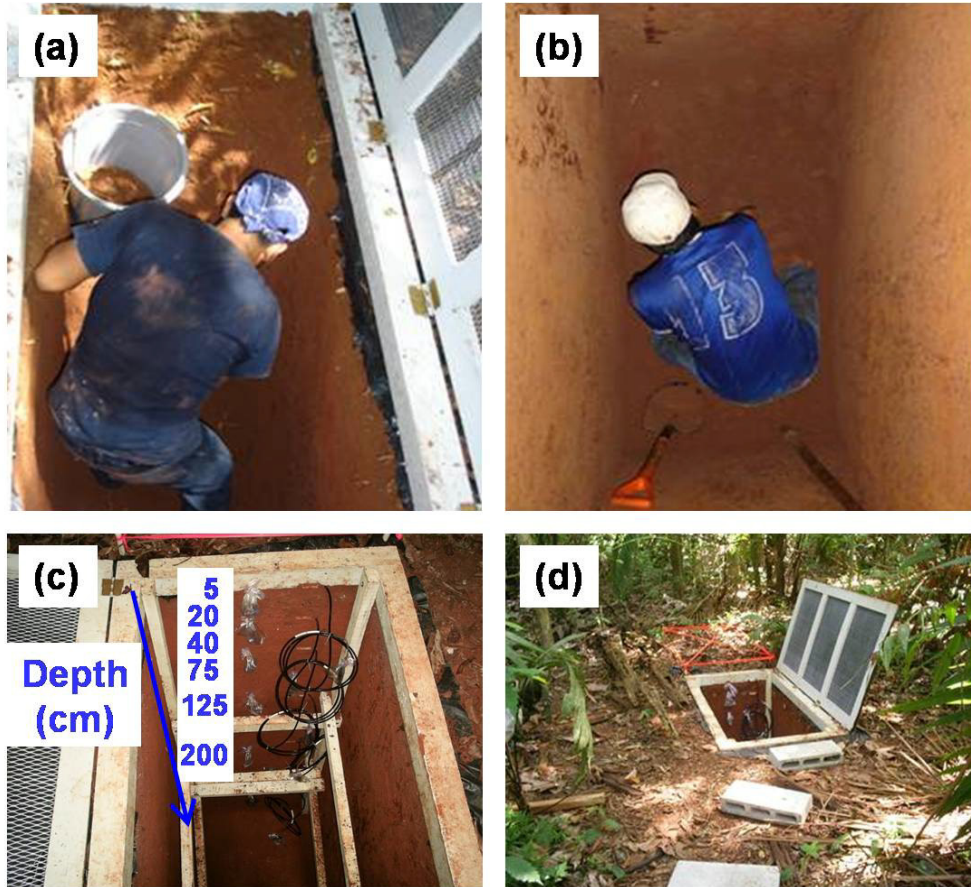


Figure 1-8. a) and b) Establishment of permanent 2.5 m deep soil pits in the lowland forest; c) pit equipped with stainless-steel tubes for air-sampling, soil moisture sensors and thermocouples at six depths down to 2 m; d) permanent soil pit with open lid. Photographs (modified) from Edzo Veldkamp.

Recently, five questions that should be priorities for future research were identified (Galloway et al., 2008). This study makes a contribution to three of them, namely:

- **How will tropical regions respond to rising N input?**
- **What is the ultimate fate of N_r ?**
- **What are the net climate effects of increasing N_r ?**

1.3 References

- Ayres RU, Schlesinger WH, Socolow RH (1994) Human impacts on the carbon and nitrogen cycles. In *Industrial ecology and global change* (eds Socolow RH, Andrews C, Berkhout F). Cambridge University Press, Cambridge, UK, 500 pp.
- Bouwman AF, Van der Hock KW, Olivier JGJ (1995) Uncertainties in the global source distribution of nitrous oxide. *Journal of Geophysical Research*, **100**, 2785-2800.
- Bruijnzeel LA, Veneklaas EJ (1998) Climatic conditions and tropical montane forest productivity: the fog has not lifted yet. *Ecology*, **79**, 3-9.
- Chambers JQ, Silver WL (2004) Some aspects of ecophysiological and biogeochemical responses of tropical forests to atmospheric change. *Philosophical Transactions of the Royal Society B*, **359**, 463-476.
- Cleveland CC, Townsend AR (2006) Nutrient additions to a tropical rain forest drive substantial soil carbon dioxide losses to the atmosphere. *Proceedings of the National Academy of Sciences*, **103**, 10316-10321.
- Dentener FJ, Drevet J, Lamarque JF, *et al.* (2006) Nitrogen and sulfur deposition on regional and global scales: a multi-model evaluation. *Global Biogeochemical Cycles*, **20**, doi:10.1029/2005GB002672.
- FAO (2000) Global forest resources assessment 2000. Food and Agriculture Organization of the United Nations, Rome, Italy, 479 pp.
- Foster P (2001) The potential negative impacts of global climate change on tropical montane cloud forests. *Earth-Science Reviews*, **55**, 73-106.
- Galloway JN, Aber JD, Erisman JW, Seizinger SP, Howarth RW, Cowling EB, Cosby BJ (2003) The Nitrogen Cascade. *BioScience*, **53**, 341-356.
- Galloway JN, Dentener FJ, Capone DG, *et al.* (2004) Nitrogen cycles: past, present and future. *Biogeochemistry*, **70**, 153-226.
- Galloway JN, Townsend AR, Erisman JW, *et al.* (2008) Transformation of the nitrogen cycle: recent trends, questions, and potential solutions. *Science*, **320**, 889-892.
- Gerold G (2008) Soil, climate and vegetation of tropical montane forests - a case study from the Yungas, Bolivia. In *The tropical mountain forest - patterns and processes in a biodiversity hotspot* Vol. 2 (eds Gradstein SR, Homeier J, Gansert D). Universitätsverlag Goettingen, Goettingen, Germany, pp. 137-162.
- Gruber N, Galloway JN (2008) An earth-system perspective of the global nitrogen cycle. *Nature*, **45**, doi:10.1038/nature06592.

-
- Hall SJ, Matson PA (1999) Nitrogen oxide emissions after nitrogen additions in tropical forests. *Nature*, **400**, 152-155.
- Harbusch M (2007) *The vertical distribution of fine roots in a lower montane rainforest in the Republic of Panama*. University of Goettingen, Goettingen, Germany, 60 pp.
- IPCC (2007) Climate Change 2007: The Physical Science Basis. Contribution of Working Group I to the Fourth Assessment Report of the Intergovernmental Panel on Climate Change (eds Solomon S, Qin D, Manning M, *et al.*). Cambridge University Press, Cambridge, UK and New York, USA, 996 pp.
- Koehler B, Corre MD, Veldkamp E, Wullaert H, Wright SJ (2009a) Immediate and long-term nitrogen oxide emissions from tropical forest soils exposed to elevated nitrogen input. *Global Change Biology*, **15**, 2049-2066.
- Koehler B, Corre MD, Veldkamp E, Sueta JP (2009b) Chronic nitrogen addition causes a reduction in soil carbon dioxide efflux during the high stem-growth period in a tropical montane forest but no response from a tropical lowland forest on a decadal time scale. *Biogeosciences*, **6**, 2973-2983.
- Leuschner C, Moser G (2008) Carbon allocation and productivity in tropical mountain forests. In *The tropical mountain forest - patterns and processes in a biodiversity hotspot* Vol. 2 (eds Gradstein SR, Homeier J, Gansert D). Universitätsverlag Goettingen, Goettingen, Germany, pp. 109-128.
- Malhi Y (2005) The carbon balance of the tropical forest biome. In *The carbon balance of forest biomes* (eds Griffiths H, Jarvis PG), pp. 356. Taylor & Francis Group, Oxon, UK and New York, USA.
- Matson PA, McDowell W, Townsend AR, Vitousek PM (1999) The globalization of N deposition: ecosystem consequences in tropical environments. *Biogeochemistry*, **46**, 67-83.
- McGroddy ME, Silver WL (2007) Nutrient-cycling and climate change in tropical forests. In *Tropical Rainforest Responses to Climatic Change* (eds Bush MB, Flenley JR). Praxis Publishing Ltd, Chichester, UK, pp. 295-316.
- Mo J, Zhang W, Zhu W, Gundersen P, Fang Y, Li D, Wang H (2007) Nitrogen addition reduces soil respiration in a mature tropical forest in southern China. *Global Change Biology*, **14**, 1-10.
- Montagnini F, Jordan CF (2005) *Tropical Forest Ecology - The basis for conservation and management*. Springer, Heidelberg, Germany, 295 pp.

-
- Richter M (2008) Tropical mountain forests - distribution and general features In *The tropical mountain forest - patterns and processes in a biodiversity hotspot* Vol. 2 (eds Gradstein SR, Homeier J, Gansert D). Universitätsverlag Goettingen, Goettingen, Germany, pp. 7-24.
- Rustad LE, Huntington TG, Boone RD (2000) Controls on soil respiration: Implications for climate change. *Biogeochemistry*, **48**, 1-6.
- Sanchez PA, Swaminathan MS (2005) Hunger in Africa: the link between unhealthy people and unhealthy soils. *Lancet*, **365**, 442-444.
- Schuur EAG (2001) The effect of water on decomposition dynamics in mesic to wet Hawaiian montane forests. *Ecosystems*, **4**, 259-273.
- Schuur EAG, Chadwick OA, Matson PA (2001) Carbon cycling and soil carbon storage in mesic to wet Hawaiian montane forests. *Ecology*, **82**, 3182-3196.
- Smith BE (2002) Nitrogenase reveals its inner secrets. *Science*, **297**, 1654-1655.
- Smithsonian Tropical Research Institute (2009). Scientific Online Databases.
<http://biogeodb.stri.si.edu/bioinformatics/en/>
- Swift MJ, Heal OW, Anderson JM (1979) *Decomposition in terrestrial ecosystems*. Blackwell Scientific Publications, Oxford, UK, 372 pp.
- Tanner EVJ, Vitousek PM, Cuevas E (1998) Experimental investigation of nutrient limitation of forest growth on wet tropical mountains. *Ecology*, **79**, 10-22.
- United Nations (2004) World Urbanization Prospects: The 2003 Revision. UN Department of Economic and Social Affairs.
- Vitousek PM, Aber JD, Howarth RW, *et al.* (1997) Human alteration of the global nitrogen cycle - Sources and consequences. *Ecological Applications*, **7**, 737-750.
- Wright SJ (2005) Tropical forests in a changing environment. *Trends in Ecology and Evolution*, **20**, 553-560.
- Yienger JJ, Levy H (1995) Empirical model of global soil-biogenic NO_x emissions. *Journal of Geophysical Research*, **100**, 11447-11464.

**Immediate and long-term nitrogen oxide emissions from
tropical forest soils exposed to elevated nitrogen input**

**BIRGIT KOEHLER, MARIFE D. CORRE, EDZO VELDKAMP,
HANS WULLAERT and S. JOSEPH WRIGHT**

2.1 Abstract

Tropical nitrogen (N) deposition is projected to increase substantially within the coming decades. Increases in soil emissions of the climate-relevant trace gases NO and N₂O are expected, but few studies address this possibility. We used N addition experiments to achieve N-enriched conditions in contrasting montane and lowland forests and assessed changes in the timing and magnitude of soil N-oxide emissions. We evaluated transitory effects, which occurred immediately after N addition, and long-term effects measured at least six weeks after N addition. In the montane forest where stem growth was N limited, the first-time N additions caused rapid increases in soil N-oxide emissions. During the first two years of N addition, annual N-oxide emissions were five times (transitory effect) and two times (long-term effect) larger than controls. This contradicts the current assumption that N-limited tropical montane forests will respond to N additions with only small and delayed increases in soil N-oxide emissions. We attribute this fast and large response of soil N-oxide emissions to the presence of an organic layer (a characteristic feature of this forest type) in which nitrification increased substantially following N addition. In the lowland forest where stem growth was neither N nor P limited, the first-time N additions caused only gradual and minimal increases in soil N-oxide emissions. These first N additions were completed at the beginning of the wet season, and low soil water content may have limited nitrification. In contrast, the 9 and 10 year N-addition plots displayed instantaneous and large soil N-oxide emissions. Annual N-oxide emissions under chronic N addition were seven times (transitory effect) and four times (long-term effect) larger than controls. Seasonal changes in soil water content also caused seasonal changes in soil N-oxide emissions from the 9 and 10 year N-addition plots. This suggests that climate change scenarios, where rainfall quantity and seasonality change, will alter the relative importance of soil NO and N₂O emissions from tropical forests exposed to elevated N deposition.

2.2 Introduction

Humans have more than doubled the rate of nitrogen (N) entering the land-based N cycle worldwide, thereby enhancing the mobility of 'reactive' nitrogen (N_r) within and between ecosystems (Vitousek *et al.*, 1997). The three main causes of anthropogenic increases of N_r are N fertilizers used in agriculture, fossil fuel combustion and cultivation of N-fixing plants (Galloway *et al.*, 2003; 2008). Until recently, enhanced inputs of N were concentrated in economically developed regions of the temperate zone, but for the coming decades deposition

of N_r is projected to increase substantially in economically emerging tropical regions such as Southeast Asia and Latin America due to demands for food and energy by growing populations with increasing per capita use of N (Galloway *et al.*, 2003; 2004; 2008).

The increase in tropical N deposition is projected to stimulate soil nitrous oxide (N_2O) and nitric oxide (NO) emissions, increase nitrate (NO_3^-) leaching with accompanying base cation losses, and enhance soil acidification (Matson *et al.*, 1999). On a global basis, atmospheric transport and subsequent deposition has become the dominant N_r distribution process and it is critical to better understand gaseous N emission rates (Galloway *et al.*, 2008). Tropical rain forests are already the largest natural source of terrestrial N_2O emissions (Bouwman *et al.*, 1995) and the third most important biome for NO emissions (Yienger & Levy, 1995). N_2O is a long-lived greenhouse gas with an atmospheric lifetime of 114 years and a 100-year global warming potential of 298 relative to CO_2 . N_2O also contributes to the depletion of stratospheric ozone. The atmospheric concentration of N_2O has increased approximately linearly by about $0.26\% \text{ yr}^{-1}$ over the past few decades. The dominant impact of NO emissions on climate is through the photochemical formation of tropospheric ozone, the third largest contributor to positive radiative forcing (IPCC, 2007). NO further generates indirect negative radiative forcing by shortening the atmospheric lifetime of methane and regulates the production of nitric acid and organic nitrates, both acid rain precursors (Crutzen, 1979).

Commonly, tropical forests growing on heavily weathered soils exhibit a conservative phosphorus (P) cycle, while tropical forests growing on younger soils exhibit a conservative N cycle, much like undisturbed temperate forest ecosystems (Walker & Syers, 1976; Vitousek, 1984). This relationship has been shown along a soil chronosequence in Hawaii where the supply of available N is low in the younger volcanic soils and increases with soil age. This contrasts with rock-derived P, which is relatively abundant in young soils but becomes increasingly bound in unavailable forms in older heavily weathered soils (Hedin *et al.*, 2003). ^{15}N signatures and N:P ratios in leaves are consistent with the hypothesis that P conservation increases and N conservation decreases with soil weathering stage on a global scale (Martinelli *et al.*, 1999; McGroddy *et al.*, 2004). A conservative N cycle is implied when the biological N demand (primarily vegetation growth) exceeds N supply (primarily N fixation, deposition and mineralization). Forest ecosystems with a conservative N cycle are characterized by small rates of soil N cycling and N losses (N leaching and gaseous N emissions; Davidson *et al.*, 2000). In contrast, the N cycle of forest ecosystems where N

supply exceeds biological N demand has been termed ‘open’ or ‘leaky’ because N losses are large relative to the amount of soil N cycling.

N-oxides are produced in soils largely by nitrification and denitrification. A large fraction of the observed variation in soil N-oxide emissions can be explained by the conceptual ‘hole-in-the-pipe’ (HIP) model, which is based on their biogeochemical controls (Firestone & Davidson, 1989; Davidson *et al.*, 2000). The HIP model proposes that the total N-oxide gas flux (NO+N₂O) is proportional to the rates of nitrification and denitrification while the relative proportion of each gas emitted from the soil is controlled by the soil aeration status. Thus, the HIP model predicts that forest ecosystems with a conservative N cycle will have lower soil N-oxide emissions while forest ecosystems with a leaky N cycle will have larger soil N-oxide emissions.

One way to evaluate potential future effects of N deposition on tropical forests is to create N-enriched conditions through N addition. Just six N-addition experiments have evaluated N-oxide emissions from tropical forest soils. These include four one-time pulse N additions and two chronic N additions. The one-time pulse N additions caused transitory (days to two weeks) increases of soil N-oxide emissions (Kaplan & Wofsy, 1988; Keller *et al.*, 1988; Bakwin *et al.*, 1990; Steudler *et al.*, 2002) as well as intermediate-term (sustained elevated emissions six months after N addition) increases of soil NO emissions (Steudler *et al.*, 2002). The two chronic N additions took place in Puerto Rican and Hawaiian montane forests dominated by single tree species. In Puerto Rico, chronic N addition doubled soil N₂O emissions and quadrupled soil NO emissions compared to the largest mean emissions from a fertile mid-successional control site (Erickson *et al.*, 2001). In an N-limited Hawaiian forest with a conservative soil N cycle, N-oxide emissions did not increase significantly after first-time N addition but did increase significantly after chronic N addition. In contrast in a P-limited Hawaiian forest with a leaky soil N cycle, N-oxide emissions increased rapidly and by much larger amounts than in the N-limited forest after both first-time and chronic N additions. Thus, the timing and magnitude of fertilizer-induced soil N-oxide emissions were influenced by the N status (i.e., N supply and demand) of the Hawaiian forest ecosystem (Hall & Matson 1999, 2003). Chronic N additions are lacking for species-rich tropical forests, and these missing experiments are needed to provide broader insight into the consequences of future N deposition on soil N-oxide emissions from the tropical mainland.

Apart from soil age/weathering stage, the N status of old-growth tropical forests is also influenced by altitude (lowland versus montane) and presence of an organic layer. Lowland

forests generally have larger N concentrations in leaf and litterfall (Tanner *et al.*, 1998), NO₃-leaching losses (Hedin *et al.*, 2003; Klinge *et al.*, 2004; Dechert *et al.*, 2005; Schwendenmann & Veldkamp, 2005), soil N-oxide emissions (Keller & Reiners, 1994; Davidson *et al.*, 2000; Purbopuspito *et al.*, 2006), and $\delta^{15}\text{N}$ signatures in leaves and soils (Martinelli *et al.*, 1999) than montane forests. This suggests that lowland forests are characterized by more leaky soil N cycling. On the other hand, thick and densely rooted organic layers are common in tropical montane forests (Edwards & Grubb, 1977) and may be important nutrient sources (Wilcke *et al.*, 2002; Röderstein *et al.*, 2005). N concentrations and cycling rates on a mass basis are larger in organic layers than in mineral soils of tropical forests (Livingston *et al.*, 1988; Vitousek & Matson, 1988; Wilcke *et al.*, 2002), but due to the small mass of the organic layer (or low bulk density) its large N-cycling rates may be unimportant on an areal basis (Livingston *et al.*, 1988).

Our present study reports the impact of first-time and chronic N additions on soil N-oxide emissions from two species-rich, old-growth tropical forests in the Republic of Panama: a lowland forest on a deeply-weathered soil and a montane forest on a less-developed volcanic soil with an organic layer. We hypothesized the following:

- 1) The lowland forest, where stem diameter growth and annual fine litterfall mass were not N limited (S.J. Wright, unpublished results; Kaspari *et al.*, 2008), should exhibit relatively large soil N-cycling rates and thus a rather leaky N cycle. This forest will react to first-time N addition with immediate increases in soil N-oxide emissions, and chronic N addition will lead to sustained larger N-oxide emissions.
- 2) The montane forest, with N-limited stem diameter growth and fine litterfall mass (Adamek *et al.*, 2009), should exhibit relatively small soil N-cycling rates and thus a conservative N cycle. However, a substantial organic layer covers the mineral soil, and we expect that first-time N addition will immediately increase soil N-cycling rates in this organic layer and consequently cause immediate increases in N-oxide emissions. Chronic N addition will lead to sustained higher N-oxide emissions.

We tested these hypotheses by intensive measurements of soil N-oxide emissions supported by measurements of soil factors known to influence gaseous N losses including temperature, moisture, extractable mineral N, and N cycling rates. This is the first study to evaluate (1) transitory and long-term soil N-oxide emissions in response to chronic N input in species-rich tropical forests and (2) the effects of elevated N input on the organic layer of a species-rich tropical montane forest.

2.3 Materials and methods

2.3.1 Approach

N-addition experiments differ from atmospheric N deposition in mode and amount in which N is added to the ecosystem. N deposition enters the ecosystem at the canopy level and through frequent inputs at relatively low concentrations, whereas fertilizer is typically applied to the soil and in one or a few large doses of high concentration. Furthermore, atmospheric N deposition normally enters an ecosystem as a combination of NH_4^+ , NO_3^- and organic N, whereas we applied fertilizer N in the form of urea. We chose urea for a practical reason: NH_4NO_3 is not sold in Panama due to security concerns.

We did not intend to simulate the mode of atmospheric deposition, but rather we intended to create an N-enriched condition, which is ultimately the result of chronic atmospheric N deposition. One ‘artifact’ of N addition is the occurrence of pronounced ‘peaks’ in soil mineral N concentrations and N-oxide emissions, which is typically a transitory effect occurring within a month following N addition (Keller *et al.*, 1988; Veldkamp *et al.*, 1998; Steudler *et al.*, 2002). We therefore differentiate the impact of N additions on soil N-oxide emissions between ‘transitory’ and ‘long-term’ effects measured within 42 days and at least six weeks following N addition, respectively. Long-term effects should be less sensitive to the type of N fertilizer because all urea-N will be hydrolyzed and processed in the soil N cycle within six weeks of N addition.

2.3.2 Study Area

The lowland study site (between 25-61 m elevation) consists of an old-growth (>300 years) semi-deciduous tropical forest (Leigh *et al.*, 1996) and is located on Gigante Peninsula (9°06'N, 79°50'W) which is part of the Barro Colorado Nature Monument, Republic of Panama. On nearby Barro Colorado Island, annual rainfall (1995-2007) averages 2650 ± 146 mm with a dry season from January to mid-May during which 297 ± 40 mm of rainfall is recorded. Ambient N deposition from rainfall was $9 \text{ kg N ha}^{-1} \text{ yr}^{-1}$, measured bi-weekly in 2006-2007 at the shore of Gigante Peninsula near the study site. The mean annual air temperature is 27.4 ± 0.1 °C. Litter mass on nearby Barro Colorado Island has a rapid turnover time of 210 days (Yavitt *et al.*, 2004). Stem diameter growth (S.J. Wright, unpublished results) and annual fine litterfall mass (Kaspari *et al.*, 2008) were not effected after five and six years of N addition, respectively.

The montane study site (between 1200-1300 m elevation) consists of an old-growth lower montane rainforest (Grubb, 1977) and is located in the Fortuna Forest Reserve in the Cordillera Central (8°45'N, 82°15'W), Chiriquí province, Republic of Panama. Mean annual rainfall is 5532 ± 322 mm (1997-2007), and rainfall distribution exhibits only a weak seasonality (11-yr average of 244–288 mm month⁻¹ from February to April and 403–683 mm month⁻¹ from March to January). Ambient N deposition from rainfall was 5 kg N ha⁻¹ yr⁻¹, measured bi-weekly in 2006-2007 at a forest clearing near the study site. The average monthly air temperature is 19 °C from December to March and 21 °C for all other months (annual mean (1999-2007) of 20.1 ± 0.1 °C). Stem diameter growth and fine litterfall mass increased compared to the control during the first two years of N addition (Adamek *et al.*, 2009). See Tables 2-1 and 2-2 for information on soil characteristics / classification and forest structure, respectively, of both sites.

Table 2-1. Soil classification and characteristics of the forest sites determined in January 2006, after eight years of N addition in the lowland site and before first N addition in the montane site.

Characteristics / Depth	Lowland *	Montane †	
Parent material	Basalt	Volcanic ash deposits	
Texture	Heavy Clay	Sandy loam	
Soil type (FAO)	Endogleyic Cambisol in the lower part to Acric Nitisol in the upper part of the landscape	Aluandic Andosols	
Soil type (USDA)	Dystrudepts	Hapludands	
Organic layer (median thickness, cm)	None	8 (25% quantile of 5 cm and 75% quantile of 12 cm, $n = 64$)	
	Control	8-yr N addition	
Organic layer		All plots	
Bulk density (g cm ⁻³)	-	-	0.07 ± 0.01
pH (1:10 H ₂ O)	-	-	4.1 ± 0.1
Total carbon (C) (mg g ⁻¹)	-	-	443.0 ± 18.7
Total nitrogen (N) (mg g ⁻¹)	-	-	22.4 ± 1.1
C/N ratio	-	-	19.9 ± 0.4
δ ¹⁵ N (‰)	-	-	0.92 ± 0.15

Total phosphorus (P) (mg kg ⁻¹)	-	-	0.72 ± 0.07
Total base cations	-	-	5.8 ± 0.6
Mineral topsoil (0-0.05 m)			
Bulk density (g cm ⁻³)	0.62 ± 0.02	0.62 ± 0.02	0.47 ± 0.02
pH (1:1 H ₂ O)	5.3 ± 0.2 a	4.5 ± 0.1 b	4.1 ± 0.1
Total C (mg g ⁻¹)	51.0 ± 5.3	47.2 ± 3.8	94.5 ± 11.4
Total N (mg g ⁻¹)	3.9 ± 0.4	3.6 ± 0.2	6.2 ± 1.0
C/N ratio	13.3 ± 0.5	13.3 ± 0.4	15.7 ± 0.6
δ ¹⁵ N (‰)	4.86 ± 0.52	5.56 ± 0.17	3.81 ± 0.42
Total P (mg g ⁻¹)	0.55 ± 0.08	0.50 ± 0.02	0.56 ± 0.05
Effective cation exchange capacity (ECEC) (mmol(+) kg ⁻¹)	205 ± 44	116 ± 8	132 ± 25
Base saturation (%)	91.8 ± 3.6 a	61.8 ± 8.6 b	20.9 ± 3.6
Mineral soil (0.05-0.5 m)			
pH (1:1 H ₂ O)	5.1 ± 0.1 a	4.9 ± 0.1 b	4.5 ± 0.1
Total C (mg g ⁻¹)	15.2 ± 1.1	14.6 ± 0.9	30.7 ± 5.8
Total N (mg g ⁻¹)	1.4 ± 0.1	1.3 ± 0.1	1.8 ± 0.3
C/N ratio	10.2 ± 0.7	11.0 ± 0.2	16.5 ± 0.8
δ ¹⁵ N (‰)	7.33 ± 0.79	8.30 ± 0.38	5.95 ± 0.23
Total P (mg g ⁻¹)	0.40 ± 0.07	0.36 ± 0.02	0.29 ± 0.04
ECEC (mmol(+) kg ⁻¹)	149 ± 48	110 ± 22	71 ± 19
Base saturation (%)	55.7 ± 7.0 a	41.4 ± 5.3 b	11.2 ± 4.6

* Means (± SE, $n = 4$) with different letter indicate differences between treatments (independent t -test at $P \leq 0.05$).

† Means (± SE, $n = 8$) did not differ between plots which were later randomly assigned to control and N addition treatment.

2.3.3 Experimental design

In the lowland, our study was conducted in the only ongoing large-scale chronic nutrient addition experiment in old-growth species rich tropical forest. The site covers a gentle slope from the northeast corner to the southwest and lacks pronounced ridges, slopes, valleys and bottomlands. The experiment includes N-addition and control plots, among other treatments, laid out in four replicates across a 26.6-ha area in a stratified random design. Each treatment

plot is 40x40 m and the distance between adjacent plots is at least 40 m. N addition started in June 1998. Just outside the long-term experimental plots, we set up four 20x20 m plots (at least 40 m apart) for first-time N addition in May 2006. In the montane forest, the experiment was set up in a paired-plots design with four replicates. Each plot is 40x40 m, and plots are separated by at least 40 m. Plots lack streams, swampy areas, gaps or clearings, and slopes >15°. Plot size is corrected for inclination (Condit, 1998). Control and N-addition treatments were randomly assigned to each pair of plots. N addition started in February 2006.

The N-addition plots received 125 kg urea-N ha⁻¹ yr⁻¹ which was split in four equal applications. In the lowland site, fertilizer was applied during the wet season with six to eight weeks between applications (May 15-30, July 1-15, September 1-15, October 15-30). In the montane site, the four N additions were spread during the year with at least seven weeks between applications. Urea was applied manually, walking back and forth across 10x10 m subplots and changing directions (east-to-west and north-to-south) in subsequent N additions. Gas flux measurement chambers were covered during plot N addition and received the exact amount of fertilizer for their area afterwards.

We measured soil N-oxide fluxes, air and soil temperatures (at 0.05 m depth), soil moisture, and soil extractable mineral N. Measurements were conducted every six weeks on all plots (specifically before N additions), and intensively (two to five times) following fertilizations on the N-addition plots. Two pre-treatment measurements in the montane site and one pre-treatment measurement in the first-time N-addition lowland site indicated that initial N-oxide fluxes did not differ between control and N-addition plots prior to manipulation. We do not have pre-treatment measurements of N-oxide fluxes from the 9 and 10-yr N-addition lowland plots. All measurements took place within 10 m of the center of each plot so that all sampling points were surrounded (buffered) by at least 10 m of forest receiving the same treatment (in case of the first-time N-addition lowland plots the buffer zone was 5 m).

2.3.4 Soil characteristics

Soil characteristics were determined in January 2006 before first treatment in the montane site. Organic layer samples were air-dried and ground before analyses. Mineral soil samples (from 0-0.05, 0.05-0.10, 0.10-0.25 and 0.25-0.50 m depth with one profile per plot) were air-dried, sieved (2 mm), and ground for analysis of total organic C, N, $\delta^{15}\text{N}$ and total P. Total C and N were measured by a CNS Elemental Analyzer (Elementar Vario EL, Hanau, Germany),

$\delta^{15}\text{N}$ by isotope ratio mass spectrometry (Finigan MAT, Bremen, Germany), and total P and total base cations (only for the organic layer samples) by pressure digestion in concentrated HNO_3 (König & Fortmann, 1996) followed by analysis of the digests using Inductively Coupled Plasma-Atomic Emission Spectrometer (ICP-AES; Spectro Analytical Instruments, Kleve, Germany). Effective cation exchange capacity (ECEC) of the mineral soil was determined from sieved samples by percolating with unbuffered 1 M NH_4Cl (König & Fortmann, 1996) and measuring cations in percolates using ICP-AES. Base saturation was calculated as percentage base cations of the ECEC. Soil pH was measured from a saturated paste mixture (1:1 and 1:10 ratio of soil to H_2O for mineral soil and organic layer, respectively). Soil bulk density was determined by the soil core method (Blake & Hartge, 1986).

Table 2-2. Forest characteristics of the lowland and montane sites.

Site	Forest structure (based on trees ≥ 0.1 m in diameter at breast height)				
	Tree height (m)	Mean basal area ($\text{m}^2 \text{ha}^{-1}$)	Tree density (trees ha^{-1})	Most abundant tree species	Trees belonging to the family <i>Fabaceae</i> (%)
Lowland	30-35	20.3	384	<i>Oenocarpus mapora</i> , <i>Dialium guianense</i> , <i>Heisteria concinna</i> , <i>Tetragastris panamensis</i> ; together contributing 28%	15
Montane	~20 (some emergent trees up to 40 m, mainly <i>O. mexicana</i>)	46.1	1039	<i>Eschweilera panamensis</i> , <i>Vochysia guatemalensis</i> , <i>Cassipourea elliptica</i> ; together contributing 38%*	4 [†]

* The palm *Colpotherinax aphanopetala* and vascular epiphytes (especially the genus *Anthurium* and *Monstera*) are also abundant.

[†] All belonging to the genus *Inga*, which is the only *Fabaceae* known from the site (J. Dalling, personal communication).

2.3.5 N-oxide flux measurements

Four permanent chamber bases (area 0.04 m², height 0.25 m, ~0.02 m inserted into the soil) were installed on each plot in a stratified random design along two perpendicular 20-m long transects that crossed in the plot center. Soil N₂O fluxes were measured using vented static chambers. Four gas samples (100 mL each) were removed at 2, 12, 22 and 32 minutes after chamber closure and stored in pre-evacuated glass containers with a teflon-coated stopcock. Gas samples were analyzed using a gas chromatograph (Shimadzu GC-14B, Columbia, USA) equipped with an electron capture detector and an autosampler (Loftfield *et al.*, 1997). Gas concentrations were determined by comparison of integrated peak areas of samples and three to four standard gases (317, 503, 1000 and 2992 ppb N₂O; Deuste Steininger GmbH, Mühlhausen, Germany). Soil NO fluxes were measured on-site using open dynamic chambers which were placed for five to seven minutes on the same chamber bases used for N₂O sampling. Flow rate through the chamber was between 450-750 mL min⁻¹. Dilution of the NO concentration in the chamber by outside air flow through the chamber is negligible during the initial linear part of the concentration increase (Bakwin *et al.*, 1990). NO was analyzed with a Scintrex LMA-3 chemiluminescence detector (Scintrex Unisearch, Ontario, Canada) after oxidation to NO₂ by a CrO₃ catalyst. The reaction vessel in the detector has a fabric wick saturated with luminol II solution, which contains additives to enhance reaction and reduce interference from other gases including ozone. Because the catalyst is sensitive to relative humidity, a known flux of ambient air dried by silica gel was mixed to the chamber air to reach a humidity of ~50%. In order to minimize potential changes in catalyst efficiency caused by variations of air humidity between calibration and measurements (Williams & Davidson, 1993) we calibrated the detector in the field before and after the four chamber flux measurements per plot using a standard gas (3400 ppb NO; Deuste Steininger GmbH, Germany).

Gas fluxes were calculated from the linear increase of gas concentration in the chamber versus time, and were adjusted for air temperature and atmospheric pressure measured at the time of sampling:

$$\Phi = \frac{V}{A} \left(\frac{P}{R \cdot T} \right) Mf \frac{\partial C}{\partial t} \quad (2-1)$$

where Φ is the flux (g N m⁻² h⁻¹), V the chamber volume (L), A the chamber area (m²), P the atmospheric pressure (Pa), R the ideal gas constant (8.315 Pa m³ mol⁻¹ K⁻¹), T the temperature

(K), M the molar mass of NO-N or N₂O-N (g mol⁻¹), $\delta C/\delta t$ the rate of gas concentration change within the chamber (ppm h⁻¹ = $\mu\text{L L}^{-1} \text{h}^{-1}$) and f a conversion factor ($10^{-9} \text{ m}^3 \mu\text{L}^{-1}$). Positive gas fluxes indicate emission from the soil; negative fluxes indicate consumption of the gas by the soil. Zero fluxes were included. NO fluxes from the open dynamic chambers were calculated using three minutes of continuous data with values logged every five seconds. In contrast, N₂O fluxes from the vented static chambers were calculated using four points in time. N₂O fluxes might be significantly underestimated if a linear model was uncritical applied, ignoring potential chamber feedbacks (especially decreasing diffusion gradient over time; Livingston *et al.*, 2006). If N₂O concentration increased asymptotically with time, both a linear and a quadratic regression model were fitted (Wagner *et al.*, 1997) and the more adequate model was chosen using the Akaike Information Criterion (AIC). The quadratic model was used in about 25% of the N₂O flux calculations. The annual N-oxide losses were approximated by applying the trapezoid rule on time intervals between measured flux rates, assuming constant flux rates per day.

2.3.6 Soil mineral N, soil moisture, and net rates of soil N cycling

Parallel to gas sampling, four samples of 0–0.05 m mineral soil (for the montane site, organic layer and mineral soil were sampled separately) were collected within the central 10x10 m of each plot. While in the field, samples were pooled for each plot, leaves and roots were manually removed, and a subsample (50-60 g fresh weight) was added to a prepared extraction bottle containing 150 mL of 0.5 mol L⁻¹ K₂SO₄ solution. The rest of the sample was stored in plastic bags for gravimetric moisture determination in the laboratory. Subsamples (40-100 g fresh weight) were dried for 24 h at 105 °C. Moisture content is expressed as percentage of water-filled pore space, assuming a particle density of 2.65 g cm⁻³ for mineral soil (Linn & Doran, 1984) and of 1.4 g cm⁻³ for organic layer (Breuer *et al.*, 2002). The soil-K₂SO₄ bottles were transported to the laboratory and stored in a refrigerator (4 °C) until extractions were performed. Extraction was done by shaking the soil-K₂SO₄ bottles for 1 hour and filtering them through K₂SO₄-prewashed filter papers (4 μm nominal pore size). Extracts were frozen immediately and remained frozen during transport by air to Germany, where analysis was conducted. NH₄⁺ and NO₃⁻ contents of the extracts were analyzed using continuous flow injection colorimetry (Cenco/Skalar Instruments, Breda, Netherlands), in which NH₄⁺ was determined using the Berthelot reaction method (Skalar Method 155-000) and NO₃⁻ was measured using the copper-cadmium reduction method (NH₄Cl buffer but

without ethylenediamine tetraacetic acid; Skalar Method 461-000). In the first six months of the study, mineral N extraction of the soil samples was conducted within three days for the lowland site and eight days for the montane site. In June 2007, we brought equipment to the field stations so that soil-K₂SO₄ extraction proceeded within 12 hours after field sampling. We compared the NO₃⁻ concentrations of the soil samples before and after June 2007, and these were not statistically different. Also, statistical analyses of treatment effects and site differences were conducted separately on mineral N concentrations before and after June 2007, to verify that observed differences were not influenced by the change in methodology.

Net rates of soil N cycling were measured in the first week of September 2006. In the lowland site, this was in the middle of the wet season and three weeks after the third N application of the year for the N-addition plots. In the montane site, this was 1.5 months after the third N application of the first-year N addition plots. Two intact soil cores were taken from the mineral soil (0-0.05 m depth) and, for the montane site, also from the organic layer within the central 10x10 m of each plot. One soil core was extracted immediately in the field with 0.5 mol L⁻¹ K₂SO₄ (as described above) to determine initial NH₄⁺ and NO₃⁻ levels (T₀). The other intact soil core was put in a plastic bag, inserted back into the soil for seven days of incubation, and afterwards extracted in the field with K₂SO₄ (T₁). Soil-K₂SO₄ extractions proceeded within 12 hours after field sampling. Net N mineralization and nitrification rates were calculated as the difference between T₁- and T₀-NH₄⁺ and NO₃⁻ concentrations, respectively.

2.3.7 Statistical analyses

Statistical analysis was carried out on the plot mean NO and N₂O fluxes (average of four chambers). If data sets were rightly skewed, we applied either a square-root or a logarithmic transformation prior to analysis (after adding a constant value if the data set included negative values). For analysis of time-series data (i.e. repeated measurements of the response variables N-oxide fluxes, soil mineral N, soil temperature and water-filled pore space) we used linear mixed effects models, where explanatory variables are included as either fixed (influencing the mean of the response variable) or random (influencing its variance) effect (Crawley, 2002). Linear mixed effects models are advantageous over repeated-measures analysis of variance because these can properly account for correlation between repeated measurements, allow to specify the within-group variance of a stratification variable, and are unaffected by randomly missing data (Gueorguieva & Krystal, 2004; Pinheiro & Bates, 2004). Our basic

model included treatment (if testing for an effect of N addition) or site (if testing for differences between lowland and montane forest) as fixed effect and the spatial replication (experimental plots) nested in time (temporal sampling scheme) as random effects. We extended the model to include (1) a variance function which allows different variances of the response variable per level of the fixed effect, and/or (2) a first-order temporal autoregressive process, which assumes that correlation between measurements decreases with increasing time distance, if this improved the relative goodness of the model fit based on the Akaike Information Criterion. We then checked the model using diagnostic residual plots and assessed the significance of the fixed effect based on analysis of variance (Crawley, 2002). For linear regression, we tested whether the slope is different from zero using analysis of variance in regression. For soil characteristics and net N-cycling rates, treatment effects and differences between sites were assessed using independent *t*-tests. Mean values in the text are given with ± 1 standard error. Missing values were excluded from analyses and effects were accepted as statistically significant if *P* value ≤ 0.05 . All analyses were conducted using R 2.6.0 (R Development Core Team, 2008).

2.4 Results

2.4.1 Soil conditions, N-cycling rates and N-oxide fluxes from control forests

Water-filled pore space (WFPS) followed a clear seasonal pattern in the lowland forest but not in the montane forest, and was much higher in the mineral soil than in the organic layer of the montane forest (Fig. 2-1a and b). Soil temperature at 0.05 m depth varied seasonally by 1.6 °C (annual mean of 25.4 °C) in the lowland forest and by 3.9 °C (annual mean of 18.1 °C) in the montane forest (Fig. 2-1c and d). Linear regressions between N-oxide fluxes and WFPS or soil temperature were not significant. WFPS and soil temperature did not differ between control and N-addition plots.

Ammonium (NH_4^+) was the dominant form of soil mineral N at both sites. In the lowland forest, NH_4^+ concentrations increased throughout the wet season until the dry season began and then decreased towards the end of the dry season, whereas nitrate (NO_3^-) concentrations were always small in the wet season and increased in the dry season (Fig. 2-2 a-d). Soil mineral N did not show a seasonal pattern in the montane forest (Fig. 2-3). NH_4^+ concentrations were larger in the organic layer of the montane forest than in the mineral soil of either forest (both *P* < 0.010) but did not differ between forests in the mineral soil. NO_3^-

concentrations were statistically indistinguishable between the organic layer of the montane forest and the mineral soil of both forests, as well as between the mineral soils of both forests.

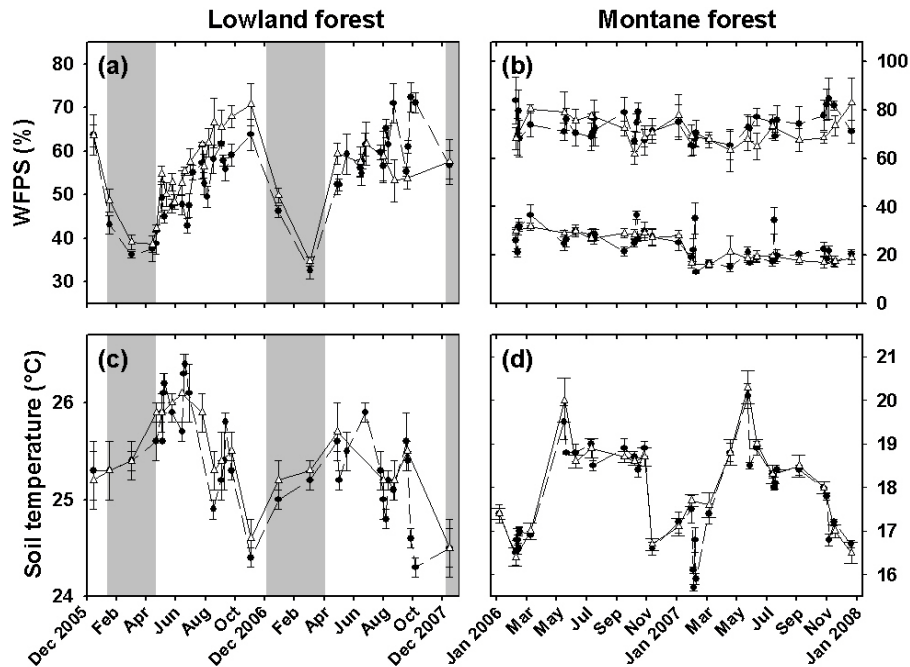


Figure 2-1. Mean (\pm SE, $n = 4$) water-filled pore space (WFPS) and soil temperature at 0.05 m depth in control (Δ) and N-addition (\bullet) lowland (a and c) and montane (b and d) forests. For WFPS in the montane forest, the upper and lower values are for 0-0.05 m mineral soil and the organic layer, respectively. Grey shading marks the dry season in the lowland forest.

Net N mineralization, which is often used as an index of plant available mineral N, was larger in the organic layer of the montane forest than in the mineral soil of either forest (both $P \leq 0.001$), and did not differ between forests in the mineral soil. Net nitrification was larger in the mineral soil of the lowland forest than in the organic layer ($P = 0.001$) and mineral soil of the montane forest ($P = 0.050$, Table 2-3).

Across the 2-yr measurement period, the lowland forest soil had larger mean NO ($P = 0.024$), N₂O ($P = 0.032$) and total N-oxide emissions ($P = 0.043$) than the montane forest soil (Tables 2-4 and 2-5). Soil N-oxide emissions were dominated by N₂O at both sites and the ratio of annual N₂O/NO fluxes was 5.6 in 2006 and 3.2 in 2007 in the lowland forest and 8.2 in 2006 and 8.0 in 2007 in the montane forest (Table 2-6).

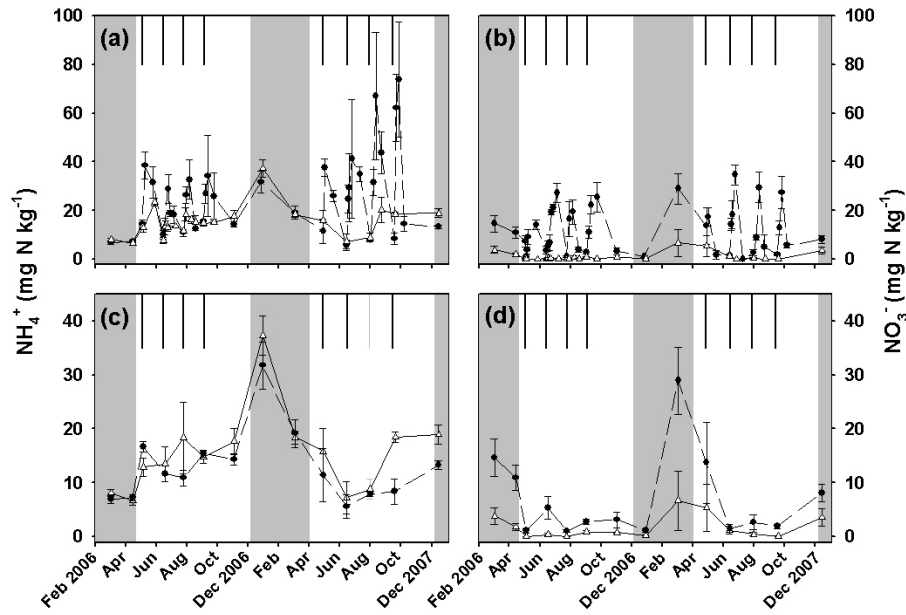


Figure 2-2. Mean (\pm SE, $n = 4$) soil extractable NH_4^+ (left side) and NO_3^- (right side) in control (Δ) and 9- and 10-yr N-addition (\bullet) lowland forest. Black vertical lines indicate dates of N addition. Grey shading marks the dry season. Upper panels (a and b) include the transitory ‘fertilization peaks’, and lower panels (c and d) show only the ‘background concentrations’ at least six weeks after an N addition.

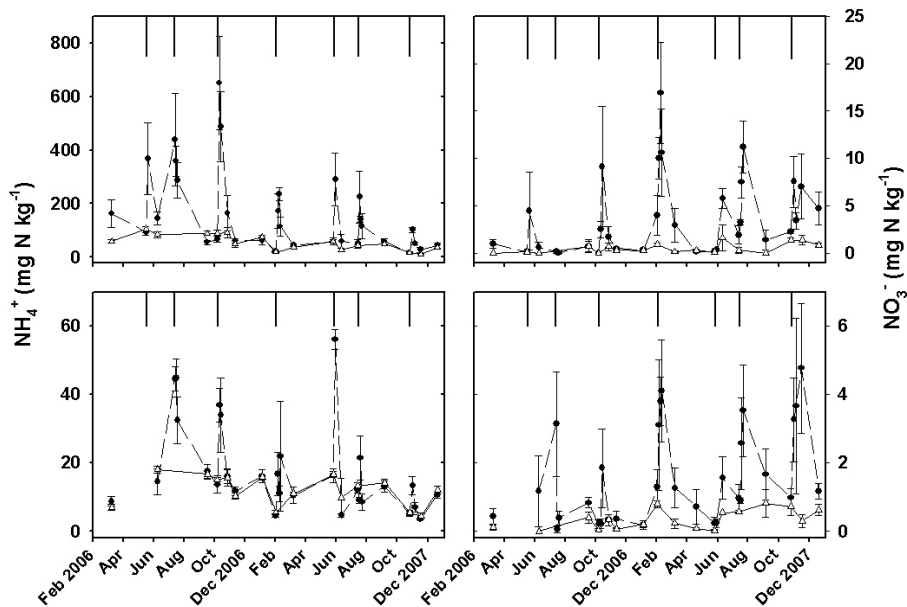


Figure 2-3. Mean (\pm SE, $n = 4$) soil extractable NH_4^+ (left side) and NO_3^- (right side) in control (Δ) and 1- and 2-yr N-addition (\bullet) montane forest. Black vertical lines indicate dates of N addition. Upper and lower panels present the organic layer and 0-0.05 m mineral soil, respectively.

Table 2-3. Mean (\pm SE; $n = 4$) net rates of soil N cycling ($\text{ng N cm}^{-2} \text{ h}^{-1}$) measured in September 2006 (wet season in the lowland forest).

Depth / N-cycling	Lowland			Montane	
	Control	1-yr N addition	9-yr N addition	Control	1-yr N addition
Organic Layer					
Net mineralization	-	-	-	258.77 \pm 32.90 b	534.33 \pm 74.20 a
Net nitrification	-	-	-	15.17 \pm 9.10 b	221.43 \pm 80.97 a
Mineral soil (0-0.05 m)					
Net mineralization	21.96 \pm 103.33	12.92 \pm 64.58	9.04 \pm 102.04	41.44 \pm 26.56	49.94 \pm 5.31
Net nitrification	140.79 \pm 80.08	193.75 \pm 25.83	178.25 \pm 114.96	-3.19 \pm 3.19 b	20.19 \pm 9.56 a

Means with different letters indicate differences between treatments (independent t -test at $P \leq 0.05$).

Table 2-4. Mean (\pm SE) soil NO and N₂O emissions from old-growth tropical lowland forests*.

Location	Mean annual temperature (°C)	Mean annual precipitation (mm)	Soil type (USDA classification)	N ₂ O (ng N cm ⁻² h ⁻¹)	NO (ng N cm ⁻² h ⁻¹)	Reference
Tapajos National Forest, Pará, Brazil (3.04°S, 54.95°W)	25	2000	Sandy loam Ultisol	1.6 \pm 0.3	8.8 \pm 5.0	Keller <i>et al.</i> (2005)
Tapajos National Forest, Pará, Brazil (3.04°S, 54.95°W)	25	2000	Clay Oxisol	7.0 \pm 0.6	9.0 \pm 2.8	Keller <i>et al.</i> (2005)
Paragominas, Pará, Brazil (2°59S, 47°31W)		1850	Haplustox	2.1	1.3	Verchot <i>et al.</i> (1999)
La Selva, Heredia, Costa Rica (10°26N, 84°0W)	25.8	3962	Inceptisols and Ultisols	6.7 \pm 3.0	1.0 \pm 0.3	Keller & Reiners (1994)
Gigante Peninsula, Republic of Panama (9° 06N, 79° 50W)	27.4	2650	Clay Dystrudepts	1.6 \pm 0.1	0.3 \pm 0.03	This study

* Only studies with at least one year of measurements for which averages are provided by the authors are included. The listing is not meant to be complete but to give an overview of the range of published data.

Table 2-5. Mean (\pm SE) soil NO and N₂O emissions from old-growth tropical montane forests*.

Location	Elevation (m)	Mean annual temperature (°C)	Mean annual precipitation (mm)	Soil type (USDA Classification)	N ₂ O (ng N cm ⁻² h ⁻¹)	NO (ng N cm ⁻² h ⁻¹)	Reference
Kohala, Hawaii (20°03, 155°41)	1122	16.1	2540	Typic Placandept	~0.5		Riley & Vitousek (1995) ^{†, §}
Wuasa, Central Sulawesi, Indonesia (120°17E, 01°25S)	1190	22.5	1590	Entisols and Inceptisols	1.1 \pm 0.1	0.5 \pm 0.2	Purbopuspito <i>et al.</i> (2006) [‡]
Rorekatimbu, Central Sulawesi, Indonesia (120°18E, 01°19S)	1800	18.3		Inceptisols	0.3 \pm 0.02	0.2 \pm 0.07	Purbopuspito <i>et al.</i> (2006) [‡]
Puncak Dingin, Central Sulawesi, Indonesia (120°18E, 01°16S)	2470	14.6		Inceptisols	1.0 \pm 0.2	0.2 \pm 0.03	Purbopuspito <i>et al.</i> (2006) [‡]
Maui, Hawaii (20°48, 156°15)	1300	16	4050	Inceptisols	\leq 0.2	\leq 0.2	Holtgrieve <i>et al.</i> (2006) ^{‡, §}
Maui, Hawaii (20°48, 156°15)	1320	16	3350	Inceptisols	1.1 \pm 0.3	8.7 \pm 4.6	Holtgrieve <i>et al.</i> (2006) ^{‡, §}
Fortuna, Republic of Panama (8° 45' N, 82° 15' W)	1200-1300	20	5532	Hapludands	1.3 \pm 0.1	0.1 \pm 0.02	This study [‡]

* The listing is not meant to be complete but to give an overview of the range of published data. For Purbopuspito *et al.* (2006) and this study average N-oxide fluxes over 1-2-yr measurements are provided by the authors. We included studies with less than one year of measurements as there are only few studies of soil N-oxide emissions from tropical montane forests.

[†] Average N₂O flux was estimated from a figure. No estimate is given for NO, but fluxes were often zero.

[‡] A substantial organic layer is mentioned by the authors.

[§] Forest dominated by a single species, *Metrosideros polymorpha*.

Table 2-6. Annual soil NO and N₂O emissions (kg N ha⁻¹, mean ± SE, *n* = 4) for control and N-addition plots, separated into transitory effects (include transitory ‘fertilization peaks’) and long-term effects (include only fluxes measured at least six weeks after an N addition).

Site	Treatment	2006		2007	
		NO	N ₂ O	NO	N ₂ O
Montane	Control	0.13 ± 0.02	1.06 ± 0.12	0.13 ± 0.02	1.26 ± 0.16
	1- and 2-yr N addition, transitory effect	0.84 ± 0.25 *	4.49 ± 1.35 *	1.95 ± 0.55 † (3.32 ± 0.52)	6.51 ± 2.65
	1- and 2-yr N addition, long-term effect	0.28 ± 0.05 ‡	2.24 ± 0.82 ‡	0.34 ± 0.12	2.31 ± 1.15
Lowland	Control	0.24 ± 0.05	1.35 ± 0.09	0.31 ± 0.06	0.98 ± 0.10
	9- and 10-yr N addition, transitory effect	2.06 ± 0.39	6.93 ± 1.82	1.44 ± 0.33	8.36 ± 1.38
	9- and 10-yr N addition, long-term effect	0.67 ± 0.18	4.97 ± 1.09	0.75 ± 0.09	3.81 ± 0.51

* Calculation includes the two pre-treatment measurements (January and February 2006).

† Calculation excludes the exceptionally high flux in March 2007 (Fig. 2-5a), which we do not consider representative for the whole integration time (inclusion would change the estimate to the value given in parentheses).

‡ Calculation excludes the two pre-treatment measurements (January and February 2006) and starts with the first long-term effect measurement of May 2006 (Fig. 2-5c and d; 102 days after the first-time N addition).

2.4.2 Transitory N addition effects (‘fertilization peaks’)

After each addition of 31.25 kg N ha⁻¹, a distinctive ‘peak’ was observed in soil N-oxide emissions (with the exception of the first-time N addition in the lowland forest, see below) and in soil mineral N concentrations. We call these ‘fertilization peaks’ and refer to them as ‘transitory’ effects. Maximum NH₄⁺ and NO₃⁻ concentrations (Figs. 2-2a, b and 2-3) and

maximum NO emissions were measured within the first two weeks while N₂O emissions peaked between the first and third week following N additions (Figs. 2-4a, b and 2-5a, b). In the lowland forest, fertilization peaks of soil N-oxide emissions increased as the wet season progressed (Fig. 2-4a and b). Twice in the montane forest, a second maximum of NO emissions occurred within five weeks after N addition (Fig. 2-5a in March 2006 and March 2007). In the montane forest, transitory N-oxide emissions reached higher levels in the second year than in the first year of N addition (Fig. 2-5a and b), and the second year fertilization peaks were in the same order of magnitude as those from the lowland forest at the height of the wet season (Fig. 2-4a and b). Maximum NO emissions reached 15.41 ± 4.49 ng N cm⁻² h⁻¹ in the montane and 20.52 ± 6.51 ng N cm⁻² h⁻¹ in the lowland forest. Maximum N₂O emissions were 29.33 ± 11.95 ng N cm⁻² h⁻¹ in the montane and 42.19 ± 5.25 ng N cm⁻² h⁻¹ in the lowland forest.

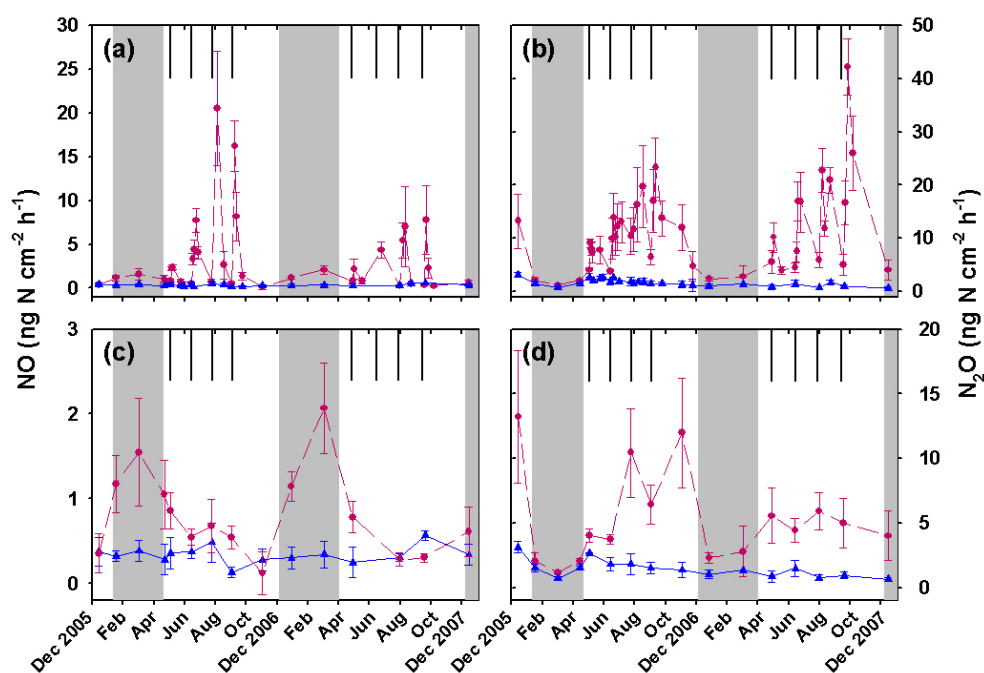


Figure 2-4. Mean (\pm SE, $n = 4$) soil NO (left side) and N₂O emissions (right side) from control (\blacktriangle) and 9- and 10-yr N-addition (\bullet) lowland forest. Black vertical lines indicate dates of N addition. Grey shading marks the dry season. Upper panels (a and b) include the transitory ‘fertilization peaks’, and lower panels (c and d) show only the ‘background fluxes’ at least six weeks after an N addition.

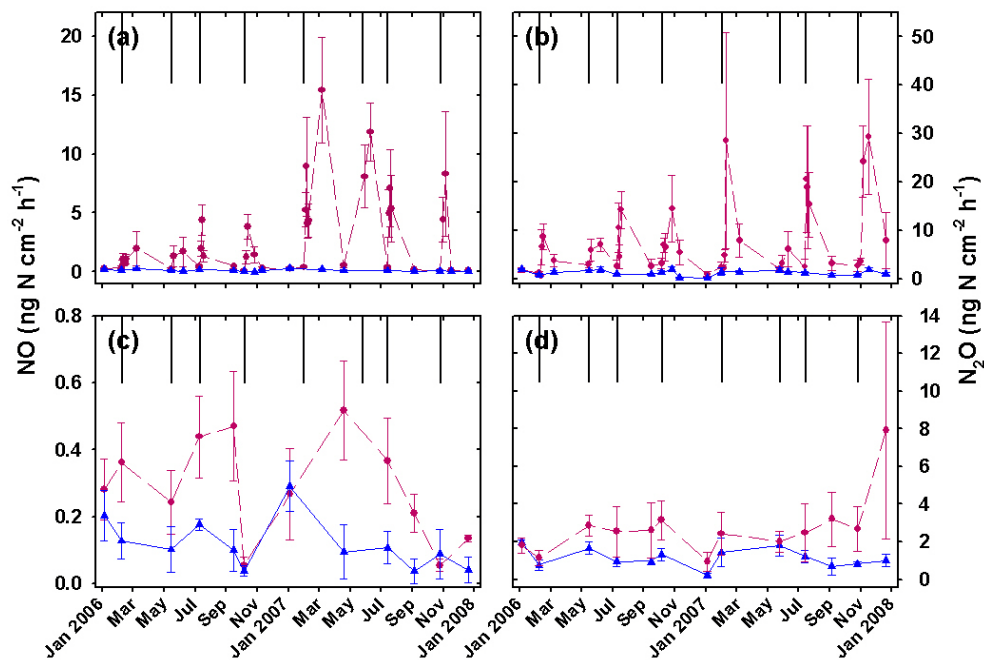


Figure 2-5. Mean (\pm SE, $n = 4$) soil NO (left side) and N₂O emissions (right side) from control (\blacktriangle) and 1- and 2-yr N-addition (\bullet) montane forest. Black vertical lines indicate dates of N addition. Upper panels (a and b) include the transitory ‘fertilization peaks’, and lower panels (c and d) show only the ‘background fluxes’ at least six weeks after an N addition. The first two fluxes are pre-treatment measurements.

2.4.3 Long-term effects of N enrichment

We assessed the effects of N enrichment by considering only the data at least six weeks after an N addition to eliminate the transitory fertilization peaks. We call these ‘background’ soil N-oxide fluxes and ‘background’ soil mineral N concentrations and refer to them as ‘long-term effects’. In the lowland forest, background NH₄⁺ concentrations did not differ between N-addition and control plots (Fig. 2-2c). Background NO₃⁻ concentrations were larger and showed a more pronounced seasonal pattern in the N-addition than the control plots ($P = 0.001$; Fig. 2-2d). As a result, the ratio of NH₄⁺/NO₃⁻ decreased with N enrichment. Net rates of soil N cycling in the lowland forest did not differ between treatments during the sampling in wet season 2006 (Table 2-3).

In the montane forest, N addition did not change background NH₄⁺ concentrations relative to the control. Background NO₃⁻ concentrations increased in the organic layer of the N-addition plots ($P = 0.022$) but not in the mineral soil. Hence, the ratio of NH₄⁺/NO₃⁻ in the

organic layer decreased with N addition. Net N mineralization and nitrification rates increased with N enrichment (Table 2-3).

In the lowland forest, background soil NO ($0.80 \pm 0.14 \text{ ng N cm}^{-2} \text{ h}^{-1}$) and N₂O ($5.32 \pm 0.90 \text{ ng N cm}^{-2} \text{ h}^{-1}$) fluxes were larger from the N-addition than the control plots ($P = 0.027$ and $P = 0.002$, respectively) and displayed a pronounced seasonal pattern. Background NO and N₂O fluxes from the N-addition plots were largest during the dry and wet seasons, respectively (Fig. 2-4c and d). In the N-addition plots, background NO fluxes were negatively correlated with WFPS (Fig. 2-6a) while the converse was true for the background N₂O fluxes (Fig. 2-6b). The logarithm of background N₂O/NO ratios was positively correlated with WFPS in the N-addition plots (Fig. 2-6c), but not in the control plots (Fig. 2-6d). Annual background soil N-oxide emissions increased by a factor of two to three for NO and a factor of four for N₂O (Table 2-6), such that the N₂O/NO ratio increased with N enrichment.

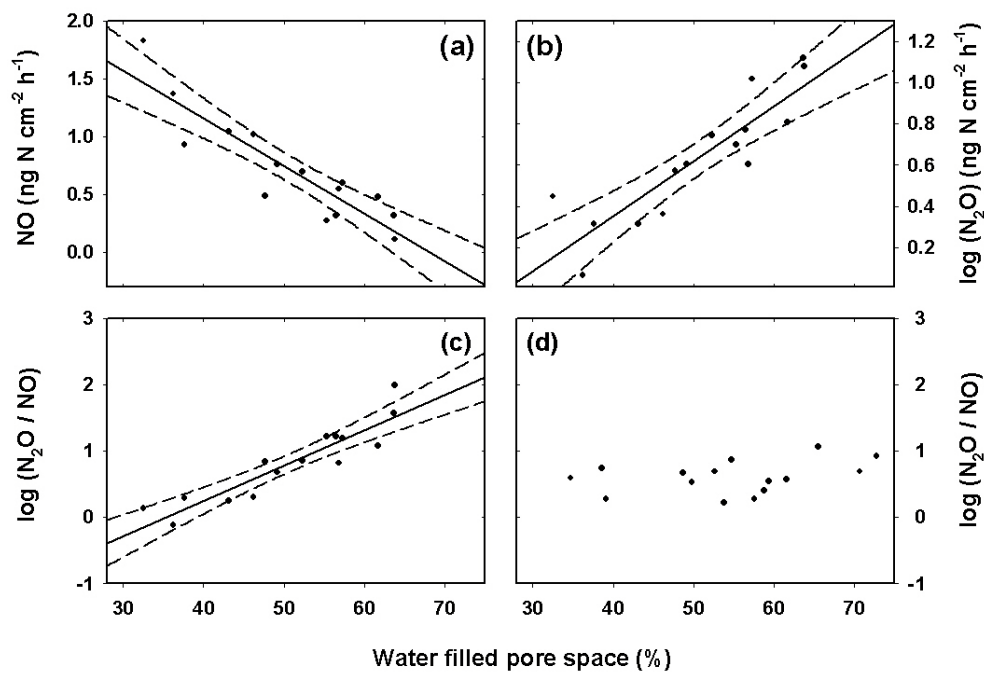


Figure 2-6. Linear regressions (95% CI, $n = 15$) between mean water-filled pore space and a) mean soil NO emissions ($y = -0.05 (\pm 0.01) x + 3.17 (\pm 0.71)$, $R^2 = 0.805$, $P < 0.001$), b) mean soil log (N₂O) emissions ($y = 0.03 (\pm 0.01) x - 0.72 (\pm 0.45)$, $R^2 = 0.756$, $P < 0.001$) and c) mean log (N₂O/NO) ratio ($y = 0.05 (\pm 0.01) x - 1.87 (\pm 0.72)$, $R^2 = 0.839$, $P < 0.001$) of four plots for the 9- and 10-yr N-addition lowland forest. Similar regression for control (d) lowland forest was not significant ($R^2 = 0.116$, $P = 0.214$). Only N-oxide fluxes measured at least six weeks after an N addition were considered.

In the montane forest, background soil NO fluxes ($0.28 \pm 0.04 \text{ ng N cm}^{-2} \text{ h}^{-1}$) from the N-addition plots were larger than controls ($P = 0.025$; Fig. 2-5c) while background soil N₂O fluxes ($2.75 \pm 0.47 \text{ ng N cm}^{-2} \text{ h}^{-1}$) did not differ from controls (Fig. 2-5d). Background N-oxide fluxes did not show a pronounced temporal pattern. Linear regressions between background N-oxide emissions and WFPS in organic layer or mineral soil were not significant. Annual background soil N-oxide emissions were two to three times larger for NO and two times larger for N₂O (Table 2-6), such that the N₂O/NO ratio decreased with N enrichment.

Background soil NO emissions from the N-addition plots were larger from the lowland than the montane forest ($P = 0.014$). Background soil N₂O and total background soil N-oxide emissions did not differ between forests, though total N-oxide emissions trended larger in the lowland forest ($P = 0.063$).

2.4.4 N-oxide fluxes following first-time N addition

In the lowland forest, first-time addition of $62.5 \text{ kg N ha}^{-1}$ (split in two equal parts and applied early in the wet season) did not affect soil N₂O fluxes but increased soil NO emissions compared to the control ($P = 0.027$). However, over a period of 60 days, only $0.05 \pm 0.02\%$ of the applied N was lost as NO-N, and most of this loss occurred after the second N addition (Fig. 2-7). In contrast, the montane forest showed immediate increases in soil N-oxide emissions after the first-time N additions compared to the control ($P = 0.012$ for NO and $P = 0.037$ for N₂O; Fig. 2-7). The losses of applied N were $0.76 \pm 0.43\%$ as NO-N and $3.09 \pm 0.84\%$ as N₂O-N within 31 days of the first N addition, and $0.48 \pm 0.33\%$ as NO-N and $1.65 \pm 0.71\%$ as N₂O-N within 25 days of the second N addition.

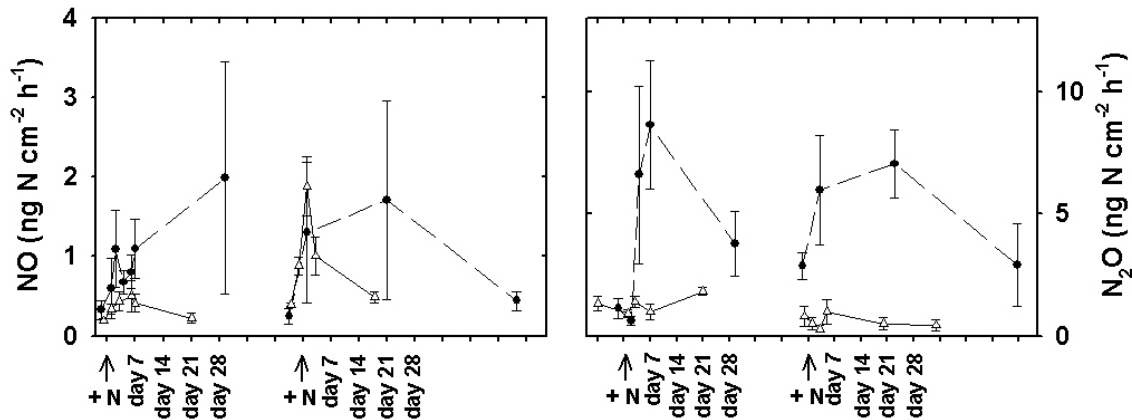


Figure 2-7. Mean (\pm SE, $n = 4$) soil NO (left side) and N₂O emissions (right side) from the first-time N addition montane (\bullet) and lowland (Δ) forest following two subsequent N additions marked with '+N' below the x-axis.

2.5 Discussion

2.5.1 Soil N cycle and N-oxide fluxes from control forests

Soil N cycles differed between the lowland and montane forests. In the lowland forest, most of the mineralized N was nitrified (Table 2-3). This suggests that mineral N production was more than sufficient for microbial immobilization, and the absence of competition from plant uptake during the 7-d incubation enabled nitrifiers to monopolize available substrate (NH₄⁺ and organic N), resulting in accumulation of NO₃⁻. In the montane forest, net nitrification rates were only 6% of net N mineralization rates in the organic layer and net NO₃⁻ immobilization occurred in the mineral soil. This indicates that a large fraction of mineral N was immobilized and the absence of plant competition for seven days failed to allow nitrifiers to accumulate NO₃⁻.

The soil N-oxide emissions from both forests were consistent with the expectations of the conceptual 'hole-in-the-pipe' (HIP) model, which hypothesizes that the total N-oxide gas flux is proportional to the rates of nitrification and denitrification (first level of control) while the relative proportion of each gas is controlled by soil aeration status (second level of control; Firestone & Davidson, 1989). Differences in N-oxide emissions between forest soils are consistent with the hypothesized first level of control with larger emissions and larger net nitrification rates in the lowland compared to the montane forest (Table 2-3). Differences in N₂O/NO ratios between forests are also consistent with the hypothesized second level of control with lower N₂O/NO ratios and lower WFPS in the lowland compared to the montane

mineral soil (Fig. 2-1a and b). Although WFPS in the montane organic layer stayed below 40% which is favorable for NO production, WFPS in the montane mineral soil was $\geq 80\%$ (Fig. 2-1b) which is optimal for N₂O production (Bollmann & Conrad, 1998).

We bring net soil N-cycling rates and N-oxide losses together to evaluate the leakiness of soil N cycles. The average soil N-oxide emissions from the lowland forest (Table 2-4) were $\sim 1\%$ of the net N-cycling rates in the top soil (Table 2-3). This characterizes a rather conservative, or less leaky, soil N cycle than we hypothesized for this lowland site where stem diameter growth and annual fine litterfall were neither N nor P limited after five and six years, respectively (S.J. Wright, unpublished results; Kaspari *et al.*, 2008). Also, the average soil N-oxide emissions from our lowland forest site were at the low end for old-growth tropical lowland forests (Table 2-4). This further suggests that our lowland forest site has a less leaky soil N cycle than has been found for tropical lowland forests with strong P-limitation (Martinelli *et al.*, 1999; Hall & Matson, 2003; Davidson *et al.*, 2007). The average soil N-oxide emissions from our montane site, which were comparable to emissions reported from other old-growth montane forests (Table 2-5), were $\sim 0.4\%$ of the net N-cycling rates in the organic layer and top mineral soil (Table 2-3). This suggests a more conservative soil N cycle relative to the lowland forest, which supports our hypothesis for this montane forest where stem diameter growth and fine litterfall were N limited (Adamek *et al.*, 2009). The soil N cycles of our forest sites thus differ in the efficiency of processing the available substrate for nitrification and in the degree of leakiness.

2.5.2 Response of soil N-oxide fluxes to N addition in the lowland forest

The small magnitude of soil N-oxide emissions following first-time N addition in the lowland forest is consistent with a relatively conservative soil N cycle. First-time N addition did not cause transitory increases in soil N-oxide emissions. Instead, there was a gradual and modest increase in soil N-oxide emissions following two subsequent N applications (Fig. 2-7). The strong dry season causes WFPS to drop below 40% (Fig. 2-1a). The first-time N addition was conducted during the transition between dry and wet season when WFPS was still between 45% and 50%. This is far below the optimum range for nitrification (Linn & Doran, 1984; Bollmann & Conrad, 1998) and might reduce nitrifying activity. Hence, water stress might also have contributed to the missing fertilization peaks of N-oxide emissions following the first-time N addition. Support for this explanation comes from the chronic N-addition plots where the fertilization peaks of N-oxide emissions at the beginning of the wet season although

substantial were clearly smaller than subsequent N-oxide peaks later in the wet season (Fig. 2-4a and b).

The initially rather conservative soil N cycle became increasingly leaky with chronic N addition. In contrast to the first-time N addition, the 9- and 10-yr N-addition plots had immediate and large transitory N-oxide emissions (Fig. 2-4a and b). Also, background soil N-oxide emissions (measured at least six weeks after N additions) were larger than controls (Fig. 2-4c and d; Table 2-6). N-oxide losses were $\sim 3.3\%$ of the net soil N-cycling rates in the chronic N-addition plots, which was also larger than controls (Tables 2-3 and 2-6). Additionally, background soil NO_3^- concentrations increased, and NO_3^- accumulated during the dry season when it reached larger concentrations than NH_4^+ (Fig. 2-2c and d). A dominance of NO_3^- relative to NH_4^+ suggests a leaky soil N cycle (Davidson *et al.*, 2000). The increase in the background $\text{N}_2\text{O}/\text{NO}$ ratio, which implies that the fluxes of the two gases are increasing unevenly, might reflect that a larger soil volume may contribute to the elevated N_2O emissions while due to its high reactivity the emitted NO should be produced within a smaller volume of the surface soil only. Supporting this assumption, N_2O concentrations in soil air are increasing down to at least 2-m depth which implies that –although further reduction to N_2 will be occurring during upward diffusion- N_2O production is not restricted to the top soil (data not reported). There was a strong correlation between background soil N-oxide emissions and WFPS in the chronic N-addition but not in the control plots (Fig. 2-6c and d). As N availability increased due to N enrichment an originally rather conservative soil N cycle, where N-oxide emissions were regulated by N availability (or the first level of control of the HIP model) was changed to an increasingly leaky soil N cycle where the second level of control (soil aeration status) caused pronounced seasonal changes in background soil N-oxide emissions.

2.5.3 Response of soil N-oxide fluxes to N addition in the montane forest

The magnitude of soil N-oxide emissions following first-time and chronic N additions in the montane forest tells us whether its response is regulated by the initial conservative soil N cycle or, as we hypothesized, by the presence of a substantial organic layer in which N mineralization and nitrification could increase substantially upon N addition. First-time N addition led to an immediate increase in soil N-oxide emissions (Figs. 2-5a, b and 2-7), and fertilization peaks of N-oxide emissions during the second-year N addition were similar to those from the chronic N-addition lowland plots. These results contrast with an N-limited

Hawaiian montane forest, where first-time N addition did not cause increases in soil N-oxide emissions (Hall & Matson, 1999; 2003). Also, the background NO emissions were larger than controls and the background N₂O emissions remained elevated two months after the last N addition in November 2007 (Fig. 2-5c and d; Table 2-6).

We largely attribute the instantaneous and sustained increase in soil N-oxide emissions in the Panamanian montane forest to a substantial increase in net N-cycling rates in the organic layer in response to N addition. Net N mineralization and nitrification rates were two and 15 fold increased, respectively, following the third N application during the first year of N addition (Table 2-3). The decrease in the background N₂O/NO ratio also suggests that the organic layer with its low WFPS (Fig. 2-1b) makes an important contribution to the soil N-oxide emissions in response to N addition. The soils in the Hawaiian forest have a horizon of organic matter as well (Lohse & Matson, 2005), but the initial N-cycling rates (mineralization and nitrification) in the top 0.1 m of soil were small and not increased after 1-yr N addition (Hall & Matson, 2003). This differing response in soil N-cycling compared to our site and consequently the small response in N-oxide emissions might partly be related to the rapid drainage of these coarse-textured soils (i.e. > 59% gravel in the mineral A horizon) causing immediate and substantial increases in N leaching losses (mainly NO₃⁻) following N addition (Lohse & Matson, 2005). In our forest, background soil N-oxide emissions expressed as a percentage of soil N-cycling rates (~0.4%) were unchanged by N addition due to large offsetting increases in N-oxide emissions and N-cycling rates in the N-addition plots. Thus, this montane forest with N-limited primary production responded to N additions with a large increase in soil N cycling while the proportion of N-oxide emissions remained small as in the model of Aber *et al.* (1998). Whether the proportion of soil N-oxide emissions to N-cycling will increase progressively with further years of N addition remains to be seen. The presence of an organic layer where N cycling increased substantially with N addition (and not the initial degree of leakiness of the soil N cycle as in the lowland forest) was the main factor regulating the response of soil N-oxide emissions to N addition in this montane forest.

2.5.4 Factors influencing soil N-oxide emissions following anthropogenic N additions

The N status of the forest and its soil N-cycling properties allow us to deduce which factors govern soil N-oxide emission response to N addition. Biological demand for N (i.e. presence

or absence of N limitation of vegetation growth) is clearly not the sole indicator of how N-oxide fluxes from tropical forest soils react to chronic N deposition. Our lowland forest, located on deeply-weathered soil, is not N limited but displayed a rather conservative soil N cycle which in combination with water stress caused a lack of fertilization peaks in N-oxide emissions following first-time N addition. Our montane forest, located on young volcanic soil, is N-limited and has a conservative soil N cycle, but the soil reacted with immediate and large N-oxide emissions following first N additions due to the large increase in nitrification activity in the organic layer. This contrasts with Hawaii, where the presence or absence of N limitation of tree growth reflected soil N-cycling characteristics across a soil chronosequence and predicted N-addition effects on soil N-oxide emissions (Hall & Matson, 1999; 2003). We therefore suggest that the status of the soil N cycle (conservative versus leaky) as well as absence/presence of an organic layer (where N-cycling rates may substantially increase) are important factors governing the response of soil N-oxide emissions from tropical forests following anthropogenic N input.

The status of the soil N cycle is likely to vary widely among lowland tropical forests (even though lowland tropical forests tend to have leakier N cycles than montane forests). Many tropical lowland forests occur on heavily-weathered soils and have a relative excess of N; however, soil texture strongly affects N-cycling processes in heavily-weathered soils across the Brazilian Amazon. Ultisols/Acrisols with a sandy loam or coarser texture tend to have more conservative soil N cycles while Oxisols/Ferralsols with a loamy or finer texture tend to have relatively leaky soil N cycles (Silver *et al.*, 2000; Sotta *et al.*, 2008). We expect that such variation in soil N cycles will influence N-oxide emissions in response to N addition.

On the other hand, many tropical montane forests occur on relatively young soils covered by thick and densely rooted organic layers (Edwards & Grubb, 1977), and their aboveground primary production is probably N limited (Tanner *et al.*, 1998). However, soil N-cycling rates can be large in the organic layer (Livingston *et al.*, 1988; Vitousek & Matson, 1988; Wilcke *et al.*, 2002). If the organic layer displays large nitrification rates (Wilcke *et al.*, 2002) or a large increase in nitrification with an increase in N availability (as was the case in our study), the soils will generally react to anthropogenic N addition with immediate increases in N-oxide emissions even if forest growth is N limited.

2.5.5 Consequences of chronic N deposition on soil N-oxide emissions from tropical lowland and montane forests

Substantial increases in the magnitude of soil N-oxide emissions can be expected from both lowland and montane tropical forests under chronic N deposition, independent of the transitory response to pulse N additions. Soil N-oxide emissions from N-limited montane forests will increase rapidly under elevated N deposition if these forests have an organic layer in which nitrification activity could substantially increase upon N addition. This contradicts the current assumption that N-limited tropical montane forests will respond to N additions with only small and delayed increases in soil N-oxide emissions. The relative contribution of N₂O to total N-oxide emissions from tropical forests on deeply weathered soils may increase. In tropical forests with a pronounced dry season, soil moisture might become the main factor regulating the type of N-oxide emitted from the soil surface as the ratio of N₂O/NO fluxes in the N-enriched lowland site strongly depended on soil water content. This suggests that climate change scenarios, where rainfall quantity and seasonality change (IPCC, 2007), will also alter the relative importance of soil N₂O and NO emissions from tropical forests exposed to anthropogenic N addition.

2.6 References

- Aber JD, McDowell W, Nadelhoffer K, *et al.* (1998) Nitrogen saturation in temperate forest ecosystems: hypotheses revisited. *BioScience*, **48**, 921-934.
- Adamek M, Corre MD, Hölscher D (2009) Early effect of elevated nitrogen input on above-ground net primary production of a lower montane rain forest, Panama. *Journal of Tropical Ecology*, **25**, 637-647.
- Bakwin PS, Wofsy SC, Fan SM, Keller M, Trumbore S, Da Costa JM (1990) Emission of nitric oxide (NO) from tropical forest soils and exchange of NO between the forest canopy and the atmospheric boundary layers. *Journal of Geophysical Research*, **95**, 16755-16764.
- Blake GR, Hartge KH (1986) Bulk density. In *Methods of soil analysis, part 1. Physical and mineralogical methods*. (ed Klute A), pp. 12. Agronomy Monograph, Soil Science Society of America, Madison, Wisconsin, USA.
- Bollmann A, Conrad R (1998) Influence of O₂ availability on NO and N₂O release by nitrification and denitrification in soils. *Global Change Biology*, **4**, 387-396.
- Bouwman AF, Van der Hock KW, Olivier JGJ (1995) Uncertainties in the global source distribution of nitrous oxide. *Journal of Geophysical Research*, **100**, 2785-2800.
- Breuer L, Kiese R, Butterbach-Bahl K (2002) Temperature and moisture effects on nitrification rates in tropical rain-forest soils. *Soil Science Society of America Journal*, **66**, 834-844.
- Condit R (1998) *Tropical forest census plots*. Springer-Verlag, Berlin, Heidelberg and R.G. Landes Company Georgetown, TX, USA., 232 pp.
- Crawley MJ (2002) *Statistical Computing, An Introduction to Data Analysis using S-Plus*. John Wiley & Sons Ltd, Chichester, UK, 761 pp.
- Crutzen PJ (1979) The role of NO and NO₂ in the chemistry of the troposphere and stratosphere. *Annual Review of Earth and Planetary Sciences*, **7**, 443-472.
- Davidson EA, Keller M, Erickson HE, Verchot LV, Veldkamp E (2000) Testing a conceptual model of soil emissions of nitrous and nitric oxides. *BioScience*, **50**, 667-680.
- Davidson EA, Reis de Carvalho JR, Figueira AM, *et al.* (2007) Recuperation of nitrogen cycling in Amazonian forests following agricultural abandonment. *Nature*, **447**, 995-999.

-
- Dechert G, Veldkamp E, Brumme R (2005) Are partial nutrient balances suitable to evaluate nutrient sustainability of land use systems? Results from a case study in Central Sulawesi, Indonesia. *Nutrient Cycling in Agroecosystems*, **72**, 201-212.
- Edwards PJ, Grubb PJ (1977) Studies of mineral cycling in a montane rain forest in New-Guinea. 1. Distribution of organic matter in vegetation and soil. *Journal of Ecology*, **65**, 943-969.
- Erickson H, Keller M, Davidson EA (2001) Nitrogen oxide fluxes and nitrogen cycling during postagricultural succession and forest fertilization in the humid tropics. *Ecosystems*, **4**, 67-84.
- Firestone MK, Davidson EA (1989) Microbiological basis of NO and N₂O production and consumption in soil. In *Exchange of trace gases between terrestrial ecosystems and the atmosphere* (eds Andreae MO, Schimel DS), pp. 7-21. John Wiley & Sons, New York.
- Galloway JN, Aber JD, Erisman JW, Seizinger SP, Howarth RW, Cowling EB, Cosby BJ (2003) The Nitrogen Cascade. *BioScience*, **53**, 341-356.
- Galloway JN, Cowling EB (2002) Reactive nitrogen and the world: 200 years of change. *Ambio*, **31**, 64-71.
- Galloway JN, Dentener FJ, Capone DG, *et al.* (2004) Nitrogen cycles: past, present and future. *Biogeochemistry*, **70**, 153-226.
- Galloway JN, Townsend AR, Erisman JW, *et al.* (2008) Transformation of the nitrogen cycle: recent trends, questions, and potential solutions. *Science*, **320**, 889-892.
- Grubb PJ (1977) Control of forest growth and distribution on wet tropical mountains: with reference to mineral nutrition. *Annual Review of Ecology and Systematics*, **8**, 83-107.
- Gueorguieva R, Krystal JH (2004) Move over ANOVA, progress in analyzing repeated-measures data and its reflection in papers published in the archives of general psychiatry. *Archives of General Psychiatry*, **61**, 310-317.
- Hall SJ, Matson PA (1999) Nitrogen oxide emissions after nitrogen additions in tropical forests. *Nature*, **400**, 152-155.
- Hall SJ, Matson PA (2003) Nutrient status of tropical rain forests influences soil N dynamics after N additions. *Ecological Monographs*, **73**, 107-129.
- Hedin LO, Vitousek PM, Matson PA (2003) Nutrient losses over four million years of tropical forest development. *Ecology*, **84**, 2231-2255.

-
- Holtgrieve GW, Jewett PK, Matson PA (2006) Variations in soil N cycling and trace gas emissions in wet tropical forests. *Oecologia*, **146**, 584-594.
- IPCC (2007) Technical Summary. In *Climate Change 2007: The Physical Science Basis. Contribution of Working Group I to the Fourth Assessment Report of the Intergovernmental Panel on Climate Change* (eds Solomon S, Qin D, Manning M, et al.), pp. 996. Cambridge University Press, Cambridge, UK and New York, NY, USA.
- Kaplan WA, Wofsy SC (1988) Emission of NO and deposition of O₃ in a tropical forest system. *Journal of Geophysical Research*, **93**, 1389-1395.
- Kaspari M, Garcia MN, Harms KE, Santana M, Wright SJ, Yavitt JB (2008) Multiple nutrients limit litterfall and decomposition in a tropical forest. *Ecology Letters*, **11**, 35-43.
- Keller M, Kaplan WA, Wofsy SC, Da Costa JM (1988) Emissions of N₂O from tropical forest soils: Response to fertilization with NH₄⁺, NO₃⁻ and PO₄³⁻. *Journal of Geophysical Research*, **93**, 1600-1604.
- Keller M, Reiners WA (1994) Soil-atmosphere exchange of nitrous oxide, nitric oxide, and methane under secondary succession of pasture to forest in the Atlantic lowlands of Costa Rica. *Global Biogeochemical Cycles*, **8**, 399-409.
- Keller M, Varner R, Dias JD, Silva H, Crill P, Cosme de Oliveira Jr. R, Asner GP (2005) Soil-Atmosphere exchange of nitrous oxide, nitric oxide, methane, and carbon dioxide in logged and undisturbed forest in the Tapajos National Forest, Brazil. *Earth Interactions*, **9**, 1-28.
- Klinge R, Martins ARA, Mackensen J, Folster H (2004) Element loss on rain forest conversion in East Amazonia: comparison of balances of stores and fluxes. *Biogeochemistry*, **69**, 63-82.
- König N, Fortmann H (1996) *Probenvorbereitungs-, Untersuchungs- und Elementbestimmungs-Methoden des Umweltanalytik-Labors der Niedersächsischen Forstlichen Versuchsanstalt, Reihe B*. University of Goettingen, Goettingen, Germany.
- Leigh EG, Rand AS, Windsor DW (1996) *The ecology of a tropical forest*. Smithsonian Press, Washington DC, 266 pp.
- Linn DM, Doran JW (1984) Effect of water-filled pore space on carbon dioxide and nitrous oxide production in tilled and nontilled soils. *Soil Science Society of America Journal*, **48**, 1267-1272.

-
- Livingston GP, Hutchinson GL, Spartalian K (2006) Trace gas emission in chambers: A non-steady-state diffusion model. *Soil Science Society of America Journal*, **70**, 1459-1469.
- Livingston GP, Vitousek PM, Matson PA (1988) Nitrous oxide flux and nitrogen transformations across a landscape gradient in Amazonia. *Journal of Geophysical Research*, **93**, 1593-1599.
- Lofffield N, Flessa H, Augustin J, Beese F (1997) Automated gas chromatographic system for rapid analysis of the atmospheric trace gases methane, carbon dioxide, and nitrous oxide. *Journal of Environmental Quality*, **26**, 560-564.
- Lohse KA, Matson PA (2005) Consequences of nitrogen additions for soil processes and solution losses from wet tropical forests. *Ecological Applications*, **15**, 1629-1648.
- Martinelli LA, Piccolo MC, Townsend AR, *et al.* (1999) Nitrogen stable isotopic composition of leaves and soil: tropical versus temperate forests. *Biogeochemistry*, **46**, 45-65.
- Matson PA, McDowell W, Townsend AR, Vitousek PM (1999) The globalization of N deposition: ecosystem consequences in tropical environments. *Biogeochemistry*, **46**, 67-83.
- McGroddy ME, Silver WL, Cosme de Oliveira Jr. R (2004) The effect of phosphorus availability on decomposition dynamics in a seasonal lowland Amazonian forest. *Ecosystems*, **7**, 172-179.
- Pinheiro JC, Bates DM (2004) *Mixed-effects models in S and S-Plus*. Springer Science and Business Media, New York, NY, USA, 528 pp.
- Purbopuspito J, Veldkamp E, Brumme R, Murdiyarso D (2006) Trace gas fluxes and nitrogen cycling along an elevation sequence of tropical montane forests in Central Sulawesi, Indonesia. *Global Biogeochemical Cycles*, **20**, GB1010, doi:3010.1029/2005GB002516.
- R Development Core Team (2008) R: A language and environment for statistical computing. R Foundation for Statistical Computing, Vienna, Austria. ISBN 3-900051-07-0, URL <http://www.R-project.org>.
- Riley RH, Vitousek PM (1995) Nutrient dynamics and nitrogen trace gas flux during ecosystem development in montane rain forest. *Ecology*, **76**, 292-304.
- Röderstein M, Hertel D, Leuschner C (2005) Above- and below-ground litter production in three tropical montane forests in southern Ecuador. *Journal of Tropical Ecology*, **21**, 483-492.

-
- Schwendenmann L, Veldkamp E (2005) The role of dissolved organic carbon, dissolved organic nitrogen and dissolved inorganic nitrogen in a tropical wet forest ecosystem. *Ecosystems*, **8**, 339-351.
- Silver WL, Neff J, McGroddy M, Veldkamp E, Keller M, Cosme R (2000) Effects of soil texture on belowground carbon and nutrient storage in a lowland Amazonian forest ecosystem. *Ecosystems*, **3**, 193-209.
- Sotta ED, Corre MD, Veldkamp E (2008) Differing N status and N retention processes of soils under old-growth lowland forest in Eastern Amazonia, Caxiuanã, Brazil. *Soil Biology and Biochemistry*, **40**, 740-750.
- Stuedler PA, Garcia-Montiel DC, Piccolo MC, Neill C, Melillo JM, Feigl BJ, Cerri CC (2002) Trace gas responses of tropical forest and pasture soils to N and P fertilization. *Global Biogeochemical Cycles*, **16**, 7-13.
- Tanner EVJ, Vitousek PM, Cuevas E (1998) Experimental investigation of nutrient limitation of forest growth on wet tropical mountains. *Ecology*, **79**, 10-22.
- Veldkamp E, Keller M, Nuñez M (1998) Effects of pasture management on N₂O and NO emissions from soils in the humid tropics of Costa Rica. *Global Biogeochemical Cycles*, **12**, 71-79.
- Verchot LV, Davidson EA, Cattânio JH, Ackerman IL, Erickson HE, Keller M (1999) Land use change and biogeochemical controls of nitrogen oxide emissions from soils in eastern Amazonia. *Global Biogeochemical Cycles*, **13**, 31-46.
- Vitousek PM (1984) Litterfall, nutrient cycling, and nutrient limitation in tropical forests. *Ecology*, **65**, 285-298.
- Vitousek PM, Aber JD, Howarth RW, *et al.* (1997) Human alteration of the global nitrogen cycle - Sources and consequences. *Ecological Applications*, **7**, 737-750.
- Vitousek PM, Matson PA (1988) Nitrogen transformations in a range of tropical forest soils. *Soil Biology and Biochemistry*, **20**, 361-367.
- Wagner SW, Reicosky DC, Alessi RS (1997) Regression models for calculating gas fluxes measured with a closed chamber. *Agronomy Journal*, **89**, 279-284.
- Walker TW, Syers JK (1976) The fate of phosphorus during pedogenesis. *Geoderma*, **15**, 1-19.
- Wilcke W, Yasin S, Abramowski U, Valarezo C, Zech W (2002) Nutrient storage and turnover in organic layers under tropical montane rain forest in Ecuador. *European Journal of Soil Science*, **53**, 15-27.

- Williams EJ, Davidson EA (1993) An intercomparison of two chamber methods for the determination of emission of nitric oxide from soil. *Atmospheric Environment*, **27A**, 2107-2113.
- Yavitt JB, Wright SJ, Kelman Wieder R (2004) Seasonal drought and dry-season irrigation influence leaf-litter nutrients and soil enzymes in a moist, lowland forest in Panama. *Austral Ecology*, **29**, 177-188.
- Yienger JJ, Levy H (1995) Empirical model of global soil-biogenic NO_x emissions. *Journal of Geophysical Research*, **100**, 11447-11464.

Biogeosciences, 6, 2973–2983, 2009
www.biogeosciences.net/6/2973/2009/
© Author(s) 2009. This work is distributed under
the Creative Commons Attribution 3.0 License.



Chronic nitrogen addition causes a reduction in soil
carbon dioxide efflux during the high stem-growth
period in a tropical montane forest but no response from
a tropical lowland forest on a decadal time scale

BIRGIT KOEHLER, MARIFE D. CORRE, EDZO VELDKAMP
and JUVIA P. SUETA

3.1 Abstract

Atmospheric nitrogen (N) deposition is rapidly increasing in tropical regions. We studied the response of soil carbon dioxide (CO₂) efflux to long-term experimental N addition (125 kg N ha⁻¹ yr⁻¹) in mature lowland and montane forests in Panama. In the lowland forest, on soils with high nutrient-supplying and buffering capacity, fine litterfall and stem-growth were neither N- nor phosphorus-limited. In the montane forest, on soils with low nutrient supplying capacity and an organic layer, fine litterfall and stem-growth were N-limited. Our objectives were to 1) explore the influence of soil temperature and moisture on the dynamics of soil CO₂ efflux and 2) determine the responses of soil CO₂ efflux from an N-rich and N-limited forest to elevated N input. Annual soil CO₂-C efflux was larger in the lowland (15.44 ± 1.02 Mg C ha⁻¹) than in the montane forest (9.37 ± 0.28 Mg C ha⁻¹). In the lowland forest, soil moisture explained the largest fraction of the variance in soil CO₂ efflux while soil temperature was the main explanatory variable in the montane forest. Soil CO₂ efflux in the lowland forest did not differ between the control and 9-11 yr N-addition plots, suggesting that chronic N input to nutrient-rich tropical lowland forests on well-buffered soils may not change their C balance on a decadal time scale. In the montane forest, first year N addition did not affect soil CO₂ efflux but annual CO₂ efflux was reduced by 14% and 8% in the 2nd and 3rd year N-addition plots, respectively, compared to the control. This reduction was caused by a decrease in soil CO₂ efflux during the high stem-growth period of the year, suggesting a shift in carbon partitioning from below- to aboveground in the N-addition plots in which stem diameter growth was promoted.

3.2 Introduction

Tropical forests contain more than 40% of the global carbon (C) stock in vegetation (IPCC, 2007), and they account for about one third of the global soil organic C storage down to a depth of one meter (Jobbágy & Jackson, 2000). Every year they cycle more than 10% of the atmospheric carbon dioxide (CO₂), the most important anthropogenic greenhouse gas (IPCC, 2007), through photosynthesis, respiration and microbial decay (Malhi, 2005). A major term in this biosphere-atmosphere CO₂ exchange is soil respiration, the second largest flux in the global terrestrial C cycle. Despite its central role in the global C cycle soil respiration remains least understood among ecosystem C processes (Luo & Zhou, 2006).

Soil temperature and moisture are important abiotic factors regulating CO₂ production in tropical forest soils (Davidson *et al.*, 2000; Schwendenmann *et al.*, 2003). Generally, rates of enzymatic respiration processes increase with temperature. The common relationship with soil moisture is that CO₂ efflux is small under dry conditions which depress root and microbial activity, reaches a maximal rate at intermediate soil moisture, and decreases again when anaerobic conditions prevail. Another regulating factor for soil respiration is nutrient availability, which in the case of nitrogen (N) is drastically increasing in tropical regions due to enhanced agricultural use of N fertilizer, cultivation of N-fixing plants, combustion of fossil fuels and biomass burning (Galloway *et al.*, 2003; 2008).

One way to evaluate potential future effects of N deposition on tropical forests is to create N-enriched conditions through N addition. Just three N-addition experiments have evaluated CO₂ efflux from tropical forest soils. Addition of 300 kg N ha⁻¹ yr⁻¹ to three submontane forests in Venezuela did not cause consistent trends in soil CO₂ efflux in the following year (Priess & Fölster, 2001). Soil CO₂ efflux was stimulated by three years of N addition (150 kg N ha⁻¹ yr⁻¹) to a Costa Rican lowland forest on an Ultisol soil. This response was accompanied by an increase in the top-soil fine root biomass (Cleveland & Townsend, 2006). In contrast, two years of N addition at the same rate to a Chinese lowland forest on an Oxisol soil reduced soil CO₂ efflux during the warm and wet growing season, while no effect was observed at lower N-addition levels (50 and 100 kg N ha⁻¹ yr⁻¹; Mo *et al.*, 2008). These differing results elucidate that responses of soil CO₂ efflux to increasing N availability may depend on N loading levels and possibly soil characteristics.

To address the question of how soil CO₂ efflux may respond to elevated N input the potential effects on root and microbial respiration need to be considered. Fine-root biomass and plant C allocation to mycorrhizal fungi typically decrease with rising N availability, which would reduce rhizosphere respiration, but to the contrary fine-root production, turnover and maintenance respiration may increase (Nadelhoffer, 2000; Norby & Jackson, 2000; Treseder, 2004). N addition can indirectly enhance microbial respiration if plant primary production and hence substrate availability are boosted (Luo & Zhou, 2006). The effects of N addition on decomposition depend on its stage: decomposition rates of light soil C fractions/fresh litter are accelerated but decomposition rates of heavier soil C fractions/humified organic matter are suppressed (Neff *et al.*, 2002). Finally, N enrichment may ultimately change soil chemical characteristics by increasing soil acidity, cation leaching (Lohse & Matson, 2005) and aluminum mobilization into the soil solution (Likens *et al.*,

1996) which may decrease microbial biomass (DeForest *et al.*, 2004) and root growth (Godbold *et al.*, 1988), consequently reducing soil respiration.

Our study reports the impact of longterm N addition (125 kg N ha⁻¹ yr⁻¹) on soil CO₂ efflux from two species-rich, old-growth tropical forests in Panama with contrasting N status: N-rich lowland forest on deeply-weathered Cambisol and Nitisol soils and N-limited montane forest on less-developed Andosol soils. In the lowland forest, annual fine litterfall, leaf litter decomposition rates (Kaspari *et al.*, 2008) and stem diameter growth were not affected by 5-6 years of N addition. Fine-root biomass at 0-0.2-m depth had not changed by 3- and 11-yr N addition (S.J. Wright, unpublished results). Soil pH and base saturation at 0-0.5 m depth were decreased after 8 years of N addition (Koehler *et al.*, 2009). In the montane forest, annual fine litterfall increased during the first two years of N addition, and the growth rates of stems in the 0.3-0.5 m diameter at breast height (dbh) class were promoted by 2- and 3-yr N addition (Adamek *et al.*, 2009a; Pame-Baldos, 2009). Fine-root biomass, production and turnover in organic layer and 0-0.2 m mineral soil did not change within 1.5-yr N addition (Adamek, 2009b). Based on these site characteristics we hypothesized that:

- 1) due to the increased soil acidity and resulting nutrient imbalances soil CO₂ efflux in the lowland forest will be smaller from the 9-11 yr N-addition than the control plots;
- 2) due to the increase in aboveground substrate supply for microbial decomposition soil CO₂ efflux in the montane forest will be larger from the 1-3 yr N-addition than the control plots.

3.3 Materials and methods

3.3.1 Study Area

The lowland study site (between 25-61 m elevation) consists of an old-growth (>300 years) semi-deciduous tropical forest (Leigh *et al.*, 1996) and is located on Gigante Peninsula (9°06'N, 79°50'W) which is part of the Barro Colorado Nature Monument, Republic of Panama. On nearby Barro Colorado Island, annual rainfall (1995-2007) averages 2650 ± 146 mm with a dry season from January to mid-May during which 297 ± 40 mm of rainfall is recorded. Ambient N deposition from rainfall was 9 kg N ha⁻¹ yr⁻¹, measured bi-weekly from 2006 to 2007 at the shore of Gigante Peninsula near the study site. Annual air temperature averages 27.4 ± 0.1 °C. The soil is derived from a dense basalt flow, has a heavy clay texture, and is classified as Endogleyic Cambisol in the lower and Acric Nitisol in the upper part of the landscape, respectively (FAO classification; alternatively Dystrudepts in USDA

classification). The soil aluminum (Al) saturation (0-0.05 m depth) was increased after 8 years of N addition (3.1 ± 2.9 and 26.6 ± 9.1 % Al on cation exchange capacity in the control and N-addition plots, respectively; $P = 0.050$).

The montane study site (between 1200-1300 m elevation) consists of an old-growth lower montane rainforest (Grubb, 1977) and is located in the Fortuna Forest Reserve in the Cordillera Central ($8^{\circ}45'N$, $82^{\circ}15'W$), Chiriquí province, Republic of Panama. Mean annual rainfall is 5532 ± 322 mm (1997-2007), and rainfall distribution exhibits a weak seasonality (11-yr average of 244–288 mm month⁻¹ from February to April and 403–683 mm month⁻¹ from March to January). Ambient N deposition from rainfall was 5 kg N ha⁻¹ yr⁻¹, measured bi-weekly from 2006 to 2007 at a forest clearing near the study site. The average monthly air temperature is 19 °C from December to March and 21 °C for all other months (annual mean 20.1 ± 0.1 °C; 1999-2007). Monthly stem diameter increments are largest between July and December and clearly smaller in the rest of the year (Adamek *et al.*, 2009a). The soil is derived from volcanic ash deposits, has a sandy loam texture, a substantial organic layer (median thickness of 8 cm) and is classified as Aluandic Andosols (FAO) or Hapludands (USDA). Before treatment, this soil had lower pH and base saturation and larger exchangeable aluminum content than the control and 8-yr N-addition lowland forest soil. 3-yr N addition did neither affect top soil pH (4.33 ± 0.10 and 4.38 ± 0.13 at 0-0.05 m depth in the control and N-addition plots, respectively) nor pH down to a depth of 0.4 m (4.76 ± 0.14 and 4.72 ± 0.16 in the control and N-addition plots, respectively). The increase in chronic mineral soil extractable NO₃⁻ concentrations, which was statistically undistinguishable from the control during the first two years of N addition, was significant concerning the 3-yr N-addition period ($P=0.015$). Detailed soil characteristics, forest structure, and temporal patterns of soil mineral N concentrations in both sites can be found in Koehler *et al.* (2009).

3.3.2 Experimental design

In the lowland, our study was conducted in the only ongoing chronic nutrient addition experiment in old-growth forest. The experiment includes N-addition and control plots laid out in four replicates across a 26.6-ha area in a stratified random design. N addition started in June 1998. In the montane forest, the experiment was set up in a paired-plots random design with four replicates. N addition started in February 2006. At both sites, each plot is 40x40 m in size and plots are separated by at least 40 m distance. The N-addition plots received 125 kg urea-N ha⁻¹ yr⁻¹ split in four equal applications. In the lowland forest, N was applied during

wet season with six to eight weeks between applications. In the montane forest, the N applications were spread during the year with at least seven weeks time-lag (for details please see Koehler *et al.* (2009)).

3.3.3 Soil CO₂ efflux, temperature and moisture measurements

From January 2006 to January 2009 we measured soil CO₂ efflux, soil temperature and soil moisture every six weeks on all plots and more intensively on the N-addition plots (two to five times within a six week period following N addition). In each plot, four permanent chamber bases were inserted ~ 0.02 m into the soil in a stratified random design along two perpendicular 20-m long transects that cross the plot's central point. Therefore, all chambers were surrounded (buffered) by at least 10 m of forest receiving the same treatment. Soil CO₂ efflux was measured during the day using vented static chambers (area 0.04 m², height 0.25 m). A study on nearby Barro Colorado Island had indicated that day and night soil CO₂ efflux was statistically undistinguishable (Kursar, 1989). Four gas samples (100 mL each) were removed at 2, 12, 22 and 32 minutes after chamber closure and stored in pre-evacuated glass containers with a teflon stopcock. Gas samples were analyzed using a gas chromatograph (Shimadzu GC-14B, Germany) equipped with an electron capture detector (Loftfield *et al.*, 1997) which was calibrated with three to four standard gases (360, 706, 1505 and 5012 ppm CO₂, Deuste Steininger GmbH, Mühlhausen, Germany). Gas fluxes were calculated from the concentration increase in the chamber versus time, and were adjusted for air temperature and atmospheric pressure measured at the time of sampling. To account for the decreasing diffusion gradient over time caused by the chamber feedback we fitted both a linear and a quadratic regression model if CO₂ concentrations increased asymptotically (Wagner *et al.*, 1997). We chose the statistically more adequate model based on the Akaike Information Criterion. The quadratic model was used in 29% of the gas flux calculations. If the concentration increase leveled out but the quadratic model was statistically inferior we excluded the respective last data points and calculated the flux based on a linear model. This data screening and calculation procedures provide that we minimized underestimations which may occur if a linear model was uncritical applied to static chamber flux data (e.g. Livingston *et al.*, 2006). Two pre-treatment measurements in the montane forest indicated that initial soil CO₂-efflux did not differ between control and N-addition plots before manipulation. We do not have pre-treatment measurements of soil CO₂ efflux from the 9-10-yr N-addition plots of

the lowland forest. The annual gaseous C losses were approximated by applying the trapezoid rule on time intervals between measured flux rates, assuming constant flux rates per day.

Parallel to gas sampling, soil temperature was measured at 0.05 m depth near each of the four chamber bases per plot. For soil moisture, four samples of 0–0.05 m mineral soil (and additionally from the organic layer at the montane site) were collected within the inner 10x10 m of each plot and pooled. A subsample was oven-dried at 105 °C for 24h. Soil moisture is expressed as percentage of water-filled pore space, assuming a particle density of 2.65 g cm⁻³ for mineral soil (Linn & Doran, 1984) and of 1.4 g cm⁻³ for organic layer (Breuer *et al.*, 2002).

3.3.4 Statistical analyses and calculations

If data sets were rightly skewed a square-root or logarithmic transformation was applied before analysis. If data sets were left-skewed a quadratic or cubic transformation was applied before analysis. Regression analyses (on treatment means) were conducted to investigate the influence of soil moisture and temperature on soil CO₂ efflux. For the lowland forest, the data of the control and N-addition plots were pooled to increase the robustness of parameter estimates. This was justified by their comparable soil CO₂ efflux, temperature and moisture (see Sect. 3). In multiple regression or if including squared terms the explanatory variables x were mean-centered and normalized before analysis [$x^*=(x-\text{mean}(x))/\text{standard error}(x)$]. Multiple regression analyses were conducted by first fitting the maximal model (containing all linear, squared and interaction terms) and progressing to the minimal adequate model through a series of single-term deletions based on F -tests (Crawley, 2002). Variance inflation factors as multicollinearity measure were < 2 in all models. Model significance was assessed by regression analysis of variance. Linear mixed effects models (on plot means) were used to test for the ‘fixed effect’ of treatment (N addition), site (lowland vs. montane forest) or season on the time-series of the response variables (i.e. the repeated measurements of soil CO₂ efflux, soil temperature and water-filled pore space). The spatial replication nested in time was included as ‘random’ effect. The models were specified as explained in Koehler *et al.* (2009) and the significance of the fixed effect was evaluated using analysis of variance (Crawley, 2002). For soil characteristics, treatment effects and/or differences between sites were assessed using independent t -tests. In all analyses concerning soil CO₂ efflux, only the fluxes measured at least 6 weeks after an N-application were considered (see Sect. 3.3). Effects were considered significant if P value ≤ 0.05 . For the montane forest, we calculated

the ratio of soil CO₂ efflux to mean monthly stem diameter growth (0.3-0.5 m dbh class) per plot based on the growth data reported in Adamek *et al.* (2009a) and Pame-Baldos (2009). If the mean stem diameter growth in a plot was effectively zero (<0.1 mm month⁻¹) these ratios were excluded as they were artificially large (>4.5 times the interquartile range). The plot ratios were normalized by division with the maximal value, and thus converted to a dimensionless measure. Mean values in the text are given with ± 1 standard error, regression parameter estimates are given with the 95% confidence level. Analyses were conducted using R 2.9.0 (R Development Core Team, 2009).

3.4 Results

3.4.1 Water-filled pore space and temperature in the control forest soils

Water-filled pore space (WFPS) showed a seasonal pattern in the lowland forest where it varied by 34% between dry and wet seasons (Fig. 3-1a). In the montane forest, WFPS was larger in the mineral soil than in the organic layer. WFPS varied less throughout the year than in the lowland (16% and 21% in organic layer and mineral soil, respectively; Fig. 3-1b). In contrast, soil temperature at 0.05 m depth varied seasonally by only 1.7 °C (annual mean of 25.5 °C) in the lowland (Fig. 3-1c) but by 3.8 °C (annual mean of 18.1 °C) in the montane forest (Fig. 3-1d). An unusually low-rainfall period in the montane forest (February to April 2007 with ~40% less rain than the 11-yr average) caused a reduction in the WFPS in both mineral soil and organic layer. With the onset of higher rainfall the WFPS re-increased in the mineral soil while it remained smaller in the organic layer until the end of the study (Fig. 3-1b). WFPS and soil temperature did not differ between control and N-addition plots at either site.

3.4.2 Soil CO₂ efflux of the control forests

Soil CO₂ effluxes were larger from the lowland (189.60 ± 7.95 mg C m⁻² h⁻¹) than the montane forest (107.29 ± 4.68 mg C m⁻² h⁻¹, $P = 0.004$, Table 3-1). In the lowland, they ranged between 83.45 ± 17.69 and 283.99 ± 36.08 mg C m⁻² h⁻¹ and displayed a distinct seasonal pattern, averaging smaller during dry season (136.96 ± 16.82 mg C m⁻² h⁻¹) than during wet season (205.20 ± 6.60 mg C m⁻² h⁻¹, $P < 0.001$, Fig. 3-2a and c). $26.18 \pm 1.50\%$ of the annual CO₂ efflux occurred during the ~130 days of dry season. WFPS explained a larger fraction of the variance in soil CO₂ efflux than soil temperature. Soil CO₂ effluxes were

maximal at an intermediate WFPS and decreased below and above this value (Fig. 3-3a). Based on a regression tree moisture limitation of soil CO₂ production took place below a WFPS of ~38 %. A regression between soil CO₂ efflux and temperature illustrates that temperature was only a relevant explanatory variable if CO₂ production was not limited by low soil moisture (Fig. 3-4a; please note that the linear regression slope would not differ if the control and N-addition plots would be analyzed separately). Accordingly, the minimal adequate multiple regression model contains not only WFPS (and its quadratic term) and soil temperature but also the interaction-term of both factors (parameter estimates \pm 95% CI):

$$CO_2 = 189.07(\pm 12.18) + 3.24(\pm 1.51)T^* + 2.09(\pm 1.18)WFPS^* - 0.22(\pm 0.14)WFPS^{*2} - 0.28(\pm 0.21)WFPS^*T^* \quad (3-1)$$

where CO_2 is mean soil CO₂ efflux ($mg\ C\ m^{-2}\ h^{-1}$), T is soil temperature at 0.05 m depth ($^{\circ}C$), $WFPS$ is water-filled pore space (%) and * indicates that the variable was mean-centered and normalized before analysis ($n = 47$, $R^2 = 0.65$, $P < 0.001$).

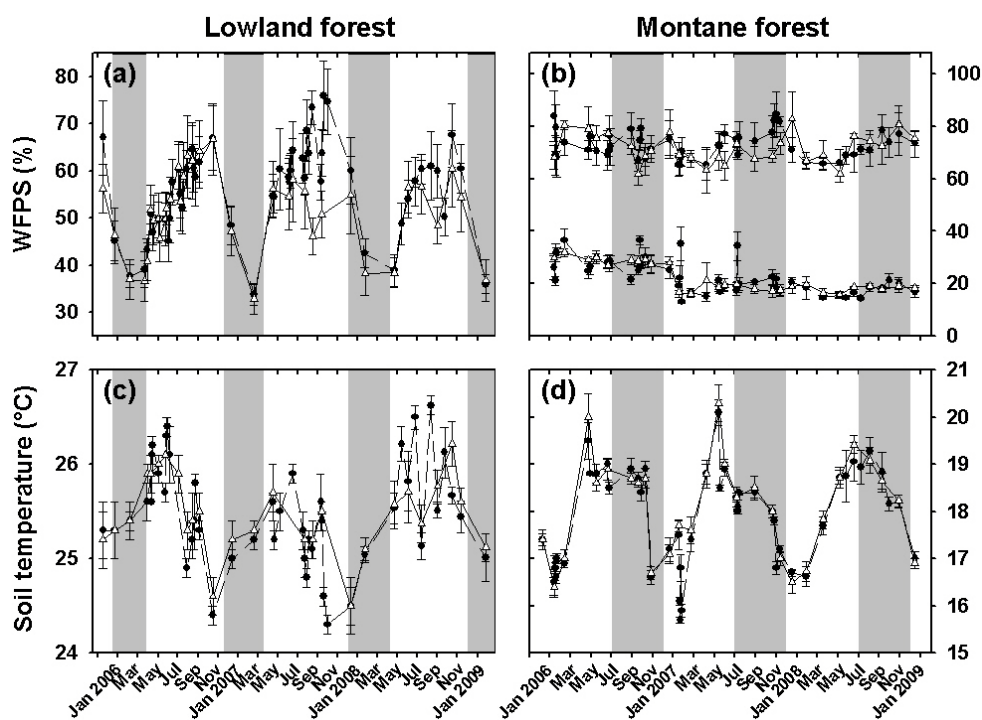


Figure 3-1. Mean (\pm SE, $n = 4$) water-filled pore space (WFPS) and soil temperature at 0.05 m depth in the control (Δ) and N-addition (\bullet) lowland (a and c) and montane (b and d) forest. For WFPS in the montane forest, the upper and lower values are for the 0-0.05 m mineral soil and organic layer, respectively. Grey shading marks the dry seasons in the lowland forest, and the high stem-growth periods in the montane forest.

Soil CO₂ effluxes from the montane forest varied less than in the lowland, between 51.27 ± 3.22 and $165.01 \pm 6.26\ mg\ C\ m^{-2}\ h^{-1}$. In 2007 and 2008 they were larger during the

high stem-growth period than during the other months ($P = 0.001$, Fig. 3-2b and d). No relationship was detected between soil CO₂ efflux and WFPS (in either organic layer or mineral soil, Fig. 3-3b), while soil CO₂ efflux increased with increasing soil temperature (Fig. 3-4b).

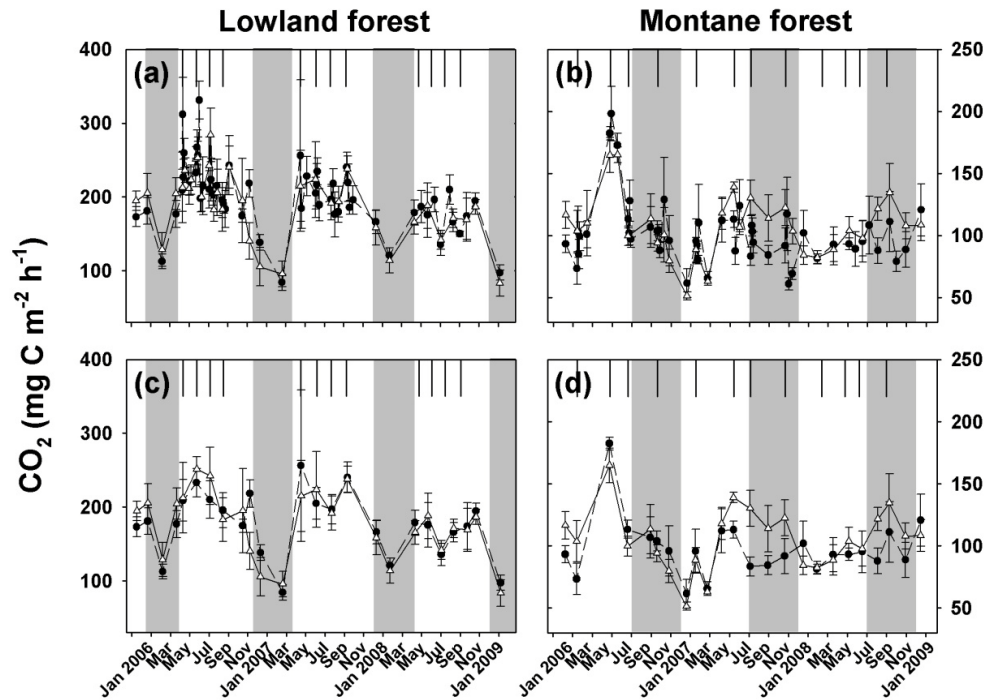


Figure 3-2. Mean (\pm SE, $n = 4$) soil CO₂ efflux from the control (Δ) and N-addition (\bullet) lowland (a and c) and montane (b and d) forest. Upper panels include the transitory fertilization effects, and lower panels show only the chronic fluxes at least 6 weeks after an N addition. Black vertical lines indicate dates of N addition. Grey shadings mark the dry seasons and the high stem-growth periods in the lowland and montane forest, respectively.

Table 3-1. Annual soil CO₂ efflux (Mg C ha⁻¹, mean ± SE, *n* = 4) for control and N-addition plots. Only CO₂ fluxes measured at least 6 weeks after an N addition have been used for this calculation (see paragraph 3.4.3).

Site	Treatment	2006	2007	2008
Montane	Control	9.93 ± 0.62	9.17 ± 0.55	9.01 ± 0.55
	1 - 3-yr N addition	(11.03 ± 0.51 [*])	7.88 ± 0.35	8.30 ± 0.22
Lowland	Control	17.12 ± 1.59	15.63 ± 0.91	13.59 ± 1.34
	9 - 11-yr N addition	16.30 ± 0.92	15.45 ± 0.87	13.84 ± 0.93

* The two pre-treatment measurements from January and February 2006 (Fig. 3-2b, d) were excluded. Note that this annual value is biased towards an overestimation because the high CO₂ efflux measured in May 2006 is not representative for the integration time it represents.

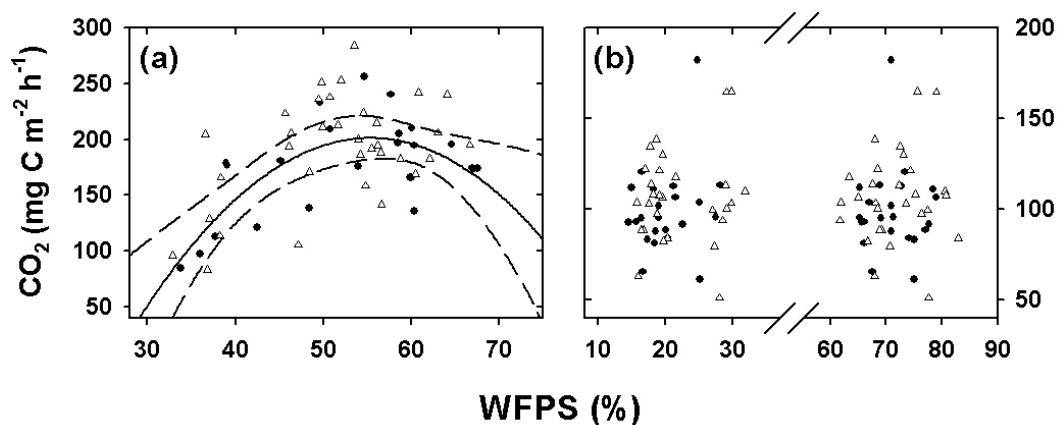


Figure 3-3. Regression analyses (parameter estimates ± 95% CI) between mean water-filled pore space (WFPS) and CO₂ efflux of the control (Δ) and N-addition (●) plots for the a) lowland [$y = 204.45 (\pm 13.06) + 1.78 (\pm 1.32) x^* - 0.35 (\pm 0.16) x^{*2}$, $R^2 = 0.42$, $n = 60$, $P < 0.001$, * denotes that the variable x was mean-centered and normalized before analysis] and b) montane forest (no significant relationships). For the lowland forest, the analysis was conducted on the pooled data of the control and N-addition plots (see Sect. 3.3.4). For the montane forest, the analysis was conducted separately for the control and N-addition plots. Data points to the left and right of the x-axis break are for the organic layer and mineral soil, respectively. For both sites, only CO₂ fluxes measured at least 6 weeks after an N addition were included (see Sect. 3.3).

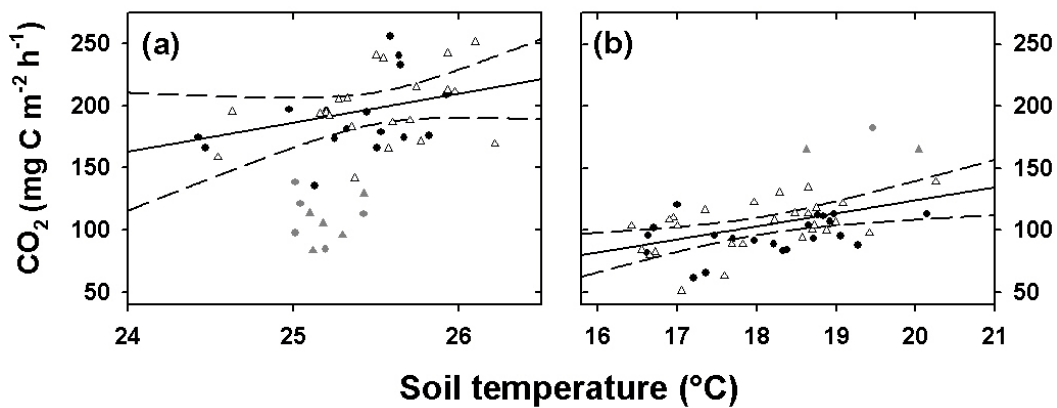


Figure 3-4. Linear regressions (parameter estimates \pm 95% CI) between mean soil temperature (0.05 m depth) and CO₂ efflux of the control (Δ) and N-addition (\bullet) plots for the a) lowland [$y = -484.45 (\pm 551.25) + 26.71 (\pm 21.67) x$, $R^2 = 0.15$, $n = 51$, $P = 0.017$] and b) montane forests [control plots: $y = -86.34 (\pm 128.13) + 10.51 (\pm 7.10) x$, $R^2 = 0.27$, $n = 26$, $P = 0.005$; N-addition plots: no significant relationship]. For the lowland forest, the analysis was conducted on the pooled data of the control and N-addition plots (see Sect. 2.4) and excluded ten data points (grey) of which soil CO₂ production was limited by low soil moisture content. For the montane forest, the analysis was conducted separately for the control and N-addition plots and excluded the three large CO₂ fluxes from May 2006 (grey; Fig. 2b and d). For both sites, only CO₂ fluxes measured at least 6 weeks after an N addition were included (see Sect. 3.3).

3.4.3 Effects of elevated N input on the chronic soil CO₂ efflux

Often, during the time when soil extractable N concentrations were artificially elevated within a month following an N application (Koehler *et al.*, 2009), transitory peaks occurred in soil CO₂ efflux (Fig. 3-2a and b). Because we are interested in evaluating the ultimate long-term effects of an N-enriched soil N-cycle on soil CO₂ efflux we excluded these transitory effects from the subsequent analyses and only considered the ‘chronic’ fluxes measured at least 6 weeks after an N-application, which are reported in the following. In the lowland forest, soil CO₂ efflux did not differ between the control and 9-11-yr N-addition plots (176.59 ± 8.64 mg C m⁻² h⁻¹, Fig. 3-2c). In the montane forest, soil CO₂ efflux did not differ between the control and N-addition plots during the first year of N addition (112.14 ± 11.53 mg C m⁻² h⁻¹). In the second year of N addition, soil CO₂ efflux was smaller from the N-addition than the control plots during the high stem-growth period (i.e. July to December, $P = 0.025$). These diminished CO₂ effluxes resulted in 14% reduction of the mean annual soil CO₂ efflux relative to the control (Fig. 3-5a, Table 3-1). A reduction of soil CO₂ efflux from the N-

addition plots was observable during the high stem-growth period in the third year as well, but these fluxes were statistically undistinguishable from the controls ($P = 0.163$; Figs. 3-2d, 3-5b, Table 3-1). The ratio of soil CO₂ efflux to monthly stem diameter growth (0.3-0.5 m dbh class) was smaller in the N-addition than the control plots ($P = 0.018$). Considering the time period since this effect emerged (i.e. May 2007) until the end of the study the reduction averaged $16 \pm 3\%$ (Fig. 3-6). Differing from the controls, soil temperature did not explain a significant fraction of the variance in soil CO₂ efflux from the N-addition plots (Fig. 3-4b; $R^2 = 0.13$, $n = 21$, $P = 0.105$).

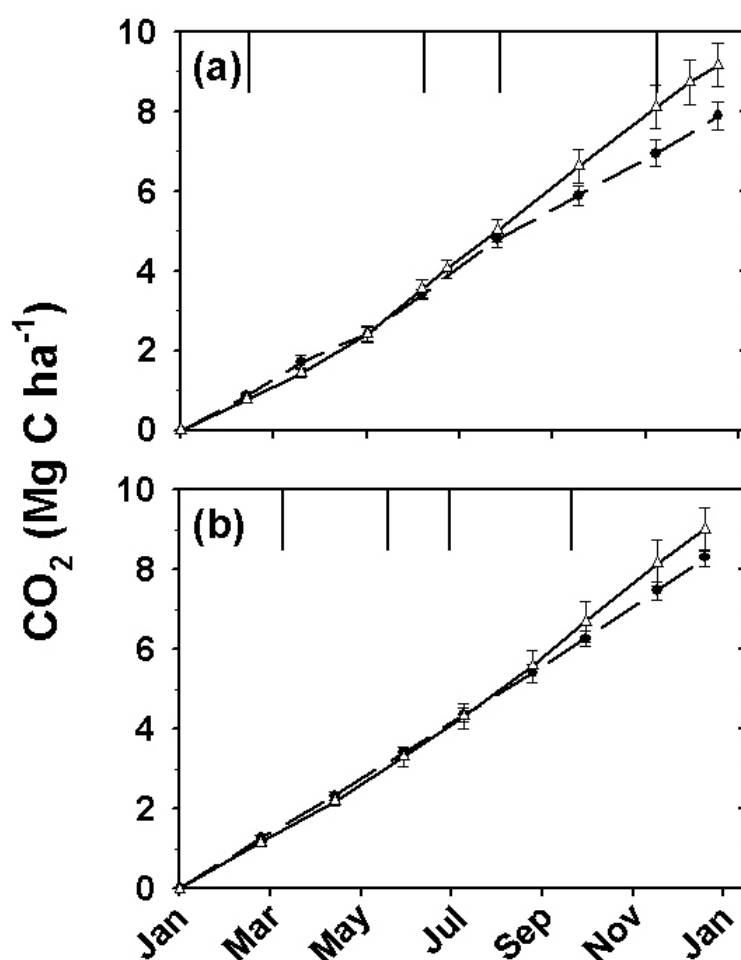


Figure 3-5. Mean (\pm SE, $n = 4$) cumulative soil CO₂ efflux from the control (Δ) and N-addition (\bullet) montane forest in a) 2007 (2-yr N addition) and b) 2008 (3-yr N addition). Only CO₂ fluxes measured at least 6 weeks after an N addition were included in this calculation (see Sect. 3.3). Black vertical lines indicate dates of N addition.

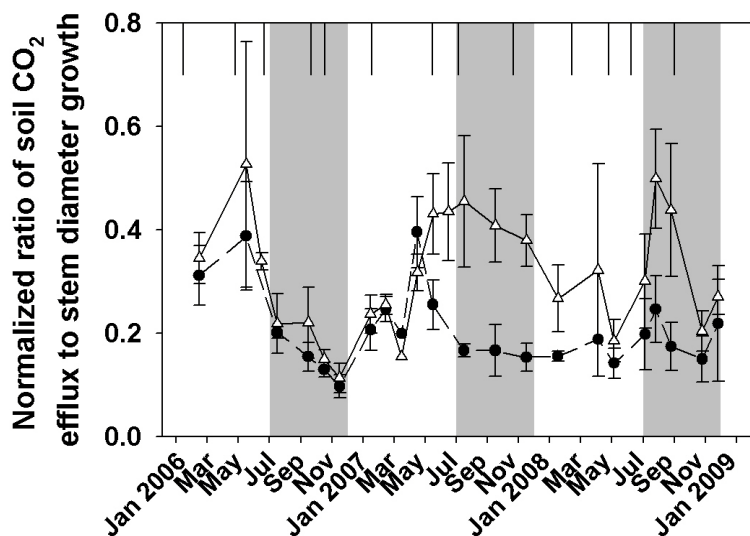


Figure 3-6. Mean (\pm SE, $n = 4$) normalized ratio of soil CO₂ efflux to monthly stem growth of trees with 0.3-0.5 m diameter at breast height from the control (Δ) and N-addition (\bullet) montane forest. Black vertical lines indicate dates of N addition. Grey shadings mark the high stem-growth periods. Only CO₂ fluxes measured at least 6 weeks after an N addition were included in this calculation (see Sect. 3.3).

3.5 Discussion

3.5.1 Soil moisture and temperature regulation on soil CO₂ efflux from the control forests

The importance of soil moisture and temperature in regulating soil CO₂ efflux, through their influence on CO₂ production by microbial and root respiration, differed between the lowland and montane forests. We did not calculate apparent Q_{10} values of soil CO₂ efflux because in the field the influence of plant phenology and soil temperature variation at an arbitrarily chosen depth can not be separated (Davidson *et al.*, 2006). The influence of plant phenology on soil respiration is mainly due to different timing of litterfall, root growth, and root turnover (Curiel Yuste *et al.*, 2004). In the lowland forest, the seasonality in rainfall and thus in soil moisture strongly influences plant phenology as well as decomposition. Leaf fall peaks during dry season when decomposition is limited by low soil moisture (Cornejo *et al.*, 1994), while nutrient mineralization rates (except for potassium) are much greater during wet than during dry season (Yavitt *et al.*, 2004). Fine root productivity is also restricted by low water supply and hardened soil during dry season. Fine roots grow rapidly during the first half of wet season and much less during the remainder of the year, and maximum fine root biomass

occurs in the transition between dry and wet season (Cavelier *et al.*, 1999; Yavitt & Wright, 2001). The soil CO₂ efflux reflected these patterns in decomposition and plant phenology. The effluxes were largest in the first half of wet season and decreased thereafter, reaching their minimum at the end of dry season (Fig. 3-2c). The regression analyses confirmed the strong influence of soil moisture on soil CO₂ efflux (Fig. 3-3a). The interaction term between soil moisture and temperature in the multiple regression model (Eq. (1)) reflects that soil CO₂ efflux only increased with temperature if CO₂ production was not limited by low soil moisture content (Fig. 3-4a). The annual soil CO₂ efflux is comparable to values reported from other old-growth tropical lowland forests (Raich & Schlesinger, 1992).

In the montane forest, only soil temperature explained a significant fraction of the variance in soil CO₂ efflux. This site receives almost double annual rainfall than the lowland forest and has lower air and soil temperatures. The fine litterfall exhibits a seasonal pattern with larger amounts falling in the windier period between ~November and February. In spite of the availability of fresh substrate for microbial decomposition, soil CO₂ effluxes were smaller during this colder period of the year (Figs. 3-1d, 3-2d). This suggests that the increase of CO₂ efflux in May was prompted by the simultaneously rising soil temperature, and that CO₂ production was hampered by low temperatures during ~February to April. However, the seasonal pattern in soil CO₂ efflux probably resulted in part from changes in root biomass and production. If these were largely temperature-independent and mainly regulated by a different factor (e.g. photosynthetically active radiation) they may have confounded the increase of soil CO₂ efflux with temperature. The annual soil CO₂ efflux is comparable to values reported from other old-growth tropical montane forests (Raich, 1998; Priess & Fölster, 2001). In the lowland forest, where soil temperature varies little throughout the year, seasonal changes in soil CO₂ efflux were mainly triggered by differences in soil moisture while the opposite seemed to be the case in the montane forest.

3.5.2 Effects of N addition on soil CO₂ efflux from the lowland forest

Soil CO₂ efflux did not differ between the control and N-addition plots in the lowland forest (Fig. 3-2c, Table 3-1) and, in combination with results from studies on fine roots, litterfall and decomposition, this suggests that both root and microbial respiration were resilient to the observed N-induced changes in soil chemical characteristics. Our measured bulk soil CO₂ efflux does not allow us to distinguish between the CO₂ sources. It is possible that an increase

in CO₂ production from one source was offset by a decrease from the other source. However, our assumption that neither root nor microbial respiration were strongly influenced by chronic N addition is in line with previous findings: 1) fine root biomass in 0-0.2-m depth had not changed by 3- and 11-yr N addition (S. J. Wright, unpublished results) and 2) neither annual leaf litterfall nor leaf litter mass loss rates were influenced by 6-yr N addition (Kaspari *et al.*, 2008).

Our result that elevated N-input did not affect soil CO₂ efflux contrasts the findings from an N-addition study in an N-rich Costa Rican lowland forest on an Ultisol soil. In that study, laboratory experiments with root-free soil showed that microbial respiration was not altered by N addition (Cleveland *et al.*, 2006; Cleveland & Townsend, 2006). In the field, however, soil CO₂ efflux was boosted by 3-yr addition of 150 kg N ha⁻¹ yr⁻¹. This rise was partly attributed to a parallel increase in the top-soil fine root biomass. A possible explanation for the contrasting results in our study and theirs is that root responses on a smaller scale of nutrient manipulation (5x5 m treatment plots in Costa Rica) may differ from - and might not reflect - responses to fertilization across entire root systems occupying larger soil volumes (40x40 m treatment plots in this study; Raich *et al.*, 1994; Ostertag, 2001; Cleveland & Townsend, 2006).

The fact that soil CO₂ efflux did not change under chronic N addition despite alterations in soil chemical traits (i.e. decrease in pH and base saturation, increase in Al saturation) may be explained by the initial soil characteristics of our site. Our soils have a higher pH, effective cation exchange capacity and base saturation than Ferralsols/Oxisols (Koehler *et al.*, 2009), and a very low Al saturation. The supply of available phosphorus (P) is possibly sufficient, i.e. litterfall and stem diameter growth did not respond to P-addition (S.J. Wright, unpublished results). Data on dissolved ions indicate that active weathering occurs in both the control and chronic N-addition plots (M.D. Corre, unpublished results). After 8 years of N addition, the top soil pH (4.5 ± 0.1) was still in the upper part of the range wherein acidity is neutralized by Al solubilization from silicates and hydrous oxides (pH 3-5, Van Breemen *et al.*, 1983). Therefore, despite the observed increase in Al saturation, the Al concentrations may not have reached a level where toxicity effects on roots and microbial biomass are expressed. After a decade of N addition, the good nutrient-supplying and buffering capacity in our soils still mitigates acidity- or Al-induced reductions of soil respiration.

With N addition ongoing we expect that our studied forest will eventually exhibit a decline in soil CO₂ efflux, as reported from N-enriched temperate forests (Bowden *et al.*,

2004) and an N-saturated tropical lowland forest on an Oxisol soil in China. The Chinese site has been receiving high atmospheric deposition of $>30 \text{ kg N ha}^{-1} \text{ yr}^{-1}$ for several decades. Aboveground primary production (fine litterfall and stem growth) was not affected by N addition (Mo *et al.*, 2008; J. Mo, personal communication). Already the control top soil pH (3.76 ± 0.01) is in the lower part of the Al-buffer range and hence a progressing N-induced acidification may increasingly manifest Al-toxicity on roots and microbial biomass. The observed decrease in soil CO₂ efflux within 2-yr experimental addition of $150 \text{ kg N ha}^{-1} \text{ yr}^{-1}$ was indeed accompanied by a decline in microbial biomass, fine root biomass (both in the top soil) and litter decomposition rates (Mo *et al.*, 2006; 2008). Our finding that soil CO₂ efflux did not change with chronic N addition to an old-growth tropical lowland forest differs from both previous studies but this is explicable by scale-related differences in root responses to N addition on the one hand and site-specific soil characteristics as well as exposure time and N-loading level on the other hand.

3.5.3 Effects of N addition on soil CO₂ efflux from the montane forest

Soil CO₂ efflux did not differ between the control and 1-yr N-addition plots but was diminished during the high stem-growth period in the second and third year of N addition (statistically distinguishable only in the second year, Fig. 3-2d). As 3-yr N addition did not alter the soil pH from the organic layer down to 0.4 m depth, this decrease was not due to acidification and pH-related changes in soil chemistry. The decline occurred simultaneously with an enhancement of stem diameter growth (Adamek *et al.*, 2009a; Pame-Baldos, 2009), yielding reduced ratios of soil CO₂ efflux to stem growth in the N-addition plots (Fig. 3-6). This link, which hints at a shift in C partitioning from below- to aboveground, persisted throughout the study period and suggests that the decline in soil CO₂ efflux was partly attributable to a decrease in rhizosphere respiration. The fact that 1.5-yr N addition did not affect fine root biomass, production or turnover in the organic layer and 0-0.2-m mineral soil (Adamek, 2009b) does not invalidate this implication because a reduction of root and root-associated respiration may also stem from a decline in the total belowground C allocation and rhizosphere C flux (Giardina *et al.*, 2004) or a decrease in root colonization with mycorrhizal fungi (Treseder, 2004; Talbot *et al.*, 2008). Also we do not have information about possible fine root responses that may have occurred after August 2007, or on coarse roots. Soil CO₂ efflux was positively correlated with soil temperature in the control plots while the same relationship was not significant in the N-addition plots (Fig. 3-4b). Based only on the

regression statistics we would not claim that this indicates a reduction of temperature sensitivity, however, it is a hypothesis which deserves further investigation. A similar response as in our studied Panamanian forest has been found in a nutrient-limited tropical Eucalyptus plantation where fertilization (with N, P, potassium and micronutrients) increased wood productivity as well as total litterfall but decreased C allocation to fine roots and reduced soil CO₂ efflux by 18% (Giardina *et al.*, 2004). Also, a recent analysis of annual C budgets for 63 forest ecosystems from temperate, boreal and tropical regions strongly supported the assumption that enhanced nutrient availability generally increases C partitioning to aboveground net primary production -mainly to wood production- while it decreases partitioning to the total belowground C flux (Litton *et al.*, 2007).

We can not exclude the possibility that, besides the shift in C partitioning from below to aboveground and a resulting diminution of rhizosphere respiration, microbial respiration may have decreased as well. Within the first two years of N addition the total fine litterfall was ~1 Mg C ha⁻¹ larger in the N-addition than the control plots (Adamek *et al.*, 2009a), enlarging the substrate pool for decomposition. In this forest with restricted decomposition, however, the mean annual input of litterfall-C (4.3 Mg C ha⁻¹ yr⁻¹) is small compared to the C stock in the organic layer (~25 Mg C ha⁻¹). N addition reduced microbial biomass and activity of ligninolytic and cellulolytic enzymes in temperate forests with organic horizons (DeForest *et al.*, 2004; Frey *et al.*, 2004) and has been attributed to retard degradation of recalcitrant C fractions, thereby causing increases in the organic matter stock of forests (Berg & Meentemeyer, 2002). Further process-oriented studies (e.g. mycorrhizal association, microbial community composition, and enzyme activities) would greatly contribute to a deeper understanding of our observed changes in the montane forest's C cycling, and would elucidate to which extent the observed shift in C allocation explains the reduction in soil CO₂ efflux.

3.5.4 Consequences of chronic N deposition on carbon cycling in tropical forests

Biological demand for N (i.e. presence or absence of N limitation on vegetation growth) was an important qualitative predictor of the response of soil CO₂ efflux to elevated soil N availability. For tropical lowland forests on soils with high nutrient-supplying and buffering capacity, where primary productivity is not N-limited, we do not expect that chronic N

addition will affect their C balance in the short term or on a decadal time scale. In the long term, soil CO₂ efflux (and forest productivity) may eventually decline as N enrichment is accompanied by a progressing soil acidification and changing soil chemical traits. However - based on our results and baring in mind that the experimental N-loading exceeded anticipated N deposition rates- this condition may take many years to develop. The onset of a decrease in soil CO₂ efflux will be strongly determined by the N loading and initial soil characteristics (e.g. pH, cation exchange capacity and base saturation). On the other hand, N addition might cause a reduction in soil CO₂ efflux from tropical montane forests which have N-limited primary productivity. Once N limitation is alleviated a relatively quick shift in C partitioning from below- to aboveground may occur. In the longer term, such shift would cause imprints on the magnitude of soil C storage.

3.6 References

- Adamek M, Corre MD, Hölscher D (2009a) Early effect of elevated nitrogen input on above-ground net primary production of a lower montane rain forest, Panama. *Journal of Tropical Ecology*, **25**, 637-647.
- Adamek M (2009b) *Effects of increased nitrogen input on the net primary production of a tropical lower montane rain forest, Panama*. Ph.D. thesis, University of Goettingen, Goettingen, Germany, 105 pp.
- Berg B, Meentemeyer V (2002) Litter quality in a north European transect versus carbon storage potential. *Plant and Soil*, **242**, 83-92.
- Boone RD, Nadelhoffer KJ, Canary JD, Kaye JP (1998) Roots exert a strong influence on the temperature sensitivity of soil respiration. *Nature*, **396**, 570-572.
- Bowden RD, Davidson EA, Savage K, Arabia C, Steudler PA (2004) Chronic nitrogen additions reduce total soil respiration and microbial respiration in temperate forest soils at the Harvard Forest. *Forest Ecology and Management*, **196**, 43-56.
- Breuer L, Kiese R, Butterbach-Bahl K (2002) Temperature and moisture effects on nitrification rates in tropical rain-forest soils. *Soil Science Society of America Journal*, **66**, 834-844.
- Cavelier J, Wright SJ, Santamaría J (1999) Effects of irrigation on litterfall, fine root biomass and production in a semideciduous lowland forest in Panama. *Plant and Soil*, **211**, 207-213.
- Cleveland C, Reed SC, Townsend AR (2006) Nutrient regulation of organic matter decomposition in a tropical rain forest. *Ecology*, **87**, 492-503.
- Cleveland CC, Townsend AR (2006) Nutrient additions to a tropical rain forest drive substantial soil carbon dioxide losses to the atmosphere. *Proceedings of the National Academy of Sciences*, **103**, 10316-10321.
- Cornejo FH, Varela A, Wright SJ (1994) Tropical forest litter decomposition under seasonal drought: nutrient release, fungi and bacteria. *Oikos*, **70**, 183-190.
- Crawley MJ (2002) *Statistical Computing, An Introduction to Data Analysis using S-Plus*. John Wiley & Sons Ltd, Chichester, England, 761 pp.
- Curiel Yuste J, Janssens IA, Carrara A, Ceulemans R (2004) Annual Q₁₀ of soil respiration reflects plant phenological patterns as well as temperature sensitivity. *Global Change Biology*, **10**, 161-169.

-
- Davidson EA, Verchot LV, Cattânio JH, Ackerman IL, Carvalho JEM (2000) Effects of soil water content on soil respiration in forests and cattle pastures of eastern Amazonia. *Biogeochemistry*, **48**, 53-69.
- Davidson EA, Janssens IA, Luo Y (2006) On the variability of soil respiration in terrestrial ecosystems: moving beyond Q₁₀. *Global Change Biology*, **12**, 154-164.
- DeForest JL, Zak DR, Pregitzer KS, Burton AJ (2004) Atmospheric nitrate deposition, microbial community composition, and enzyme activity in Northern Hardwood Forests. *Soil Science Society of America Journal*, **68**, 132-138.
- Frey SD, Knorr M, Parrent JL, Simpson RT (2004) Chronic nitrogen enrichment affects the structure and function of the soil microbial community in temperate hardwood and pine forests. *Forest Ecology and Management*, **196**, 159-171.
- Galloway JN, Aber JD, Erisman JW, Seizinger SP, Howarth RW, Cowling EB, Cosby BJ (2003) The Nitrogen Cascade. *BioScience*, **53**, 341-356.
- Galloway JN, Townsend AR, Erisman JW, *et al.* (2008) Transformation of the nitrogen cycle: recent trends, questions, and potential solutions. *Science*, **320**, 889-892.
- Giardina CP, Binkley D, Ryan MG, Fownes JH, Senock RS (2004) Belowground carbon cycling in a humid tropical forest decreases with fertilization. *Oecologia*, **139**, 545-550.
- Godbold DL, Fritz E, Hüttermann A (1988) Aluminum toxicity and forest decline. *Proceedings of the National Academy of Sciences*, **85**, 3888-3892.
- Grubb PJ (1977) Control of forest growth and distribution on wet tropical mountains: with reference to mineral nutrition. *Annual Review of Ecology and Systematics*, **8**, 83-107.
- IPCC (2007) In *Climate Change 2007: The Physical Science Basis. Contribution of Working Group I to the Fourth Assessment Report of the Intergovernmental Panel on Climate Change* (eds Solomon S, Qin D, Manning M, *et al.*), pp. 996. Cambridge University Press, Cambridge, UK and New York, NY, USA.
- Jobbágy EG, Jackson RB (2000) The vertical distribution of soil organic carbon and its relation to climate and vegetation. *Ecological Applications*, **10**, 423-436.
- Kaspari M, Garcia MN, Harms KE, Santana M, Wright SJ, Yavitt JB (2008) Multiple nutrients limit litterfall and decomposition in a tropical forest. *Ecology Letters*, **11**, 35-43.
- Koehler B, Corre MD, Veldkamp E, Wullaert H, Wright SJ (2009) Immediate and long-term nitrogen oxide emissions from tropical forest soils exposed to elevated nitrogen input. *Global Change Biology*, **15**, 2049-2066.

-
- Kursar TA (1989) Evaluation of soil respiration and soil CO₂ concentration in a lowland moist forest in Panama. *Plant and Soil*, **113**, 21-29.
- Leigh EG, Rand AS, Windsor DW (1996) *The ecology of a tropical forest*. Smithsonian Press, Washington DC, USA, 266 pp.
- Likens GE, Driscoll CT, Buso BC (1996) Long-term effects of acid rain: response and recovery of a forest ecosystem. *Science*, **272**, 244-246.
- Linn DM, Doran JW (1984) Effect of water-filled pore space on carbon dioxide and nitrous oxide production in tilled and nontilled soils. *Soil Science Society of America Journal*, **48**, 1267-1272.
- Litton CM, Raich JW, Ryan MG (2007) Carbon allocation in forest ecosystems. *Global Change Biology*, **13**, 2089-2109.
- Livingston GP, Hutchinson GL, Spartalian K (2006) Trace gas emission in chambers: A non-steady-state diffusion model. *Soil Science Society of America Journal*, **70**, 1459-1469.
- Loftfield N, Flessa H, Augustin J, Beese F (1997) Automated gas chromatographic system for rapid analysis of the atmospheric trace gases methane, carbon dioxide, and nitrous oxide. *Journal of Environmental Quality*, **26**, 560-564.
- Lohse KA, Matson PA (2005) Consequences of nitrogen additions for soil processes and solution losses from wet tropical forests. *Ecological Applications*, **15**, 1629-1648.
- Luo Y, Zhou X (2006) *Soil respiration and the environment*. Elsevier Academic Press, Burlington, San Diego and London, UK, 316 pp.
- Malhi Y (2005) The carbon balance of the tropical forest biome. In *The carbon balance of forest biomes* (eds Griffiths H, Jarvis PG), pp. 356. Taylor & Francis Group.
- Mo J, Brown S, Xue J, Fang Y, Li Z (2006) Response of litter decomposition to simulated N deposition in disturbed, rehabilitated and mature forests in subtropical China, *Plant and Soil*, **282**, 135-151.
- Mo J, Zhang W, Zhu W, Gundersen P, Fang Y, Li D, Wang H (2008) Nitrogen addition reduces soil respiration in a mature tropical forest in southern China. *Global Change Biology*, **14**, 403-412.
- Nadelhoffer KJ (2000) The potential effects of nitrogen deposition on fine-root production in forest ecosystems. *New Phytologist*, **147**, 131-139.
- Neff JC, Townsend AR, Gleixner G, Lehman SJ, Tumbull J, Bowman WD (2002) Variable effects of nitrogen additions on the stability and turnover of soil carbon, *Nature*, **419**, 915-917.

-
- Norby RJ, Jackson RB (2000) Root dynamics and global change: seeking an ecosystem perspective. *New Phytologist*, **147**, 3-12.
- Ostertag R (2001) Effects of nitrogen and phosphorus availability on fine-root dynamics in Hawaiian montane forests. *Ecology*, **82**, 485-499.
- Pame-Baldos A (2009) Above-ground net primary productivity and leaching losses in a tropical montane forest exposed to elevated nitrogen input, M.Sc. thesis, University of Goettingen, Goettingen, Germany, 36 pp.
- Priess J, Fölster H (2001) Microbial properties and soil respiration in submontane forests of Venezuelan Guyana: characteristics and response to fertilizer treatments. *Soil Biology and Biochemistry*, **33**, 503-509.
- Raich JW (1998) Aboveground productivity and soil respiration in three Hawaiian rain forests. *Forest Ecology and Management*, **107**, 309-318.
- Raich JW, Riley RH, Vitousek PM (1994) Use of root-ingrowth cores to assess nutrient limitation in forest ecosystems. *Canadian Journal of Forest Research*, **24**, 2135-2138.
- Raich JW, Schlesinger WH (1992) The global carbon dioxide flux in soil respiration and its relationship to vegetation and climate, *Tellus*, **44**, 81-99.
- R Development Core Team (2009) R: A language and environment for statistical computing. R Foundation for Statistical Computing, Vienna, Austria. ISBN 3-900051-07-0, URL <http://www.R-project.org>.
- Schwendenmann L, Veldkamp E, Brenes T, O'Brien JJ, Mackensen J (2003) Spatial and temporal variation in soil CO₂ efflux in an old-growth neotropical rain forest, La Selva, Costa Rica. *Biogeochemistry*, **64**, 111-128.
- Talbot JM, Allison SD, Treseder KK (2008) Decomposers in disguise: mycorrhizal fungi as regulators of soil C dynamics in ecosystems under global change. *Functional Ecology*, **22**, 955-963.
- Treseder KK (2004) A meta-analysis of mycorrhizal responses to nitrogen, phosphorus, and atmospheric CO₂ in field studies. *New Phytologist*, **164**, 347-355.
- Van Breemen N, Mulder J, Driscoll CT (1983) Acidification and alkalization of soils, *Plant and Soil*, **75**, 283-308.
- Wagner SW, Reicosky DC, Alessi RS (1997) Regression models for calculating gas fluxes measured with a closed chamber. *Agronomy Journal*, **89**, 279-284.
- Yavitt JB, Wright SJ (2001) Drought and irrigation effects on fine root dynamics in a tropical moist forest, Panama. *Biotropica*, **33**, 421-434.

Yavitt JB, Wright SJ, Kelman Wieder R (2004) Seasonal drought and dry-season irrigation influence leaf-litter nutrients and soil enzymes in a moist, lowland forest in Panama. *Austral Ecology*, **29**, 177-188.

An inverse analysis reveals limitations of the soil-CO₂
profile method to calculate CO₂ production for well-
structured soils

BIRGIT KOEHLER, ERWIN ZEHE, MARIFE D. CORRE and EDZO VELDKAMP

- MANUSCRIPT IN PREPARATION -

4.1 Abstract

Soil respiration is the second largest flux in the global carbon cycle but the underlying below-ground process, carbon dioxide (CO₂) production, can not be measured in the field. The production has frequently been calculated from the vertical gas diffusive flux divergence, known as ‘soil-CO₂ profile method’. For a tropical lowland forest in Panama this method gave inconsistent results when using ‘empirical’ diffusion coefficients (D) calculated based on soil porosity and moisture. The objective of this study was to investigate whether these inconsistencies were caused by (1) the applied interpolation and solution methods, (2) uncertainties in describing the profile of D using empirical equations or (3) the assumptions of the profile method. We show that the calculated production strongly depends on the function used to interpolate between measured CO₂ concentrations. Using an inverse analysis we deduce which D would be required to explain the observed CO₂ concentrations if the profile method were valid. In the top soil, this ‘inverse’ D closely resembled the empirical D . In the deep soil, however, the inverse D increased sharply while the empirical did not. This deviation disappeared upon conducting a constrained fit parameter optimization. A radon (Rn) mass balance model, in which diffusion is calculated based on these D , simulated the observed Rn profiles reasonably well. However, the constrained inverse D underestimated the measured CO₂ concentrations. Finally, it gave depth-constant fluxes and hence zero production in the CO₂-profile method. We suggest that, in well-structured soils, the method fails due to a missing description of steady state CO₂ exchange fluxes across water-filled pores. These are driven by the different diffusivities in inter- vs. intra-aggregate pores which create permanent CO₂ gradients if separated by a ‘diffusive water barrier’. We conclude that the assumptions of the profile method are inaccurate for soils with pore networks which exhibit spatial separation between places of CO₂ production and upward diffusion.

4.2 Introduction

Soil respiration, the efflux of CO₂ which is produced mainly by roots and decomposition of litter and organic matter, is the second largest flux in the global terrestrial carbon (C) cycle (IPCC, 2007). Because of its magnitude even small changes in soil CO₂ production can affect atmospheric CO₂ concentrations and hence global warming. Despite this central role in the global C cycle soil respiration remains among the least understood ecosystem C fluxes (Luo and Zhou, 2006).

Typically, CO₂ production diminishes and CO₂ concentration increases as gas diffusion becomes increasingly restricted with soil depth (Amundson and Davidson, 1990). The CO₂ efflux at the soil-air interface is normally measured using chamber techniques while no direct field methods exist to measure soil CO₂ production at a specific soil depth. Mathematical models have been used to calculate soil CO₂ production with soil depth. In CO₂-production-transport models microbial and root respiration are described on the process-scale (e.g. Simunek and Suarez, 1993; Fang and Moncrieff, 1999). An application of such models requires knowledge of several parameters for which information may not be available. A simpler approach is the 'soil-CO₂ profile method' to calculate production rates from measured concentration profiles using gas diffusion modeling (De Jong and Schappert, 1972, 1978). This method has been used in several studies (Davidson and Trumbore, 1995; Gaudinski *et al.*, 2000; Hirsch *et al.*, 2002; Risk *et al.*, 2002a, b; Davidson *et al.*, 2004; Fierer *et al.*, 2005; Jassal *et al.*, 2005; Davidson *et al.*, 2006; Schwendenmann and Veldkamp, 2006; Hashimoto *et al.*, 2007; Sotta Doff *et al.*, 2007; Risk *et al.*, 2008). The assumptions of the soil-CO₂ profile method are that 1) gas diffusion in the air phase is the only relevant CO₂ transport pathway in soils and 2) CO₂ concentrations in the soil gas and water phase are in steady state, i.e. changes over time can be neglected. The CO₂ flux is described using Fick's first law of diffusion and, according to the model perception, the difference between the amount of CO₂ entering and leaving a soil layer is produced or consumed at that depth.

Application of the soil-CO₂ profile method requires accurate knowledge of the soil gas diffusion properties. As the calculated soil CO₂ production rates are directly proportional to D it is a highly sensitive model parameter, i.e. a doubling throughout the profile results in a doubling of the calculated CO₂ production. D is generally calculated choosing one of several functions that describe its relationship with soil properties like porosity and moisture (hereafter termed 'empirical' D ; e.g. Penman, 1940; Currie, 1961; Millington and Quirk, 1961; Millington and Shearer, 1971; Moldrup *et al.*, 2000). To determine the diffusion gradient, data on CO₂ concentrations in soil air are needed as further model input. In most of the above mentioned studies, measured CO₂ concentrations were linearly interpolated before numerically calculating production using the method of finite differences. In three studies, the measured CO₂ concentrations were interpolated using exponential (Gaudinski *et al.*, 2000; Davidson *et al.*, 2006) or quadratic (Jassal *et al.*, 2005) functions, calculating CO₂ flux and production either analytically or numerically. Uncertainties in depth-specific production rates and/or partially negative rates often led to the following simplifications: CO₂ production was

summed over large depth intervals, and the CO₂ production of the top soil was estimated by subtracting the calculated subsoil CO₂ production from the measured soil CO₂ efflux. Suggested explanations for the encountered difficulties range from an insufficient mathematical description of the relationship between D and the soil moisture content (DeJong and Schappert, 1972) to inaccurately interpolated CO₂ concentration profiles, especially in the top soil where ‘hot spots’ of CO₂ production might occur (Davidson and Trumbore, 1995). Presently, large uncertainties remain when using gas diffusivity models in soils (Davidson *et al.*, 2006), which of course also introduces uncertainty in the conclusions drawn from the model results.

We conducted a study in a tropical lowland forest in Panama in which we wanted to calculate depth-specific soil CO₂ production rates. When we applied the soil-CO₂ profile method on a 2-yr time series of soil CO₂ concentrations we encountered similar problems as the ones described in earlier studies. The objective of the present study was to test the following hypotheses:

During application of the soil-CO₂ profile method

- (1) the procedures to interpolate between the measured CO₂ concentrations strongly influence the calculated CO₂ fluxes and production.
- (2) uncertainties in describing the depth distribution of D using soil characteristics cause inconsistencies.
- (3) the perception of the processes governing soil CO₂ dynamics is inappropriate and/or incomplete.

To test these hypotheses we compared different methods for the CO₂ interpolation and the solution of the soil-CO₂ profile method. Furthermore, we set up an inverse analysis to deduce which D would be required to explain the observed CO₂ concentrations assuming the soil-CO₂ profile method is valid (hereafter termed ‘inverse’ D). To test the accuracy of the determined empirical and inverse D we used a radon (Rn) mass balance model. Finally, we verified the validity of the assumptions of the soil-CO₂ profile method based on its mathematical derivation and the inverse modeling results.

4.3 Materials and methods

4.3.1 Measurements

Study Area

The study site is located between 25-61 m elevation in an old-growth semi-deciduous tropical lowland forest on Gigante Peninsula (9°06'N, 79°50'W) which is part of the Barro Colorado Nature Monument, Republic of Panama (Leigh *et al.*, 1996). On nearby Barro Colorado Island annual rainfall (1995-2007) averages 2650 ± 146 mm with a dry season from January to mid-May during which 297 ± 40 mm of rainfall is recorded. The mean annual air temperature is 27.4 ± 0.1 °C. Soils are derived from a basalt flow, have a heavy clay texture, and are classified as Endogleyic Cambisol in the lower parts of the landscape to Acric Nitisol in the upper parts of the landscape (FAO classification; alternatively Dystrudepts in USDA classification). Detailed soil characteristics and information on forest structure have been published earlier (Koehler *et al.*, 2009b; Corre *et al.*, in press).

Experimental design

From May 2006 to June 2008 we measured soil CO₂ efflux, CO₂ concentrations in air (0.1 m above the soil surface) and in soil air at six depths down to 2 m. Furthermore we detected soil moisture and temperature at the same soil depths. The measurements were conducted in an approximately 6-weekly schedule in three replicated plots which are separated by about 500 m distance.

Soil CO₂ concentration profiles and soil CO₂ efflux measurements

In each of the three replicate plots we established one permanent 2.5 m deep soil pit. Stainless steel tubes (3.2 mm outer diameter) were installed horizontally into the pit walls at 0.05, 0.2, 0.4, 0.75, 1.25 and 2 m depth. In the top 1 m tubes were 1 m long while the tubes at 1.25 m and 2 m depth were 1.8 m long to account for the pit wall effect on CO₂ concentrations (Schwendenmann *et al.*, 2003). Tubes were perforated at one end and closed with a septum holder at the other end protruding from the pit wall. Soil air was sampled in evacuated glass containers (100 mL) closed with a teflon stopcock. Before sampling, 20 mL of air were discarded to remove the 'dead volume' from the sampling tubes. Previous testing had shown that at least 300 mL could be withdrawn from a tube without changing CO₂ concentrations. Soil air samples were analyzed using a gas chromatograph (Shimadzu GC-14B, Columbia, MD, USA) equipped with an electron capture detector (Loftfield *et al.*, 1997) which was

calibrated with three to four standard gases (360, 706, 1505, 5012 and 39977 ppm CO₂, Deuste Steininger GmbH, Mühlhausen, Germany). Wet season soil air-sampling below 1 m was restricted because the groundwater table often rose above this depth. In one pit CO₂ concentrations at 0.05 m were always higher than at 0.2 m depth. For the model calculations these high values at 0.05 m depth were replaced by concentrations interpolated from the other two pits. Soil CO₂ effluxes were measured by air sampling from four vented static chambers per plot with subsequent gas chromatographic analysis, and were calculated based on a quadratic or linear regression model using the Akaike Information Criterion as statistical decision tool. A detailed method description of the flux measurements can be found in (Koehler *et al.*, 2009a).

Soil ²²²Rn concentration profiles

We measured ²²²Rn concentration profiles in soil air twice both at the end of dry season and the height of wet season. In each of the three soil pits soil air was sampled in pre-evacuated scintillation flasks (Lucas cells 110A and 300A, Pylon Electronics, Ontario, Ottawa, Canada) in which alpha particle emission from radioactive decay was detected using a portable radiation monitor (AB-5, Pylon Electronics). The ‘background activity’ of the Lucas cells was determined after repeatedly evacuating the cell and flushing them with nitrogen gas followed by a time span of at least 24 hours. Mean background was 0.88 ± 0.04 counts per minute (cpm). During sampling, the air was filtered for ambient alpha particles (PTFE-membrane 0.45 μm , Minisart SRP25, Sartorius, Goettingen, Germany) and dried using a CaCl₂-column (30 mL). Sampling proceeded from 0.05 m (lowest concentrations) to 2 m depth (highest concentrations). The sampling system was repeatedly flushed with ambient air in between samplings. A delay of at least 3.5 h permitted the establishment of the radioactive equilibrium of ²¹⁸Po and ²¹⁴Po after which alpha decays were counted for six 5-minute intervals within 24 hours. Mean background activity was subtracted from mean sample activity. Activities (cpm) were converted to Bq m⁻³ and corrected for the counting efficiency, for decay during the counting interval and the interval between sampling and measurement (Pylon Electronics, 1989). The cells counting efficiencies, determined after transferring a known amount of ²²²Rn into a Lucas cell using a flow through Rn source (Pylon Model RN-1025-20, Pylon Electronics), ranged from 71 to 82%.

Laboratory measurements of soil ²²²Rn production

Soil samples from the same depths used for air sampling (~150 g dry weight from each of the six depths of the three replicate pits) were air-dried and incubated for 12-18 days in air-tight jars (1700 mL) to permit ²²²Rn to build up and approach equilibrium with the parent isotope ²²⁶Ra. Between 89 and 96% of the equilibrium production rate is reached during this incubation time. Rn concentrations Rn (Bq m⁻³) were determined from duplicate air samples as described above. Afterwards, the same soil samples were adjusted to soil moisture contents representative for wet season conditions and the incubation and Rn determination was repeated. The equilibrium Rn production rates P (Bq kg⁻¹) were calculated as:

$$P = \frac{Rn \cdot V_g}{m} f \quad (4-1)$$

where V_g is the air volume in the incubation jar (m³), m is the dry soil weight (kg) and f is a conversion factor to equilibrium production rate ($f = 1 - 0.5^n$ with $n =$ number of ²²²Rn half lives passed during the incubation time). V_g is the difference between the jar volume and the soil-occupied volume as well as, for the wet soil incubations, the volume of added water.

Additional measurements in the soil pits

Soil bulk density was determined from two undisturbed 250 cm³ soil cores (Blake and Hartge, 1986) sampled during pit establishment at the six depths where air sampling tubes were installed. Soil-water characteristic curves (laboratory pF curves) were determined on one undisturbed 250 cm³ soil core per sampling depth from two soil pits, with a suction membrane in the low suction range (0-330 hPa) and a pressure membrane device in the higher suction range (1000-15000 hPa). Thermocouple T-probes (Omega Engineering, Deckenpfronn, Germany) were attached at the perforated end of the air sampling tubes, and water content probes (Campbell Scientific CS616, Logan, Utah) were installed next to them. Some clay types (our soils have a heavy clay texture with up to 70% clay; Koehler *et al.*, 2009b) can attenuate the CS616 probe response as described by the manufacturers standard calibration and, consequently, a soil specific calibration is required (Campbell Scientific, 2002-2006). To establish this soil specific sensor calibration we used four undisturbed 4000 cm³ soil samples taken during the establishment of one of the pits and basically followed the procedure described by (Veldkamp and O'Brien, 2000) but used a quadratic calibration function instead of a 3-phase-model because it achieved better performance. Soil samples were first water-saturated and during subsequent drying (at 24°C in the laboratory), both sensor output and gravimetric soil moisture were determined daily for two weeks. The CS616 sensors are

temperature dependent and signals were converted to 20°C using the manufacturer's formula. Our soil specific calibration function was $VWC \text{ (cm}^3 \text{ cm}^{-3}\text{)} = -0.002 x^2 + 0.149 x - 2.101$ ($R^2 = 0.87$, $n = 58$, $P < 0.001$) where VWC is the volumetric water content and x is the sensor period signal (ms). This calibration achieved a root mean squared error (RMSE) of 0.049 compared to a RMSE of 0.135 if the manufacturer's standard calibration function would be applied.

Empirical calculation of gas diffusion coefficients D

To calculate D for the depths of air sampling we used a semi-empirical cut- and random-rejoin-type model for aggregated porous media (Millington and Shearer, 1971). The required input parameters are D in free air ($0.139 \text{ cm}^2 \text{ s}^{-1}$ for CO₂ (Pritchard and Currie, 1982) and $0.11 \text{ cm}^2 \text{ s}^{-1}$ for ²²²Rn (Sasaki *et al.*, 2006) at $T_0 = 273.2 \text{ K}$ and $P_0 = 1013 \text{ hPa}$), the total inter- and intra-aggregate pore space and the water distribution between them. Soil total porosity was calculated from bulk density assuming a particle density of 2.65 g cm^{-3} for mineral soil (Linn and Doran, 1984). Considering that inter-aggregate pores drain quickly we calculated inter-aggregate porosity as the difference between water content at saturation and at field-capacity (Radulovich *et al.*, 1989), which we defined as the water content remaining after applying a suction of 10 kPa to the water-saturated soil (Hillel, 1998). The intra-aggregate porosity is the difference between total and inter-aggregate porosity. To estimate the water distribution between the pore classes we assumed that water can only occur in the inter-aggregate pores if the intra-aggregate pores are water saturated and are completely air-filled if the VWC is below field-capacity (Collin and Rasmuson, 1988). To account for the temperature dependence of diffusion we multiplied D with the term $(T/T_0)^n$ where T is the soil temperature during air sampling (K), T_0 is 273.2 K and n is 1.75 for CO₂ (Campbell, 1985).

4.3.2 Model approach and calculation methods

Derivation of the soil-CO₂ profile method

In order to discuss the validity and limitations of the soil-CO₂ profile method, which has been suggested by DeJong & Schappert (1972), we establish its derivation based on the mass balance of CO₂ in soils which can be modeled as:

$$\frac{\partial C_T}{\partial t} = \frac{\partial \theta C_w}{\partial t} + \frac{\partial (\theta_s - \theta) C_g}{\partial t} = -\frac{\partial}{\partial z} \left(q_g C_g + q_w C_w - D_g \frac{\partial C_g}{\partial z} - D_w \frac{\partial C_w}{\partial z} \right) + S \quad (4-2)$$

where C_T is the total concentration of CO₂ in the gas phase (C_g) and the water phase (C_w ; ng cm⁻³); t is time (s), θ is the volumetric soil water content (cm³ cm⁻³), z is depth (cm), θ_s is total soil porosity (cm³ cm⁻³), q is the mass flux (cm s⁻¹) of water or air, D is the effective diffusion coefficient (cm² s⁻¹) and S are CO₂ sources and sinks (ng cm⁻³ s⁻¹). Assuming horizontal homogeneity, the diffusive fluxes are expressed according to Fick's first law of diffusion in one spatial dimension. Positive fluxes are defined as upward (towards the atmosphere), and negative fluxes as downward (towards deeper soil). The equilibrium concentrations of CO₂ in the water and gas phase can be described according to Henry's law:

$$\frac{C_w}{C_g} = k_H := \frac{k_1}{k_2} \quad (4-3)$$

where k_H is Henry's law constant, and k_1 and k_2 are the dissolution and volatilization rate coefficients, respectively. Assuming absence of CO₂ sinks in soils (hence S is CO₂ production) and neglecting convective transport and diffusion in the water phase, the mass balances in the gas and water phases are given as:

$$\frac{\partial(\theta_s - \theta)C_g}{\partial t} = -\frac{\partial}{\partial z} \left(-D_g \frac{\partial C_g}{\partial z} \right) + S_g - k_1 C_g + k_2 C_w \quad (4-4)$$

$$\frac{\partial \theta C_w}{\partial t} = S_w + k_1 C_g - k_2 C_w \quad (4-5)$$

where S_g and S_w denote the fractions of CO₂ production which first occur in the gas and water phase, respectively. When diffusive CO₂ exchange across the air-water interface and subsequent mixing is much faster than temporal changes in CO₂ concentration one can assume that equilibrium establishes instantaneously. Eq. (4-5) then reduces to a diagnostic equation:

$$k_2 C_w = S_w + k_1 C_g \quad (4-6)$$

Insertion of eq.(6) into eq.(4) allows elimination of C_w :

$$\frac{\partial(\theta_s - \theta)C_g}{\partial t} = -\frac{\partial}{\partial z} \left(-D_g \frac{\partial C_g}{\partial z} \right) + S_g + S_w \quad (4-7)$$

Finally, assuming steady state in the air phase, one obtains:

$$S_T = S_w + S_g = -\frac{\partial}{\partial z} \left(D_g \frac{\partial C_g}{\partial z} \right) \quad (4-8)$$

This equation is well known as fundament of the ‘soil-CO₂ profile method’ (DeJong and Schappert, 1972), where the total CO₂ production is calculated based on the vertical divergence of CO₂ diffusion in the gas phase.

Parameterization of the profile method

According to the soil-CO₂ profile method the CO₂ production profile can be calculated from eq. (4-8) if the derivatives of the soil CO₂ concentration profiles and the profile of *D* are known. To achieve the first requirement, a continuously mathematical function (that can be differentiated) is used for interpolating the measured CO₂ concentrations on a regular vertical grid. For our site we chose the asymmetric sigmoidal Gompertz function (Richards, 1959) to approximate this distribution (Fig. 4-1a):

$$C_g = ae^{be^{cz}} \quad (4-9)$$

Estimates for the parameters *a*, *b* and *c* were obtained using non-linear least square fitting to the measured CO₂ concentration profiles. The first derivative describes the concentration gradient driving gaseous diffusion (Fig. 4-1b):

$$\frac{\partial C_g}{\partial z} = abce^{cz+be^{cz}} \quad (4-10)$$

The second derivative is the curvature of the concentration profile (Fig. 4-1c). In case of a constant *D* it would be the proportional to *S*:

$$\frac{\partial^2 C_g}{\partial z^2} = abc^2 e^{cz+be^{cz}} (1 + be^{cz}) \quad (4-11)$$

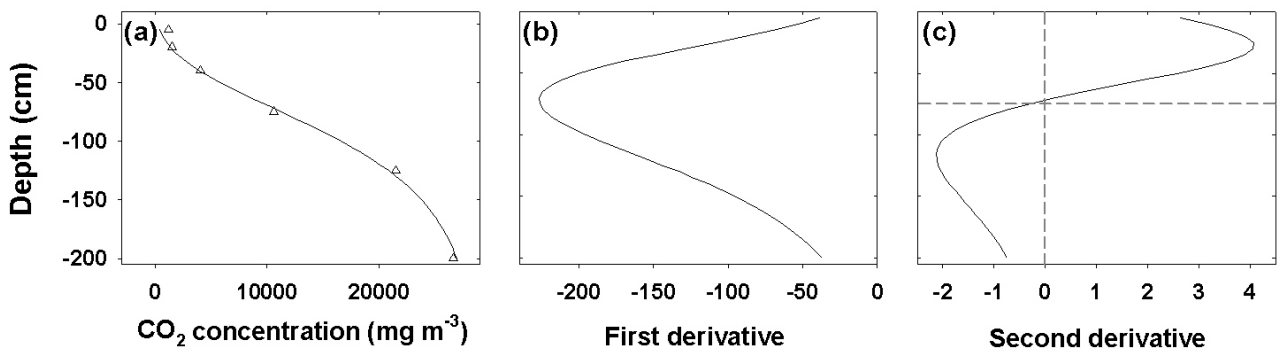


Figure 4-1. a) Sigmoidal function used to approximate the profiles of CO₂-concentrations in soil air measured at our site (Δ) and its first (b) and second derivative (c) which are relevant terms in the soil CO₂-profile method (eq. 4-8).

To parameterize D (second requirement) we 1) used the empirical function by Millington and Shearer (1971) as described above and 2) set up an inverse method to obtain a relation for D using the derivatives of the function fitted to the observed steady state gas profile (eqs. 4-10 and 4-11). We explain this inverse calculation starting from eq. (4-8), which can also be written as:

$$S_T = -\frac{\partial D_g}{\partial z} \frac{\partial C_g}{\partial z} - D_g \frac{\partial^2 C_g}{\partial z^2} \quad (4-12)$$

S_T must be greater or equal zero:

$$-\frac{\partial D_g}{\partial z} \frac{\partial C_g}{\partial z} - D_g \frac{\partial^2 C_g}{\partial z^2} \geq 0 \quad (4-13)$$

Eq. (4-13) can be rearranged such that the unknown terms are on the left-hand side and the known terms are on the right-hand side:

$$-\frac{\partial D_g}{\partial z} \frac{1}{D_g} \geq \frac{\frac{\partial^2 C_g}{\partial z^2}}{\frac{\partial C_g}{\partial z}} \quad (4-14)$$

Inserting eqs. (4-10) and (4-11) in the right-hand side of eq. (4-14) gives:

$$-\frac{\partial D_g}{\partial z} \frac{1}{D_g} \geq c + bce^{cz} \quad (4-15)$$

Definite integration of the left hand side of eq. (4-15) from depth z to the surface ($z = 0$) gives:

$$\int_0^z -\frac{\partial D_g}{\partial z} \frac{1}{D_g} \partial z = -\ln\left(\frac{D_{gz}}{D_0}\right) \quad (4-16)$$

Analogous, indefinite integration of the right-hand side of eq. (4-15) gives:

$$\int c + bce^{cz} dz = cz + be^{cz} + \text{const} \quad (4-17)$$

where *const* is an integration constant. Based on equations 4-16 and 4-17 follows:

$$-\ln\left(\frac{D_{gz}}{D_0}\right) \geq cz + be^{cz} + \text{const} \quad (4-18)$$

By taking the exponential of eq. (4-18) we get our target expression, an equation to calculate D as function of z :

$$D_g \leq D_0 e^{-cz - be^{cz} - \text{const}} \quad (4-19)$$

Thereby, *const* is given as:

$$const \leq \ln \frac{D_0}{D_g} - cz - be^{cz} \quad (4-20)$$

In the simulations, we converted *const* to the correct scale by multiplying our inverse ‘maximal’ profile of *D* (eq. 4-14) with the factor ‘empirical *D*/inverse *D*’ at all depths. Due to this, the inverse *D* at the upper boundary (*z* = 0) becomes equal to the empirical *D* calculated for 0-0.05 m depth.

In a next step we fitted the sigmoidal function to the measured CO₂ profiles such that *D* must always increase monotonically with *z*, i.e. increase from deeper soil towards the soil surface (see paragraph 4.4.2). Mathematically this implies the condition $\partial D/\partial z > 0$. The first derivative of eq. (4-19) reads:

$$\frac{\partial D_g}{\partial z} \leq D_0 e^{-cz - be^{cz} - const} (-c - cbe^{cz}) \quad (4-21)$$

From eq. (4-21) it can be recognized that the constraint $\partial D/\partial z > 0$ is fulfilled when the term in brackets becomes positive, thus:

$$-c - cbe^{cz} > 0 \quad (4-22)$$

We used the method of simulated annealing to conduct the constrained optimization (Kirkpatrick *et al.*, 1983).

Implementations of the profile method

To compare our parameterization with results of the ‘traditional’ soil CO₂-profile method (eq. 4-8) we conducted the following calculations: First, we determined CO₂ fluxes and production using the empirical *D* and 1) the method of finite differences after linear interpolation between measured CO₂ concentrations on a regular vertical grid (DeJong and Schappert, 1972; Davidson and Trumbore, 1995), 2) the analytical solution of an exponential interpolation function (Gaudinski *et al.*, 2000) and 3) the analytical solution of our chosen sigmoidal interpolation function (eq. 4-9). Secondly, we calculated the inversely determined CO₂ fluxes and production (inserting eqs. 4-10, 4-11, 4-19 and 4-21 in eq. 4-12). Mass based CO₂ production rates (per soil volume) were converted to area based production rates by multiplying with the depth of the soil layer. The sum of all area based production rates is the mineral soil CO₂ production of the total profile, or the modeled CO₂ flux. We only calculated CO₂ production for profiles where we could measure CO₂ concentrations down to 1.25 or 2 m depth. All calculations were conducted using MATLAB[®] 7.0.1 (The MathWorks, Natick, MA, USA, 2004).

Rn mass balance model

We set up a one-dimensional Rn mass balance model which considers production, decay in water and gas phase, gaseous diffusion and exchange between the gas and water phase assuming instantaneous equilibration (Davidson and Trumbore, 1995; Schwendenmann and Veldkamp, 2006). We used this model to test the validity of D by comparing steady state simulated with measured profiles of Rn concentrations. The Rn production rates were adjusted to the soil moisture during Rn sampling based on the production rates measured from dry and wet soil. We established Dirichlet boundary conditions, specifying the Rn concentration measured at 0.05 m as upper and at 2 m depth as lower boundary condition. For the other depths the initial Rn concentration in soil air was calculated depending on the measured soil water content. The model was solved with MATLAB[®] 7.0.1 (The MathWorks, 2004) using an explicit numerical method on a 0.05 m vertical grid until steady state was established.

Statistical analyses and calculations

Statistical analyses were conducted using *R 2.9.0* (R Development Core Team, 2009). If data sets were rightly skewed, we applied either a square-root or a logarithmic transformation before analysis. If data sets were left-skewed, a quadratic or cubic transformation was applied before analysis. Linear mixed effects models (on plot means) were used to test the time series of the response variables for a ‘fixed’ effect of season (VWC, soil temperature, air-filled porosities and soil CO₂ efflux) or calculation method (D), including the spatial replication nested in time as ‘random’ effects. The models were specified as explained in Koehler *et al.* (2009b) and the significance of the fixed effect was assessed using analysis of variance (Crawley, 2002). For soil porosities and Rn production rates we assessed differences between seasons and incubations (dry vs. wet) using independent t -tests. Effects were considered significant if P value ≤ 0.05 . We calculated the root mean squared error (RMSE) to characterize the goodness of fit of the interpolation functions to the measured CO₂ concentrations. Mean values in the text are given with ± 1 standard error.

4.4 Results

4.4.1 Volumetric water content, temperatures, ²²²Rn and CO₂ concentrations down to 2 m soil depth

The volumetric water content (VWC) increased with soil depth and was smaller during dry than wet season at all sampling depths (all $P < 0.001$). Mean soil temperatures ranged between 24.9 ± 0.1 and 25.2 ± 0.1 °C, and varied seasonally by 2.4 and 2.1°C at 0.05 and 0.2 m depth, respectively, and by 1.3 to 1.7 °C below (data not shown). ²²²Rn concentrations increased with soil depth and exhibited a sigmoidal profile shape both during dry and wet season (Fig. 4-2). Soil CO₂ concentrations averaged 830.47 ± 35.31 ppm at 0.1 m above the soil surface, and increased with soil depth. The strongest increase occurred down to 0.2 m depth where concentrations averaged 0.31 ± 0.02 % during dry season and 0.65 ± 0.06 % during wet season. At 2 m depth CO₂ concentrations were up to 55 times higher than the concentration above the soil surface, with an annual mean of 4.22 ± 0.32 %. CO₂ concentrations displayed a pronounced seasonality especially in the top 0.75 m soil, with highest concentrations at the end of wet season and lowest concentrations at the end of dry season (Fig. 4-3).

4.4.2 Soil porosity and empirical diffusion coefficients

In general, both total and inter-aggregate soil porosities decreased with soil depth. Also air-filled porosities decreased from top to deep soil with the sharpest decline in the top 0.4 m soil, and were smaller during wet than dry season at all sampling depths (all $P < 0.013$; Table 4-1). The empirical D resembled this depth pattern of air-filled porosities (Fig. 4-4a and b). It was smaller during wet than dry season down to 1.25 m (all $P < 0.037$) but did not differ seasonally at 2 m depth.

4.4.3 Simulated steady state ²²²Rn concentrations

The Rn production rates decreased with soil depth, and were larger but statistically undistinguishable from the wet compared to the dry soil (Table 4-1). Using the Rn production rates and the empirical D in the Rn mass balance model, the simulated steady state concentrations were higher than measured during dry season (Fig. 4-2a), but matched the measured concentrations well during wet season (Fig. 4-2b). A sensitivity analysis shows that

the steady state model solution is more sensitive to changes in the Rn production rates than in D (inset in Fig. 4-2a).

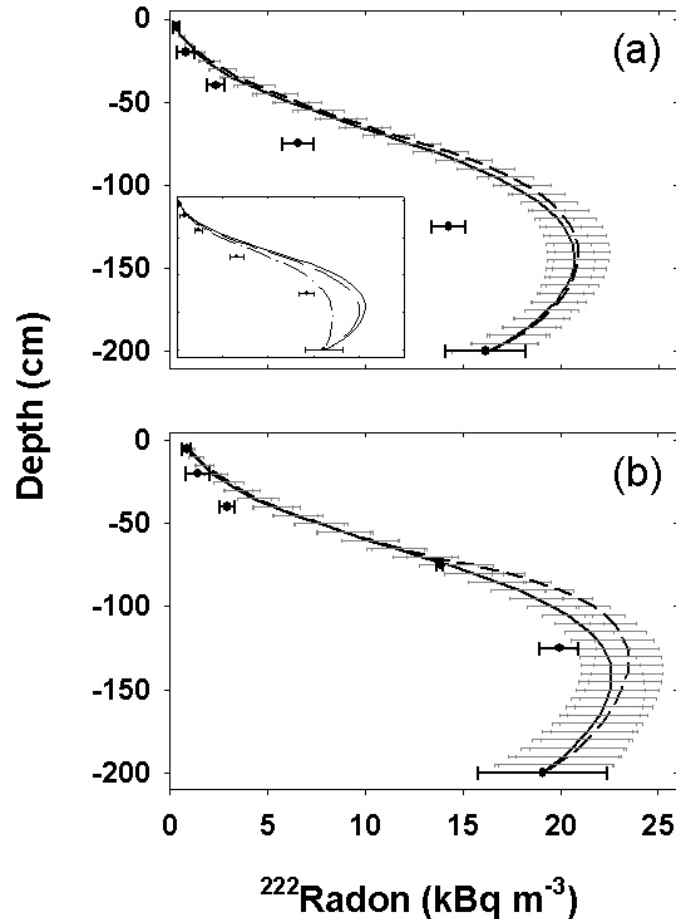


Figure 4-2. Mean (\pm SE, $n = 3$) measured Rn concentrations in soil air (\bullet) during a) dry and b) wet season. The lines show the steady state profiles (\pm SE, $n = 3$) simulated with a Rn mass balance model using the constrained inverse diffusion coefficients (D ; —) and the empirical D (---). The inset graph in a) illustrates the sensitivity of the simulated Rn concentrations: The lines display the steady state modeled concentration profile using the inverse D (—), the response towards a 20% increase in D (---) and the response towards a 20% reduction in the Rn production rates (- · -).

4.4.1 CO₂ fluxes and production rates calculated with the empirical D and different implementations of the profile method

The best fit to the measured CO₂ concentrations was achieved with a sigmoidal function (RMSE=0.14 \pm 0.04). An exponential function gives a worse goodness of fit (RMSE=0.22 \pm

0.04; Fig. 4-4c and d). When using the empirical D together with the sigmoidal function in the profile method the resulting CO₂ flux would show a slight increase from deep to top soil. In contrast, when using the exponential function instead, the flux would increase sharply towards the surface, which gave a three-fold larger mean surface flux (Fig. 4-5a). The simulated CO₂ production based on a sigmoidal function would be close to zero, become slightly negative at some depths and display a peak in the top soil. The exponential function would lead to very small CO₂ production rates below a depth of 0.75 m, which would increase sharply towards the surface (Fig. 4-5b). We do not present the results based on linearly interpolated CO₂ concentrations in combination with finite-difference solutions for reasons discussed in paragraph 4.5.1.

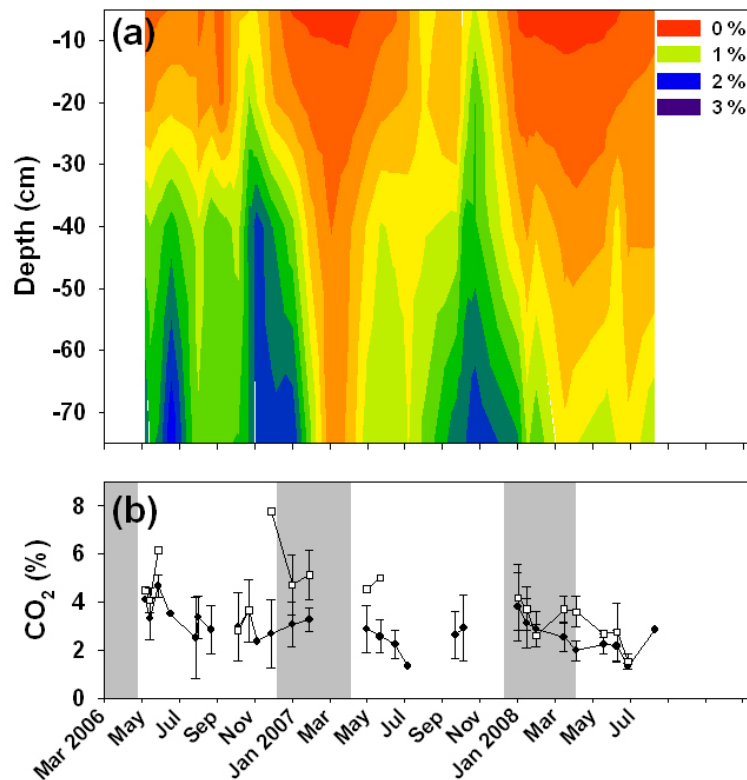


Figure 4-3. Mean CO₂ concentrations in soil air (%) with a) interpolated between the four sampling depths in the top 75 cm soil ($n = 3$, SE range between 0.002 and 0.65 %) and b) for $\bullet = 1.25$ m and $\square = 2$ m depth (\pm SE, $n = 3$). Grey shadings in b) mark the dry seasons and missing wet season data are when high groundwater level restricted deep air-sampling. Deep CO₂ concentrations are missing for the end of dry season 2007 due to analytical problems but top soil concentrations were determined.

The measured soil CO₂ effluxes averaged $198.10 \pm 9.18 \text{ mg C m}^{-2} \text{ h}^{-1}$ and were smaller during dry season ($113.38 \pm 13.84 \text{ mg C m}^{-2} \text{ h}^{-1}$) than wet season ($212.60 \pm 6.97 \text{ mg C m}^{-2} \text{ h}^{-1}$, $P < 0.001$). Any of the applied solution methods would give a ‘seasonality’ in the total soil CO₂ production (i.e. the modeled CO₂ flux). However, use of the empirical D with the sigmoidal function resulted in production rates that were too small compared to the measured effluxes. Use of the exponential function would increase the calculated production rates three-fold, at times overestimating at times underestimating the measured effluxes (Fig. 4-6). Using the empirical D in combination with linearly interpolated CO₂ concentrations and the method of finite differences gives CO₂ production rates that increase with the resolution of the interpolation grid (not shown).

Table 4-1. Mean (\pm SE) soil total porosity ($\text{cm}^3 \text{ cm}^{-3}$, $n = 3$), its inter-aggregate ($n = 2$) and air-filled fractions (% of total porosity, $n = 3$) and radon production rates from air-dried and wet-season moist soil samples (Bq kg^{-1} air-dry soil, $n = 3$).

Depth (cm)	Porosity				Radon production	
	Total	Inter-aggregate	Air-filled during dry season	Air-filled during wet season	Air-dry soil	Wet-season moist soil
-5	0.78 ± 0.02	29.8 ± 7.9	56.0 ± 0.5	40.5 ± 1.1	2.8 ± 0.6	4.4 ± 0.9
-20	0.71 ± 0.01	12.8 ± 3.7	35.3 ± 0.04	28.5 ± 0.3	2.0 ± 0.5	3.2 ± 0.4
-40	0.62 ± 0.01	11.2 ± 5.0	20.0 ± 3.0	17.1 ± 2.2	1.8 ± 0.4	2.5 ± 0.5
-75	0.57 ± 0.01	11.3 ± 5.1	11.3 ± 1.2	9.6 ± 0.9	1.7 ± 0.2	2.8 ± 0.4
-125	0.57 ± 0.02	5.4 ± 0.4	11.1 ± 3.6	9.6 ± 3.2	1.6 ± 0.3	2.4 ± 0.3
-200	0.58 ± 0.03	$2.5 \pm \text{n.a.}$	11.3 ± 4.6	10.6 ± 4.2	1.3 ± 0.3	2.5 ± 0.6

4.4.1 CO₂ fluxes and production rates calculated with the inverse D in the profile method

When we calculated the inverse D based on non-linear least-square fitting of the sigmoidal function to the measured CO₂ profile it closely resembled the empirical D in the top ~ 0.75 m soil during dry season and in the top 0.40 m during wet season. Below these depths and in

contrast to the empirical D , the inverse D increased sharply. After adding the constraint that D must decrease monotonically with soil depth (eq. 4-22), the inverse D resembled the empirical D throughout the profile but was slightly larger ($P < 0.001$ at all sampling depths, Fig. 4-4a and b). This constrained inverse D gave a similar result as the empirical when used in the Rn mass balance model (Fig. 4-2). However, it did not reproduce the measured soil CO₂ concentrations which were underestimated (RMSE=0.46 ± 0.10; Fig. 4-4c and d).

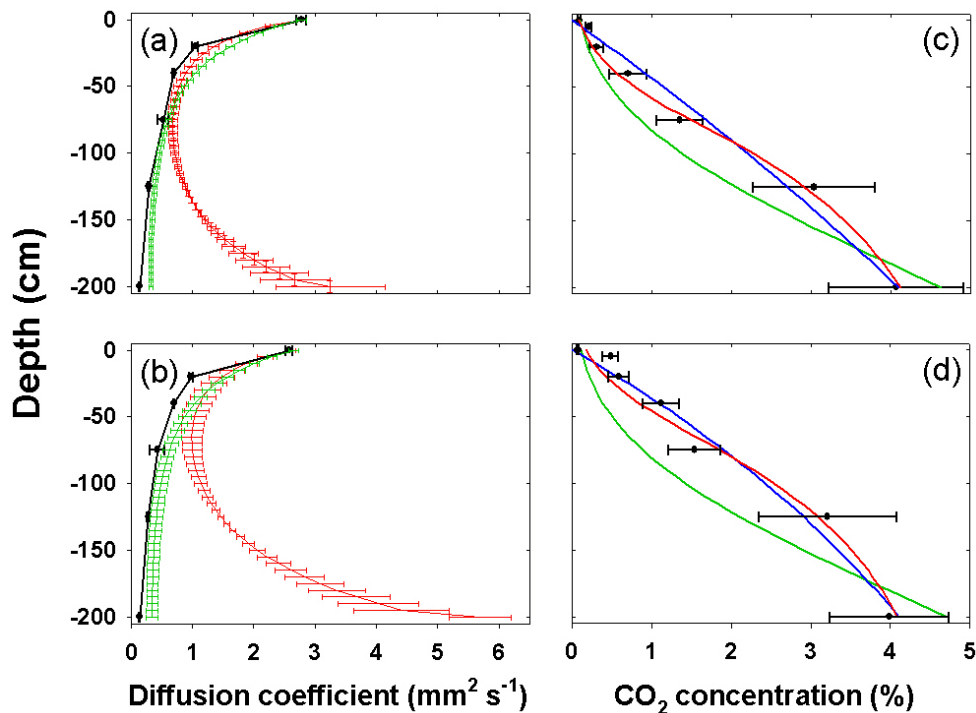


Figure 4-4. Left panels: Mean (\pm SE, $n = 3$) dry (a) and wet season (b) empirical (\bullet), unconstrained inverse ($-$) and constrained inverse ($-$) diffusion coefficients. Right panels: Mean measured (\bullet , \pm SE, $n = 3$) and interpolated CO₂ concentrations in soil air during dry (c) and wet season (d) using the sigmoidal function with an unconstrained parameter choice ($-$), the sigmoidal function with a constrained parameter choice ($-$) and an exponential function ($-$).

Using the inverse D and the corresponding CO₂-concentrations in the profile method, the resulting CO₂ flux was depth-constant (Fig. 4-5a) which means that the ‘CO₂ production’ would be zero at all depths. Using eq. (4-12) it can be shown that this is true in general: D is positive at all depths (Fig. 4-4a and b). The first derivative of a sigmoidal function $\delta C/\delta z$ is negative (<0) at all depths (Fig. 4-1b) while its second derivative is positive in the top and negative in the deep soil (Fig. 4-1c). Thus, to get positive CO₂ production terms, also $\delta D/\delta z$ must be positive at all depths which is sensible concerning that the empirical D indeed

decreases monotonically with depth at our site (Fig. 4-4a and b). In the inverse analysis, this condition was not immediately fulfilled but the solution could be forced to meet it by implying the parameter constraint of eq. (4-22) (Fig. 4-4a and b). In the top soil, a further requirement for positive CO₂-production terms is that:

$$\left| \frac{\partial D_g}{\partial z} \frac{\partial C_g}{\partial z} \right| > \left| D_g \frac{\partial^2 C_g}{\partial z^2} \right| \quad (4-24).$$

Inserting the respective terms (eqs. 4-10, 4-11, 4-19 and 4-21) shows that the absolute values of the left and right-hand expressions are the same:

$$\frac{|-c - cbe^{cz}|}{|c + cbe^{cz}|} = 1 \quad (4-25)$$

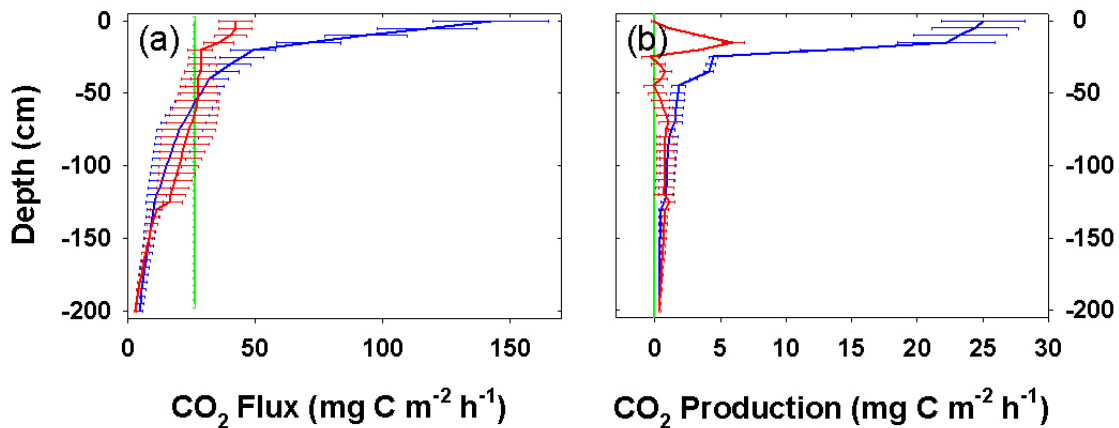


Figure 4-5. Mean (\pm SE, $n = 3$) soil CO₂ a) fluxes and b) ‘production rates’ calculated with the soil-CO₂ profile method. The different solutions were obtained using the empirical diffusion coefficient (D) with a sigmoidal (—) and an exponential (—) function to interpolate between the measured CO₂ concentrations, and using the constrained inverse D (—).

This explains formally why the condition of eq. (4-24) could not be fulfilled, and why the inversely modeled CO₂ production was zero at all depths (Fig. 4-5b). We conducted a similar inverse analysis to calculate profiles of D and S with an exponential function (equivalent to eqs. 4-15 to 4-19 with $C_g = a(1 - e^{-bz})$, not shown). The first derivative of the resulting profile of D was always <0 and consequently the CO₂ production was negative at all depths. Also in this case it was impossible to receive a solution where $S > 0$.

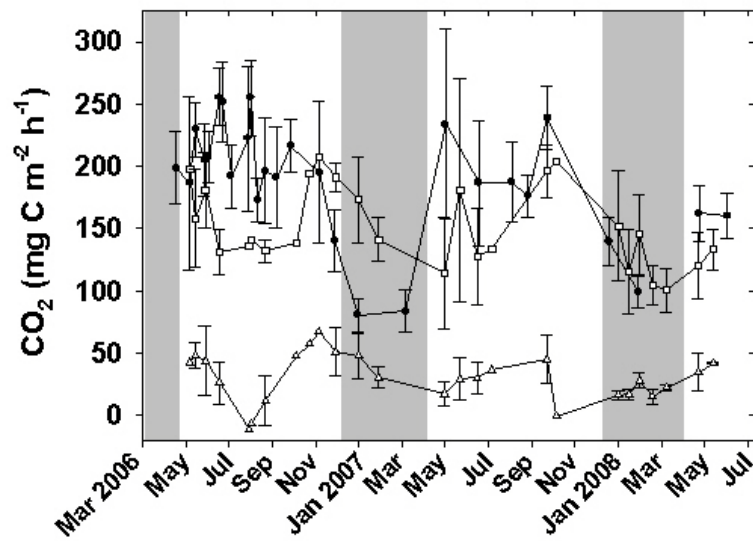


Figure 4-6. Measured (•) and modeled mean soil CO₂ flux (\pm SE, $n = 3$) using the empirical diffusion coefficients D with a sigmoidal (Δ) or exponential (\square) function to approximate the measured CO₂ profiles.

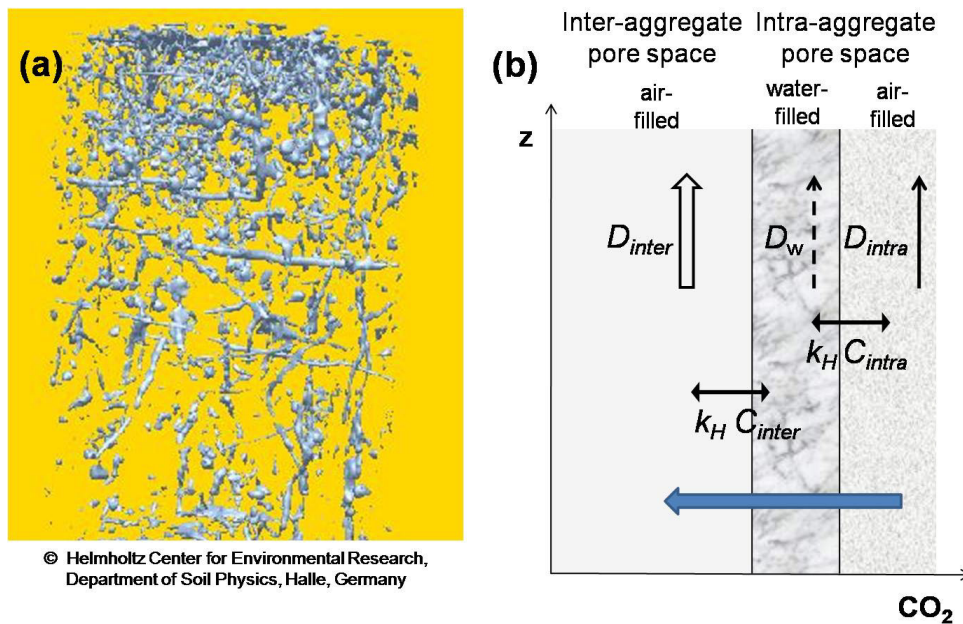


Figure 4-7. a) X-ray computed tomography scan of the inter-aggregate pores >2 mm (blue) in a Terra fusca soil. The image covers a height of ~ 0.25 m. b) Conceptual graph illustrating the CO₂ exchange at the interfaces between air- and water-filled pores. For simplicity, an equilibration according to Henry's law is assumed ($C = \text{CO}_2$ concentration, $k_H = \text{Henry's law constant}$). The different upward errors illustrate that the diffusion coefficients D are larger in air-filled inter-aggregate (D_{inter}) than intra-aggregate pores (D_{intra}), and smallest in water-filled pores (D_w). This results in a CO₂ gradient and hence a net exchange flux which persists during steady state (blue error).

4.5 Discussion

4.5.1 The influence of the function to interpolate between the measured CO₂ concentrations

Vertical interpolation between measured CO₂ concentrations is necessary to apply the soil-CO₂ profile method for a refined depth resolution. In several studies the CO₂ concentrations were linearly interpolated and the concentration gradient driving diffusion ($\delta C/\delta z$) was calculated numerically using the method of finite differences. Finite differences, however, can only be used to approximate the derivatives of continuous functions while in these studies the method was applied on a set of linear functions which changed at the measurement depths. As $\delta C/\delta z$ remains undefined at those depths the calculated CO₂ production rates depend on the depth resolution of the finite difference grid. This influence was already observed by De Jong *et al.* (1978) who reported that: ‘The discrepancies between the static chamber and soil-CO₂ profile estimates decreased as the calculations for the latter method were based on thicker soil layers’. This is, however, a mathematical artifact and we conclude that the combination of linear interpolation with finite differences leads to false results. When applying the profile method, the interpolation between measured CO₂ concentrations should be conducted by means of continuous and differentiable functions.

Selection of an adequate interpolation function is critical because in the profile method the calculated flux will only be accurate if the concentration gradient ($\delta C/\delta z$) is described correctly. In our case, the observed steady state soil gas profile could be best described using a sigmoidal function (Figs. 4-2, 4-4c and d). This functional type has not been used before but for several other studies the shape of soil Rn and CO₂ profiles suggests that it would have resulted in good fits as well (e.g. Dörr and Münnich, 1990; Elberling, 2003; Jassal *et al.*, 2004; Fierer *et al.*, 2005; Schwendenmann and Veldkamp, 2006). In our study, the resulting CO₂ production was unrealistically small compared to the measured CO₂ effluxes (Fig. 4-6). Use of an exponential interpolation would lead to more ‘ecologically reasonable’ results (both flux and production profiles increase towards the surface, Fig. 4-5) but this is largely caused by the fact that the negative first and second derivatives of an exponential function increase monotonically as well. An exponential function (as was e.g. used in Gaudinski *et al.*, 2000; Davidson *et al.*, 2006) does not match the observed steady state Rn profile (Fig. 4-2), has a worse goodness of fit than the sigmoidal function (Fig. 4-5) and the resulting CO₂ fluxes do not reproduce the measured CO₂ fluxes either (Fig. 4-6). Simply replacing the sigmoidal with an exponential interpolation function, however, increased the calculated areal production rates

on average threefold which clearly casts doubt on the forecasting power of the profile method. Parameterizing the profile method with the function which best describes our sites' steady state soil gas distribution yielded inconsistencies similar to the ones reported in earlier applications.

4.5.2 The influence of uncertainties in the depth distribution of D

As, in the soil CO₂-profile method, CO₂ production is directly proportional to D the choice of a function to describe it has been identified as a major source of uncertainty in earlier studies. For example, when using two different models to calculate D for the same site, the resulting organic horizon CO₂ production differed by a factor of two (Gaudinski *et al.*, 2000; Davidson *et al.*, 2006). Furthermore an empirically calculated D yielded over- or under-predictions of up to two orders of magnitude compared to values measured *in situ* (Risk *et al.*, 2008). Our chosen model to calculate D based on soil properties (Millington and Shearer, 1971) performs well in aggregated clay soils (Collin and Rasmuson, 1988), and the resulting empirical D s were comparable to those calculated for Oxisol soils of lowland forests in Brazil (Davidson and Trumbore, 1995) and Costa Rica (Schwendenmann and Veldkamp, 2006). The results from the Rn mass balance model suggest that our calculated D was adequate during wet season conditions (Fig. 4-2b). Although the Rn concentrations were overestimated in the dry season simulation (Fig. 4-2a) the results were better than with alternative empirical models to calculate D . The Rn mass balance model is sensitive to the Rn production rates (inset in Fig. 4-2a) which we measured in laboratory incubations with disturbed soil samples. Soil moistures during the incubations were not identical to conditions encountered during the field campaigns when Rn was sampled and, therefore, the Rn production rates were interpolated. As the more sensitive model parameter is subject to these experiment-related uncertainties we deem the achieved simulated Rn concentrations accurately enough to assume the empirical D is reasonably well constrained.

We tested this assumption by comparing the empirical with inversely modeled D s. The pattern of the air-filled porosity, which determines the distribution of D , indicates that the observed subsoil-increase of the unconstrained inverse D was unrealistic (Table 4-1). However, the fact that the additional constraint gave an inverse D which matched the empirical D amazingly well (Fig. 4-4a and b) supports the assumption that the latter is accurate. However, the CO₂ concentrations which corresponded with these constrained inverse D s were too small (Figs. 4-4c and d), and the inversely modeled CO₂ production was

zero (Fig. 4-6). We therefore conclude from the inverse analysis that our measured CO₂ profiles can not be explained when gas diffusion is the only described process, but that a further CO₂ sink is missing in the mathematical description. As the inverse analysis of an exponential function gave inconsistent results as well this conclusion is independent of the function we chose to approximate the CO₂ profile.

4.5.3 Processes governing soil CO₂ dynamics

The key assumptions of the soil-CO₂ profile method are that convective soil CO₂ transport in water is negligible, and that CO₂ equilibration between air and water phase occurs instantaneously (paragraph 4.3.2). The limiting factor here is the diffusive velocity of CO₂ in water (D_w), which is $1.94 \cdot 10^{-5} \text{ cm}^2 \text{ s}^{-1}$ at 25°C (Tse and Sandall, 1979). For the dry season, evaporative water losses, which cause a continuous increase in the air-filled porosity and consequently a decrease in CO₂ concentrations, might violate the steady state assumption (compare eq. 4-2). However, the observed soil moisture reduction of $\sim 0.2 \text{ cm}^3 \text{ cm}^{-3}$ at 0.05 m depth (not shown) results in a CO₂ ‘dilution’ of only $\sim 5\%$ from December to April. Deeper in the soil, where the drying is less and CO₂ concentrations larger, this effect is even smaller. For the wet season, we estimated the water flow velocity at which the time scale of convection τ_A approaches the characteristic diffusion time τ_D of a CO₂ molecule through a water-filled circular pore. τ_D is $\sim 10^2 \text{ s}$ for a pore diameter of 1 mm (upper end of the size range of intra-aggregate pores; Hillel, 1998), thus τ_A would need to surpass 10^{-5} m s^{-1} . Natural soils usually contain a net of well connected non-capillary macropores (including inter-aggregate pores ϵ_{inter}). Preferential flow velocity through ϵ_{inter} can increase to the order of 10^{-4} m s^{-1} for short periods during heavy rainfall (Beven and Germann, 1982; Blume *et al.*, 2008). The fact that the average air-filled porosity exceeded ϵ_{inter} even during wet season (Table 4-1) adverts to the occurrence of such rapid, event-based water transport at our site. The velocity required to disturb the diffusive CO₂ equilibration between gas and water phase, however, might never be reached in the clay soil matrix given its small hydraulic conductivity. We thus conclude that, except for short periods during heavy storms, both key assumptions of the profile method are usually fulfilled at our site.

We suggest that the inter-aggregate pore system plays a key role for the required missing CO₂ sink which we saw remains active during periods of low hydrologic activity. This network is usually fairly well connected in aggregated soils (see e.g. Fig. 4-7a) and, because of faster ‘preferential’ diffusion, better aerated than the intra-aggregate air-filled

pores (α_{intra}) (Hillel, 1998). This results in CO₂ concentrations in the inter-aggregate air-filled pores (α_{inter}) which are considerably smaller than in α_{intra} . If soil air in inter- and intra-aggregate pores is separated by a water film, the equilibrium CO₂ concentration for the water phase is different at the respective interfaces. This yields a CO₂ gradient across the water film which results in diffusive CO₂ leakage into α_{inter} (Fig. 4-7b). As the diffusion in α_{intra} and water is much slower than in α_{inter} these gradients can not be depleted during steady state conditions. Deeper in the soil, ϵ_{inter} and D are smaller resulting in a higher CO₂ accumulation in the intra-aggregate pores. This explains why, according to the results of our inverse analysis, the largest CO₂ sink was needed in the subsoil and why the deviation between empirical and unconstrained inverse D were more pronounced during wet than dry season (Fig. 4-4a and b). The same steady state exchange process occurs close to the soil surface where soil water has interfaces with the differing CO₂ concentrations in α_{intra} , α_{inter} and free air. Considering that, the concept of defining one D that represents the gas diffusive transport in an aggregated soil may not be justified for the soil CO₂-profile method if there is no continuous network of air-filled pores.

Strong support for this theory comes from the Rn mass balance simulations which, in contrast to the soil-CO₂ profile method, include the exchange between gas and water phase. The Rn simulations captured the shape of the measured profiles which confirms that, despite the poor solubility of Rn (Sander, 1999), inclusion of soil water and the coupling between the water and gas phase are relevant during steady state. For CO₂, which is much more soluble, this will even be more important. A similar argument has been suggested as explanation for failed attempts to calculate soil N₂O fluxes with the so-called 'gradient method' (Heincke and Kaupenjohann, 1999). These authors equally point out that the water phase can cause a separation between gas production and transport. We propose that the use of the soil-CO₂ profile method is problematic when calculating CO₂ production for well-structured soils with a connected, well-aerated network of macropores. Such macropore network is typical for many soils (Zehe and Sivapalan, 2009), especially under natural forests (Beven and Germann, 1982; Blume *et al.*, 2008). If these soils have diffusive water barriers between ϵ_{inter} and ϵ_{intra} , steady state CO₂ transfer into α_{inter} cannot be neglected.

4.5.4 Implications of this study for soil CO₂ production modeling

The soil-CO₂ profile method has been widely applied because of its simplicity. However, inconsistencies have been reported in many of the respective studies, and also by the authors who developed the method. We found evidence that the inconsistencies may not mainly be caused by inaccurate interpolation or parameterization but more likely by the omission of soil water in the CO₂ mass balance setup. For well-structured soils, inclusion of water is required to describe the steady CO₂ exchange between the soil gas and water phases which is caused by persistent CO₂ gradients between un-connected inter- and intra-aggregate air-filled pores. As our inverse analysis was only based on the vertical CO₂ distribution and the assumptions of the profile method this conclusion is independent from the ecosystem where we conducted our study. Consequently, we may only improve our understanding of soil CO₂ dynamics using process-based CO₂-production-transport models which consider the CO₂ mass balance in both gas and water phase.

4.6 References

- Amundson RG, Davidson EA (1990) Carbon dioxide and nitrogenous gases in the soil atmosphere. *Journal of Geochemical Exploration*, **38**, 13-41.
- Beven KJ, Germann PF (1982) Macropores and water flow in soils. *Water Resources Research*, **18**, 1311-1325.
- Blake GR, Hartge KH (1986) Bulk density. In *Methods of soil analysis, part 1. Physical and mineralogical methods*. (ed Klute A). Agronomy Monograph, Soil Science Society of America, Madison, Wisconsin, USA, 12 pp.
- Blume T, Zehe E, Bronstert A (2008) Investigation of runoff generation in a pristine, poorly gauged catchment in the Chilean Andes II: Qualitative and quantitative use of tracers at three spatial scales. *Hydrological Processes*, **22**, 3676-3688.
- Campbell GS (1985) *Soil physics with BASIC, transport models for soil-plant systems*. Elsevier Science Publishers B.V., Amsterdam, The Netherlands, 150 pp.
- Campbell Scientific (2002-2006) CS616 and CS625 water content reflectometers, Instruction manual.
- Collin M, Rasmuson A (1988) A comparison of gas diffusivity models for unsaturated porous media. *Soil Science Society of America Journal*, **52**, 1559-1565.
- Corre MD, Veldkamp E, Arnold J, Wright SJ (in press) Impact of elevated N input on N cycling and retention of soils under old-growth lowland and montane forests in Panama, *Ecology*.
- Crawley MJ (2002) *Statistical Computing, An Introduction to Data Analysis using S-Plus*. John Wiley & Sons Ltd, Chichester, England, 761 pp.
- Currie JA (1961) Gaseous diffusion in porous media. Part 3-Wet granular materials. *British Journal of Applied Physics*, **12**, 275-281.
- Davidson EA, Ishida FY, Nepstad DC (2004) Effects of an experimental drought on soil emissions of carbon dioxide, methane, nitrous oxide, and nitric oxide in a moist tropical forest. *Global Change Biology*, **10**, 718-730.
- Davidson EA, Trumbore SE (1995) Gas diffusivity and production of CO₂ in deep soils of the eastern Amazon. *Tellus*, **47**, 550-565.
- Davidson EA, Savage KE, Trumbore SE, Borken W (2006) Vertical partitioning of CO₂ production within a temperate forest soil. *Global Change Biology*, **12**, 944-956.
- DeJong E, Schappert HJV (1972) Calculation of soil respiration and activity from CO₂ profiles in the soil. *Soil Science*, **113**, 328-333.

- De Jong E, Redmann RE, Ripley EA (1978) A comparison of methods to measure soil respiration, *Soil Science*, **127**, 300-306.
- Dörr H, Münnich KO (1990) ²²²Rn flux and soil air concentration profiles in West-Germany. Soil ²²²Rn as tracer for gas transport in the unsaturated soil zone. *Tellus*, **42B**, 20-28.
- Elberling B (2003) Seasonal trends of soil CO₂ dynamics in a soil subject to freezing. *Journal of Hydrology*, **276**, 159-175.
- Fang C, Moncrieff JB (1999) A model for soil CO₂ production and transport 1: Model development. *Agricultural and Forest Meteorology*, **95**, 225-236.
- Fierer N, Chadwick OA, Trumbore SE (2005) Production of CO₂ in soil profiles of a California annual grassland. *Ecosystems*, **8**, 412-429.
- Gaudinski JB, Trumbore SE, Davidson EA, Zheng S (2000) Soil carbon cycling in a temperate forest: radiocarbon-based estimates of residence times, sequestration rates and partitioning of fluxes. *Biogeochemistry*, **51**, 33-69.
- Hashimoto S, Tanaka N, Kume T, Yoshifuji N, Hotta N, Tanaka K, Suzuki M (2007) Seasonality of vertically partitioned soil CO₂ production in temperate and tropical forest. *Journal of Forest Research*, **12**, 209-221.
- Heincke M, Kaupenjohann M (1999) Effects of soil solution on the dynamics of N₂O emissions: a review. *Nutrient Cycling in Agroecosystems*, **55**, 133-157.
- Hillel D (1998) *Environmental soil physics*. Academic Press, San Diego, California, 771 pp.
- Hirsch A, Trumbore SE, Goulden ML (2002) Direct measurement of the deep soil respiration accompanying seasonal thawing of a boreal forest soil. *Journal of Geophysical Research*, **108**, 8221-8230.
- IPCC: *Climate Change 2007: The Physical Science Basis. Contribution of Working Group I to the Fourth Assessment Report of the Intergovernmental Panel on Climate Change*, Cambridge University Press, Cambridge, UK and New York, USA, 2007.
- Jassal R, Black A, Novak M, Morgenstern K, Nesic Z, Gaumont-Guay D (2005) Relationship between soil CO₂ concentrations and forest-floor CO₂ effluxes. *Agricultural and Forest Meteorology*, **130**, 176-192.
- Jassal RS, Black TA, Drewitt GB, Novak MD, Gaumont-Guay D, Nesic Z (2004) A model of the production and transport of CO₂ in soil: Predicting soil CO₂ concentrations and CO₂ efflux from a forest floor. *Agricultural and Forest Meteorology*, **124**, 219-236.
- Kirkpatrick S, Gelatt CDJ, Vecchi MP (1983) Optimization by simulated annealing. *Science*, **220**, 671-680.

- Koehler B, Corre MD, Veldkamp E, Sueta JP (2009a) Chronic nitrogen addition causes a reduction in soil carbon dioxide efflux during the high stem-growth period in a tropical montane forest but no response from a tropical lowland forest in decadal scale. *Biogeosciences*, **6**, 2973-2983.
- Koehler B, Corre MD, Veldkamp E, Wullaert H, Wright SJ (2009b) Immediate and long-term nitrogen oxide emissions from tropical forest soils exposed to elevated nitrogen input, *Global Change Biology*, **15**, 2049-2066.
- Leigh EG, Rand AS, Windsor DW (1996) *The ecology of a tropical forest*. Smithsonian Press, Washington DC, USA, 266 pp.
- Linn DM, Doran JW (1984) Effect of water-filled pore space on carbon dioxide and nitrous oxide production in tilled and nontilled soils. *Soil Science Society of America Journal*, **48**, 1267-1272.
- Loftfield N, Flessa H, Augustin J, Beese F (1997) Automated gas chromatographic system for rapid analysis of the atmospheric trace gases methane, carbon dioxide, and nitrous oxide. *Journal of Environmental Quality*, **26**, 560-564.
- Luo Y, Zhou X (2006) *Soil respiration and the environment*. Elsevier Academic Press, Burlington, San Diego and London, UK, 316 pp.
- Millington RJ, Quirk JM (1961) Permeability of porous solids. *Transactions of the Faraday Society*, **57**, 1200-1207.
- Millington RJ, Shearer RC (1971) Diffusion in aggregated porous media. *Soil Science*, **111**, 372-378.
- Moldrup P, Olesen T, Schjønning P, Yamaguchi T, Rolston DE (2000) Predicting the gas diffusion coefficient in undisturbed soil from soil water characteristics. *Soil Science Society of America Journal*, **64**, 94-100.
- Penman HL (1940) Gas and vapor movements in the soil (I). The diffusion of vapors through porous solids. *Journal of Agricultural Science*, **30**, 437-461.
- Pritchard DT, Currie JA (1982) Diffusion coefficients of carbon-dioxide, nitrous-oxide, ethylene andthane in air and their measurement. *Journal of Soil Science*, **33**, 175-184.
- Pylon Electronics (1989) Using Pylon model 110A and 300A Lucas cells with the Pylon model AB- 5, Instruction manual.
- Radulovich R, Solorzano E, Sollins P (1989) Soil macropore size distribution from water breakthrough curves. *Soil Science Society of America Journal*, **53**, 556-559.

-
- R Development Core Team (2009) A language and environment for statistical computing. R Foundation for Statistical Computing, Vienna, <http://www.R-project.org>.
- Richards FJ (1959) A flexible growth function for empirical use. *Journal of Experimental Botany*, **10**, 290-300.
- Risk D, Kellman L, Beltrami H (2002a) Carbon dioxide in soil profiles: Production and temperature dependence. *Geophysical Research Letters*, **29**, doi:10.1029/2001GL014002, 012002.
- Risk D, Kellman L, Beltrami H (2002b) Soil CO₂ production and surface flux at four climate observatories in eastern Canada. *Global Biogeochemical Cycles*, **16**, 1122, doi:10.1029/2001GB001831.
- Risk D, Kellman L, Beltrami H (2008) A new method for in situ gas diffusivity measurement and applications in the monitoring of subsurface CO₂ production. *Journal of Geophysical Research*, **113**, G02018, doi:10.1029/2007JG000445.
- Sander R (1999) Compilation of Henry's Law Constants for inorganic and organic species of potential importance in environmental chemistry, <http://www.mpch-mainz.mpg.de/~sander/res/henry.html>, Max-Planck Institute of Chemistry, Mainz.
- Sasaki T, Gunji Y, Okuda T (2006) Transient-diffusion measurement of radon in Japanese soils from a mathematical viewpoint. *Journal of Nuclear Science and Technology*, **43**, 806-810.
- Schwendenmann L, Veldkamp E, Brenes T, O'Brien JJ, Mackensen J (2003) Spatial and temporal variation in soil CO₂ efflux in an old-growth neotropical rain forest, La Selva, Costa Rica. *Biogeochemistry*, **64**, 111-128.
- Schwendenmann L, Veldkamp E (2006) Long-term CO₂ production from deeply weathered soils of a tropical rain forest: evidence for a potential positive feedback to climate warming. *Global Change Biology*, **12**, 1-16.
- Simunek J, Suarez DL (1993) Modeling of carbon dioxide transport and production in soil 1. Model development. *Water Resources Research*, **29**, 487-497.
- Sotta Doff E, Veldkamp E, Schwendenmann L, *et al.* (2007) Effects of an induced drought on soil carbon dioxide (CO₂) efflux and soil CO₂ production in an Eastern Amazonian rainforest, Brazil. *Global Change Biology*, **13**, 2218-2229.
- Tse FC, Sandall OC (1979) Diffusion coefficients for oxygen and carbon dioxide in water at 25°C by unsteady state desorption from a quiescent liquid. *Chemical Engineering Communications*, **3**, 147-153.

Veldkamp E, O'Brien JJ (2000) Calibration of a frequency domain reflectometry sensor for humid tropical soils of volcanic origin. *Soil Science Society of America Journal*, **64**, 1549-1553.

Zehe E, Sivapalan M (2009) Treshold behavior in hydrological systems as (human) geoecosystems: Manifestations, controls and implications. *Hydrology and Earth System Science*, **13**, 1273-1297.

CHAPTER

5

Synthesis

5.1 How will tropical regions respond to rising nitrogen input?

Based on this study results (Chapters 2 and 3) I expect the following responses of soil trace gas emissions from tropical forests exposed to elevated N input:

1. The magnitude of soil N-oxide emissions will increase substantially.
2. The onset of elevated soil N-oxide emissions will be strongly influenced by the initial leakiness of the forests soil N cycle.
3. Soil N-oxide emissions from montane forests will enlarge immediately if the forest soil has an organic layer where nitrification activity may increase substantially. This can be expected even if the soil N cycle is conservative and the forests' primary productivity N limited.
4. The relative contribution of N₂O to the total soil N-oxide emissions from forests on deeply weathered soils may increase.
5. In forests with a pronounced dry season soil moisture may become the main factor regulating the type of soil emitted N-oxides. Changes in precipitation patterns and soil moisture regime due to climate change will immediately reflect in the ratio of soil N₂O/NO emissions.
6. In lowland forests on soils with high nutrient-supplying and buffering capacity, where primary productivity is neither N- nor P-limited, soil respiration may not change in the short term or on a decadal time scale.
7. Soil respiration may decrease relatively quickly in montane forests with N-limited primary productivity, and a shift in C partitioning from below- to aboveground may occur. In the longer term, such shift would cause imprints on the magnitude of soil C storage.

5.2 What is the ultimate fate of reactive nitrogen?

This study traced the fate into the atmosphere in form of nitric and nitrous oxide (Chapter 2). In total, on average 5.0 and 6.4% of the applied fertilizer N (125 kg N ha⁻¹ yr⁻¹) was soil emitted as N-oxides from the montane and lowland forest, respectively. This includes the fertilizer induced peaks, which are a transitory experimental artifact following the application of a high N dose. This is the first study to also investigate long-term soil N-oxide emissions from N-enriched tropical forests. Those were defined as emissions occurring at least six weeks after an N application, i.e. excluding the artificially high fertilizer induced peak emissions. These long-term effects should be comparable to soil N-oxide emissions from

tropical forest which became N-enriched by chronic atmospheric N deposition. On average 1.6 and 2.9% of the applied N was lost to long-term soil N-oxide emissions in the montane and lowland forest, respectively (Table 5-1).

Table 5-1. Percentage of the experimentally added reactive N ($125 \text{ kg N ha}^{-1} \text{ yr}^{-1}$) that was emitted from the lowland and montane forest soils as N-oxides.[†] The emission response is separated into transitory effects (include transitory ‘fertilization peaks’) and long-term effects (include only fluxes measured at least six weeks after an N addition).

Site (years of N addition)	Effect	2006		2007	
		NO	N ₂ O	NO	N ₂ O
Montane (1- and 2-yr)	Transitory effect	0.57 ± 0.19	2.76 ± 1.15	2.49 ± 0.49	4.21 ± 2.22
	Long-term effect	0.12 ± 0.05	1.66 ± 0.67	0.19 ± 0.09	1.13 ± 0.82
Lowland (9- and 10-yr)	Transitory effect	1.46 ± 0.29	4.46 ± 1.52	0.90 ± 0.23	5.90 ± 1.18
	Long-term effect	0.35 ± 0.11	2.89 ± 0.93	0.35 ± 0.03	2.26 ± 0.47

[†] = $100 * ((\text{kg N ha}^{-1} \text{ yr}^{-1} \text{ emitted from the N-addition plot} - \text{kg N ha}^{-1} \text{ yr}^{-1} \text{ emitted from the control plot}) / 125 \text{ kg N ha}^{-1} \text{ yr}^{-1})$

This percentage does not include losses in form of N₂ due to complete denitrification, and does not consider ammonia volatilization. Soil N₂ emissions are difficult to measure in the field (Butterbach-Bahl *et al.*, 2002). Tropical forest soils are poorly studied concerning their N₂ emissions, i.e. a recent review on forest soils only included temperate soils. Nearly all of those had been studied in the laboratory rather than in the field and the compilation yielded a highly variable N₂-N/(N₂+N₂O-N)-ratio (Schlesinger, 2009). Ammonia volatilization especially occurs in dry and alkaline soils. Undisturbed tropical forests, where soils are normally wet and acidic, have previously been considered zero-emission ecosystems. In our N-addition plots, N may have been emitted as ammonia immediately following urea application and hydrolysis (Schlesinger & Hartley, 1992). Such ammonia emissions would however not affect the above estimate of long-term N losses to the atmosphere. Our observed increases in long-term soil N-oxide emissions following N enrichment are of major importance concerning the impact on atmospheric chemistry and radiative forcing, however,

N-oxide emission to the atmosphere was only the fate of a minor fraction of the added N. The remaining bulk was thus lost to leaching and is located in other environmental compartments apart from the atmosphere, including the soil and vegetation. These fates of N are partly investigated in the other sub-studies of the NITROF-project.

5.3 What are the net climate effects of increasing reactive nitrogen?

This study investigated the effects of increasing N_r on the emission of climate relevant trace gases from tropical forest soils. The following paragraphs will only consider climate change via tropospheric radiative forcing while other climate effects (e.g. stratospheric ozone depletion by N_2O) will not be discussed. Due to their different radiative properties and atmospheric life-times greenhouse gases (GHG) differ in their climate warming influence. The warming influence in relation to CO_2 may be expressed through a common metric, the ‘ CO_2 –equivalent’ emission. This is the amount of CO_2 emission that would cause the same time-integrated radiative forcing as an emitted amount of a non- CO_2 GHG or a mixture of GHGs. The CO_2 equivalents are obtained by multiplying the GHG emission by its ‘Global Warming Potential’ (GWP) for the given time horizon (IPCC, 2007). The metric of GWPs has been subjected to several points of criticism but retained some favour because of its simple design as well as its applicability and transparency compared to proposed alternatives (Fuglestvedt *et al.*, 2003). It remains the recommended metric to compare future climate impacts of emissions from long-lived GHGs, which dominate radiative forcing (IPCC, 2007). Atmospheric NO causes two opposing effects on radiative forcing through ozone enhancements on the one hand and CH_4 reductions on the other hand. The complex nonlinear chemistry and short lifetime of NO make calculations of a GWP for its emissions very uncertain (Shine *et al.*, 2005). Due to the lack of agreement even on the sign of the GWP for NO among different studies a central estimate is not available (IPCC, 2007), and NO was thus not included in the calculations which are presented in the following.

In both control forests and throughout seasons the soil CO_2 efflux dominated the soil emission budget. The contribution of soil N_2O -emissions to the total soil CO_2 -equivalent emission ranged from 1.0 to 1.6% and was usually smaller than the standard error of CO_2 emissions. In the montane forest, where soil N_2O emissions increased (Chapter 2) and soil CO_2 efflux decreased with 2-yr N-addition (Chapter 3), the contribution of N_2O to the soil CO_2 -equivalent emission increased to on average 5%. The total net CO_2 -equivalent emission did not differ between control and 2-yr N-addition plots. In the lowland forest, 9-10 yr N-

addition increased soil N₂O emissions substantially (Chapter 2) while soil CO₂ efflux did not change (Chapter 3). The contribution of N₂O emissions to the soil CO₂-equivalent emission remained small with on average 2.3 and 4.0 % during dry and wet season, respectively. The increase in soil N₂O emissions did not cause a detectable effect in the total soil CO₂-equivalent emission in either season (Table 5-2). Considering N₂O and CO₂, two of the three most important long-lived GHGs, no net effect of chronic N-addition on the soil CO₂-equivalent emission was detected in either forest.

Table 5-2. Mean (\pm SE, $n = 4$) soil emissions of CO₂ (g CO₂ m⁻² yr⁻¹) and N₂O (g N₂O m⁻² yr⁻¹) for control and N-addition plots of the lowland and montane forest. For N₂O, the values in brackets give the respective CO₂-equivalent flux (g CO₂-equivalents m⁻² yr⁻¹) using the 100-yr GWP of 298 (IPCC, 2007).

Site	Treatment	Season	CO ₂	N ₂ O	Total CO ₂ -equivalent flux
Montane	Control *	-	3034.78 \pm 201.19	0.16 \pm 0.02 (48.86 \pm 6.90)	3083.65 \pm 207.60
	2-yr N addition *	-	2633.48 \pm 118.40	0.46 \pm 0.25 (137.93 \pm 74.48)	2771.41 \pm 173.23
Lowland	Control	Dry	4572.66 \pm 542.14	0.15 \pm 0.01 (45.77 \pm 3.53)	4618.43 \pm 541.07
	9- and 10-yr N addition	Dry	4307.47 \pm 268.80	0.33 \pm 0.08 (99.80 \pm 24.23)	4407.27 \pm 279.72
	Control	Wet	6700.18 \pm 595.10	0.25 \pm 0.02 (74.53 \pm 7.18)	6774.71 \pm 601.14
	9- and 10-yr N addition	Wet	6738.63 \pm 420.15	0.94 \pm 0.20 (280.32 \pm 59.89)	7018.95 \pm 361.20

* Only the data of 2007 (second year N addition when soil CO₂ efflux decreased) were included in this assessment.

As this assessment was based on soil emissions only these budgets do not represent the net ecosystem radiative forcing effect following N enrichment. While there are no canopy processes concerning N₂O, forests photosynthetically fix atmospheric CO₂ in the same order of magnitude as they emit CO₂ from their soils (Mooney *et al.*, 1987). If the above assessment could be calculated for net ecosystem C exchange instead of soil respiration the relevance of

soil N₂O emissions would strongly increase. In the lowland forest, the elevated magnitude of soil N₂O emissions following chronic N-addition (Chapter 2) would cause a significant increase in the ecosystem CO₂-equivalent flux, representing the increase in ecosystem positive radiative forcing which is unambiguously caused by the enlarged soil N₂O emissions. In the montane forest, primary production increased with 2-3-yr N-addition (Adamek, 2009; Pame-Baldos, 2009) while soil respiration decreased (Chapter 3). If the above calculations could be based on net ecosystem C exchange, the decrease in the CO₂-equivalent flux – and thus the reduction in positive radiative forcing (Table 5-2) - might be significant. The calculation of soil CO₂ equivalent fluxes sets the considered GHGs in relation to each other but it is important to be aware that these CO₂ equivalents do not represent the net ecosystem radiative forcing.

5.4 From trace gas production to soil surface flux

Using chamber measurements to determine gas flux rates at the soil-air interface is a common methodology in soil trace gas assessments (Livingston & Hutchinson, 1995). However, the interpretation of these flux rates together with data on related above- and belowground parameters (e.g. fine root biomass, litterfall, soil extractable mineral N, temperature and moisture) remains indirect. Gas production, consumption and transport, the belowground processes determining the soil surface flux rates, remain unknown. Hampering a direct investigation neither gas production nor consumption at a specific depth can be measured in the field. Therefore, mathematical models may be a useful tool to describe and study them, and contribute to a more extensive system understanding. Exemplary model questions would be how much deep soil N₂O production contributed to the surface emission, and if this contribution or the production and consumption patterns have changed with N enrichment, or whether the decreased CO₂ production in the N-enriched montane forest was mainly located in the mineral soil or the organic layer.

Acknowledging this importance to assess the belowground processes the third part of the thesis was dedicated to the mathematical modeling of gas production and transport. At the onset of that sub-study the assumption was that the ‘soil-CO₂ profile method’ (DeJong & Schappert (1972)) could be used to reliably calculate depth-specific soil CO₂ production rates. However, as the inverse analysis revealed limitations and inconsistencies of the method the objective was re-defined to resolve which steady-state process is missing in the current model setup (Chapter 4). The continuative research questions which emerged during the course of

this study may be addressed in follow-up studies building on the results from this modeling analysis.

5.5 Suggestions for future research

I mainly see further potential to build on the model analysis presented in Chapter 4. A first step could be to set up a simple CO₂-production-transport model, similar to the one used for radon, which considers production, gaseous diffusion and exchange between gas and water phase. This model setup proved sensitive towards the production term (paragraph 4.4.3). Microbial and root production could be parameterized using existing approaches, e.g. the ones implemented in PATCIS (Fang & Moncrieff, 1999). PATCIS describes soil organic matter decomposition as linear process using decomposition rates from a labile and a resistant fraction, assuming that a constant fraction of CO₂ arises from the decomposition of a unit of dry organic matter. Root respiration is described using specific root respiration rates and root biomass for different size classes, assuming that they are linearly related. Furthermore, influences of soil moisture, temperature and oxygen concentration on soil respiration are considered. Implementing and running this model would elucidate if the inconsistencies that were encountered upon use of the soil-CO₂ profile method can be resolved by adding a phase exchange term, as hypothesized in paragraph 4.5.3.

If such an expanded but still simple model would give consistent and reliable results it could be used on the existing data set of CO₂ profiles from the lowland forest to investigate e.g. which environmental parameters regulate the depth-specific soil CO₂ production rates during dry and wet season (e.g. soil moisture, temperature, litterfall, photosynthetic active radiation), and whether there was a response to N-addition. Based on the results presented in Chapter 2 (i.e. no differences in soil CO₂ efflux after a decade of N-addition) I hypothesize that soil CO₂ production did not differ between treatments either. However, N-induced soil acidification and subsequent changes in soil chemical characteristics will progress within the coming years. As a result, soil CO₂ production and efflux may decrease from the N-addition plots compared to the control (paragraph 3.5.2). If this would be the case during the time that soil CO₂ efflux and concentrations are still measured within the ongoing NITROF-project, model simulations might determine at which soil depths the decrease in soil CO₂ production is occurring and possibly contribute to the question which production source (i.e. root or microbial respiration) is mainly decreasing.

Next, it would be interesting to parameterize other existing CO₂-production-transport models which include a more complex process description, considering for example additional CO₂ transport pathways and/or soil water dynamics (e.g. PATCIS; Fang & Moncrieff (1999); HYDRUS; Šimůnek & Suarez (1993)), for the same lowland site. The main objectives of such study would be to 1) compare the soil CO₂ production rates determined by a simple steady state model suitable for geo-scientific studies with limited parameter availability with the results from a (transient) process-based model, 2) advance system understanding from potential differences in the model outputs, 3) divide soil CO₂ production in its components (i.e. microbial and root respiration) and 4) simulate the response of soil CO₂ production to modifications in the considered regulating parameters.

5.6 References

- Adamek M, Corre MD, Hölscher D (2009) Early effect of elevated nitrogen input on above-ground net primary production of a lower montane rain forest, Panama. *Journal of Tropical Ecology*, **25**, 637-647.
- Butterbach-Bahl K, Willibald G, Papen H (2002) Soil core method for direct simultaneous determination of N₂ and N₂O emissions from forest soils. *Plant and Soil*, **240**, 105-116.
- DeJong E, Schappert HJV (1972) Calculation of soil respiration and activity from CO₂ profiles in the soil, *Soil Science*, **113**, 328-333.
- Fang C, Moncrieff JB (1999) A model for soil CO₂ production and transport 1: Model development. *Agricultural and Forest Meteorology*, **95**, 225-236.
- Fuglestvedt JS, Berntsen TK, Godal O, Sausen R, Shine KP, Skodvin T (2003) Metrics of climate change: Assessing radiative forcing and emission indices. *Climatic Change*, **58**, 267-331.
- IPCC (2007) Climate Change 2007: The Physical Science Basis. Contribution of Working Group I to the Fourth Assessment Report of the Intergovernmental Panel on Climate Change (eds Solomon S, Qin D, Manning M, *et al.*). Cambridge University Press, Cambridge, UK and New York, USA, 996 pp.
- Livingston GP, Hutchinson GL (1995) Enclosure-based measurement of trace gas exchange: applications and sources of error In *Biogenic trace gases: Measuring emissions from soil and water* (eds Matson PA, Harriss RC). Blackwell Scientific Publications, Oxford, UK, pp. 14-51.
- Mooney HA, Vitousek PM, Matson PA (1987) Exchange of materials between terrestrial ecosystems and the atmosphere. *Science*, **238**, 926-932.
- Pame-Baldos A (2009) *Above-ground net primary productivity and leaching losses in a tropical montane forest exposed to elevated nitrogen input*. M.Sc. thesis, University of Goettingen, Goettingen, Germany.
- Schlesinger WH, Hartley AE (1992) A global budget for atmospheric NH₃. *Biogeochemistry*, **15**, 191-211.
- Schlesinger WH (2009) On the fate of anthropogenic nitrogen. *Proceedings of the National Academy of Sciences*, **106**, 203-208.

Shine KP, Berntsen TK, Fuglestvedt JS, Sausen R (2005) Scientific issues in the design of metrics for inclusion of oxides of nitrogen in global climate agreements. *Proceedings of the National Academy of Sciences*, **102**, 15768-15773.

Šimůnek J, Suarez DL (1993) Modeling of carbon dioxide transport and production in soil 1. Model development. *Water Resources Research*, **29**, 487-497.

Declaration of originality, certificate of authorship and declaration about data contributions of the co-authors to the presented manuscripts

I hereby declare that this thesis entitled 'Soil nitrogen oxide and carbon dioxide emissions from a tropical lowland and montane forest exposed to elevated nitrogen input' is my own work and has been written by me. It has not previously been submitted in any form for another degree at any university or other institute of tertiary education. Information derived from the published and unpublished work of others has been acknowledged in the text and a list of references is given in the bibliography. I certify that the manuscripts presented in chapters 2, 3 and 4 have been written by me as first author.

Chapter 2: Marife D. Corre and Edzo Veldkamp provided the data on soil characteristics (Table 2-1). S. Joseph Wright provided the raw data on forest structure of the lowland site (Table 2-2; data analysis by me). Markus Adamek provided the data on forest structure of the montane site (Table 2-2). Marife D. Corre provided the data on net rates of soil N cycling (Table 2-3). Hans Wullaert provided the data on soil N-oxide fluxes following first-time N-addition in the lowland forest (used within Fig. 2-7; statistical analysis and graphing by me).

Chapter 3: Juvia P. Sueta provided the soil CO₂ efflux, extractable N, moisture and temperature data for September 2008 to February 2009 (statistical analysis and graphing by me). Markus Adamek and Angelica Pame-Baldos provided the data on stem-growth in the montane forest (used within Fig. 3-6).

Biggit Kohler

Curriculum vitae

PERSONAL INFORMATION

Date of birth 26.05.1980
Place of birth Rendsburg
Citizenship German

EDUCATION AND RESEARCH EXPERIENCE

06/1990 - 06/1999 High school, intensive courses mathematics and biology
10/1999 - 07/2005 Studies of Geoecology, University of Potsdam, Germany
Main subjects 'Mathematical modeling in geoecology and hydrology' and 'Limnoecology'
10/2005 - 02/2009 PhD-Dissertation in the program 'Biodiversity and Ecology',
University of Goettingen, Germany
10/2005 - 10/2008 Research Associate at the Buesgen-Institute,
Ecopedology of the Tropics and Subtropics,
University of Goettingen, Germany
2005/2006 18 months of PhD-Research at the Smithsonian Tropical
Research Institute, Republic of Panama
Since 10/2008 Research Associate at the Institute of Water and Environment,
Technical University of Munich, Munich, Germany

PUBLICATIONS

Koehler B (2005) *Resource competition between mixotrophic algae and heterotrophic aquatic organisms for organic carbon - mathematical modeling and experiments*. Diploma-thesis, University of Potsdam, Potsdam, Germany, 100 pp.

Kamjunke N, Koehler B, Wannicke N, Tittel J (2008) Algae as competitors of heterotrophic bacteria for glucose. *Journal of Phycology*, **44**, 616-623.

Koehler B, Corre MD, Veldkamp E, Wullaert H, Wright SJ (2009) Immediate and long-term nitrogen oxide emissions from tropical forest soils exposed to elevated nitrogen input. *Global Change Biology*, **15**, 2049-2066.

Koehler B, Corre, MD, Veldkamp E, Sueta JP (2009) Chronic nitrogen addition causes a reduction in soil carbon dioxide efflux during the high stem-growth period in a tropical montane forest but no response from a tropical lowland forest on a decadal time scale. *Biogeosciences*, **6**, 2973-2983.

Acknowledgements

I wish to thank Marife D. Corre for enabling me to conduct my PhD-thesis in her very interesting and challenging NITROF-project and for acting as referee for this thesis. Her and Edzo Veldkamp for the well preparation of the project, instructing me to the field and laboratory measurements, for discussions and critical advice.

Erwin Zehe for acting as co-referee for this thesis, for inspiring collaboration, discussions and for his ongoing motivation and support in many ways.

S. Joseph Wright for his kind support and motivating discussions during my stay at the Smithsonian Tropical Research Institute in Panama, for data sharing and for his constructive and helpful criticism of the first manuscript.

Nuestros asistentes en el campo y laboratorio en Panama que invirtieron una energía y motivación enorme: Rodolfo Rojas, Carlos Sanchez, Ignacio Delcid, Olivier Gonzalez, Omar Hernandez y Rufino Gonzalez.

The people who in various occasions invested time and energy to help me with the technical equipment, especially Norman Loftfield, Milton García, Flore Jaimes, Hans Mühlhahn and Michael Gründel.

All the helpful people at the Smithsonian Tropical Research Institute and in Gamboa who supported or motivated me in many ways, especially Oris Acevedo, Raineldo Urriola, Llorie and Jay Gibson, Pastor Bill Wilbur, Elizabeth and Egbert Leigh, Ben Turner, Marc Seid, Bettina Engelbrecht, Hubert Herz, Carlos Espinoza, Melida Ruiz and the 'guardabosques'.

Dem Labor-Team des Büsgen-Institutes der Universität Göttingen für die engagierte und sorgfältige Bearbeitung der Projektproben.

The people who took time for getting me acquainted with methodology and for helpful discussions, especially Luitgard Schwendenmann, Ulrike Talkner and Christoph Scherber.

Ute Krökel für ihre stete Hilfsbereitschaft und die rasche Bearbeitung langer Vorschuss-Abrechnung in unterschiedlichen Währungen.

The Robert Bosch Foundation for funding the NITROF-Project including this study and the Smithsonian Tropical Research Institute for excellent logistical and technical support.

Dirk Gansert for coordinating the Ph.D. program 'Biological Diversity and Ecology', for help and advice as well as for the organization of very interesting colloquiums.

Katrin Wolff, Daniel Weymann and Oliver von Straaten for their constructive comments on Chapters 1 and 5, and all the PhD-Students of the Buesgen-Institute for a great time in Göttingen.

Mis queridos amigos con cuales compartí un tiempo maravilloso en Panama, y con cuales me unen unos recuerdos muy especiales e inolvidables, en especial: Dumas Gálvez, Isis Lopez, Gogi Kalka, Julia Barske y Hans Sollberger.

Meinen lieben mir unersetzlichen Freunden für wunderschöne gemeinsame Stunden und Jahre...meiner Familie für ihre liebevolle Unterstützung und Begleitung...und Christian für die gemeinsame Zeit.